IMPACT OF CLIMATE CHANGE ON HYDROPOWER GENERATION: CASE OF SHIRORO DAM, NIGERIA

BY

ODOOM, Peter Rock Ebo

MTech/SPS/2015/6074

A THESIS SUBMITTED TO THE POSTGRADUATE SCHOOL FEDERAL UNIVERSITY OF TECHNOLOGY, MINNA, NIGERIA IN PARTIAL FULFILLMENT OF THE REQUIREMENTS FOR THE AWARD OF THE DEGREE OF MASTER OF TECHNOLOGY (MTech) IN CLIMATE CHANGE AND ADAPTED LAND USE

MARCH, 2018

DECLARATION

I hereby declare that this thesis titled: **"Impact of Climate Change on Hydropower Generation: Case of Shiroro Dam, Nigeria"** is a collection of my original research work and it has not been presented for any other qualification anywhere. Information from other sources (published or unpublished) has been duly acknowledged.

ODOOM, Peter Rock Ebo …….

MTech/SPS/2015/6074 SIGNATURE & DATE
FEDERAL UNIVERSITY OF TECHNOLOGY,
MINNA, NIGERIA.

CERTIFICATION

The thesis titled**: "Impact of Climate Change on Hydropower Generation: Case of Shiroro Dam, Nigeria"** by ODOOM, Peter Rock Ebo, (MTech/SPS/2015/6074) meets the regulations governing the award of the degree of Master of Technology (MTech) of the Federal University of Technology, Minna and it is approved for its contribution to scientific knowledge and literary presentation.

Prof O. D. Jimoh ……
Major Supervisor Signature & Date

Prof. A. A. Okhimamhe ……
Director WASCAL, FUT Minna Signature & Date

Prof. M.G. M. Kolo ……
Dean, Postgraduate School Signature & Date

DEDICATION

I dedicate this research work to the Almighty God and to my family especially, my loving mother and siblings.

ACKNOWLEDGEMENTS

I appreciate and thanks the Almighty God for His guidance and faithfulness throughout the course of this study. My profound thanks and gratitude to my Supervisor, Prof. O. D. Jimoh, for his exceptional patiece and guidance through constructive advice and comments. Also to Prof. A. A. Okhimamhe, Director of WASCAL CC&ALU programme in FUT Minna who put all of her effort for my successfully acquisition of NiMeT data and encouragement. I would want to appreciate Mr. Isaiah Dr Saratu Usman Ibrahim for her assistance during course of this work. My appreciation also goes to WASCAL, CC&ALU FUT Minna staff for their understanding and assistance. My profound acknowledgement go to Prof. A. Amedkudzi and Miss Marian Osei of the Department of Physics, College of Science in Kwame Nkrumah University of Science and Technology for their assistance and guidance in understanding the Soil and Water Assessment Tool (SWAT) model calibration and validation. I will also want to express my deepest gratitude and thanks to Prof K. Ogunjobi, Dr. V. Ajayi and the entire staff of West African Climate System Centre in Federal University of Technology, Akure for their kindness, hospitality and provision of CORDEX data for assessing climate change impact in this work.

Also, I want to express my sincere gratitude to my colleagues and friends WASCAL Batch C – 2017 students; Miss Susan O. Simon, Mr. Saberma D. Ragatoa, Mr. Paul M. Iboko, Fafa O. Cham, Miss Lucette Adet, Mr. Sanoussi M. Sani, Mr. Gildas M. L. Guidigan, Mr. Charles L. Sanou and Mr. Sidibe Mohamed for their kindness and continuous support and assistance towards the completion of this work.

Finally, I also like to thank the Vice Chancellor Federal University of Technology Minna, and his management for offering enabling learning environment for the success of the programme. My sincere appreciation goes to the Federal Ministry of Education and

Research (BMBF) and West African Science Service Centre on Climate Change and Adapted Land Use (WASCAL) for providing the scholarship and financial support for this programme.

ABSTRACT

This study assessed the climate change impacts to streamflow and energy production in Shiroro Hydro power dam, located in a Guinean savannah zone in Niger State, Nigeria. Rainfall (1981-2015), streamflow (1990-2014), temperature (minimum and maximum) (1981-2015) data were collected from Nigeria Meteorological Agency (Nimet) and homogenisation test performed on the data using RHtestsV4. The trend in the data was evaluated using the Mann-Kendall and Sen's slope techniques. Assessment of streamflow was done by utilising the Soil and Water Assessment Tool (SWAT). Remote Sensing datasets such as Digital Elevetion Model, FAO soil map and Moderate Resolution Imaging Spectroradiometer (MODIS) land cover were utilised in ArcSWAT to set up the watershed. Climate Forecast System Reanalysis (CFSR) was downloaded and served as the climate datasets for forcing the SWAT model. Streamflow data obtained were divided into two with the first part used for calibration and the other part for validation of the watershed model. Downscaled NCC-NorESM1-M with WRF model output (precipitation, maximum and minimum temperature) under RCP 4.5 and 8.5 scenarios were extracted for the study area and streamflow simulated for the projected data in ArcSWAT. A stochastic dynamic model was employed to assess climate change impact on hydropower generation using the simulated output from the SWAT model. The results from the trend test showed existence of positive trend in both precipitation and temperature (average temperature) for Kaduna and Zaria whilst Minna and Jos indicate presence of negative trend in average temperature with Jos precipitation showing no significant trend and Minna precipitation series revealing a positive and significant trend. The calibration results of streamflow were unsatisfactory for R^2 = 0.51 and NSE=0.43 whilst PBIAS = -2 was very good. The uncertainty criteria of the model p-factor was 0.79 and r-factor 1.27 which were within the recommended range. The R^2= 0.79 and NSE= 0.77 and PBIAS = 15 values were good during the validation period with p-factor = 0.77 and r-factor = 0.77. Streamflow increased significantly from the baseline period (1990-2014) when compared with the projected future scenarios for both RCP 4.5 ad 8.5. Generally, energy production were observed to increase alongside revenue generation in the future but reliability of the plant was below the acceptable 0.75 reliability.

Table of Content

LIST OF TABLES

LIST OF FIGURES

LIST OF ABBREVIATIONS

ACF	Autocorrelation Function
AEJ	African Easterly Jet
AFWA	Air Force Weather Agency
AGCM	Atmospheric Global Circulation Model
CFSR	Climate Forecast System Reanalysis
CORDEX	Coordinated Regional Downscaling Experiment
DEM	Digital Elevation Model
FAO	Food and Agricultural Organization
FSL	Forecast Systems Laboratory
GCM	Global Climate Model
GCS	Geographic Coordinate System
GIS	Geographical Information System
HRUs	Hydrological Response Units
IRENA	International Renewable Energy Agency
IPCC	Intergovernmental Panel on Climate Change
ITD	Inter Tropical Discontinuity
LULC	Land use and land lover
MODIS	Moderate Resolution Imaging Spectroradiometer
NASA	National Aeronautics and Space Administration
NCEP	National Center for Environmental Prediction
NIMET	Nigeria Meteorological Agency
NOAA	National Oceanic and Atmospheric Administration
OGCM	Ocean General Circulation Models
PACF	Partial Autocorrelation Function
PET	Potential Evapotranspiration
RCM	Regional Climate Model
RCP4.5	Representative Concentration Pathway Realistic Scenario
RCP8.5	Representative Concentration Pathway Pessimistic Scenario

RH	Relative Humidity
SCS	Soil Conservation Service
SRES	Special Report on Emissions Scenarios
SRTM	Shuttle Radar Topography Mission
SSS	Shared Social
SWAT	Soil and Water Assessment Tool
TEJ	Tropical Easterly Jet
USGS	United States Geological Survey
UTM	Universal Transverse Mercator
WACS	West Africa Climate System
WASCAL	West Africa Science Service Centre on Climate Change and Adapted Land Use
WGS 84	World Geodetic System 1984
WMO	World Meteorological Organization
WRF	Weather Research and Forecasting Model
WRI	World Resource Institute

CHAPTER ONE

1.0 INTRODUCTION

1.1 Background to the Study

Renewable energy options have become critical to the mitigation of climate change as they provide alternative sources to energy. Renewable energy sources are the primary and clean sources of energy. Fourteen percent (14%) of the energy demand of the world are satisfied by renewable energy sources, such as geothermal, hydropower, solar, biomass, wind and marine energies (Panwar *et al.*, 2011). The use of renewable energy has widely been accepted as a decarbonizing option of energy and also because of its ability to replenish itself. World Resources Institute (2017) established that the energy sector accounts for about 72% of all global emissions of greenhouse gases in 2013. Increasing twice the percentage of renewable energy in the power generation market by the year 2030 could mitigate half of the global required emissions reduction level and with improved energy efficiency can bring down the global average rise in temperature to the targeted value of below 2 °C which will avert the incidence of catastrophic climate change (IRENA, 2015).

Advancements have been made in the hydropower technologies since its inception and therefore makes it a mature technology. Water utilised by hydropower installations fluctuate temporally. Nonetheless, the manageable output delivered by hydropower facilities that have reservoirs can be utilised to satisfy demands of electricity during peak hours and help to balance electricity systems that have large quantities of variable renewable energy generation. Some hydropower dams have multipurpose functionality as they are utilised for supply of energy, portable water, navigation and drought control, irrigation purposes and flood control.

Hydropower is an importance source of renewable energy in the world which supplied 16.4 % of global power supply in the year 2013. Hydropower have become very important to the worlds national pool of energy sources with an increase in the development activity in the past decade and approximately satisfying 1000 GW of the world's energy demand from total installed capacity with 2013 alone recording 40 GW of installed capacity (World Energy Council, 2015). In Nigeria alone, hydropower accounts for 16 % of the total energy capacity installed as at the year 2014 (Let *et al.,* 2015). Nevertheless, hydropower facilities are vulnerable to climate change impact and affect this affects power generation. It is important for vulnerability assessment to climate change vulnerable measurements is important to be quantified in order to protect existing hydropower. The operation of hydropower reservoirs often designed for additional application and uses, for example, flood control, irrigation, drought control, navigation, and portable drinking water, in association to the supply of energy. Despite the significance of hydropower, Chiang *et al.* (2013) iterated that hydropower is associated with some social, environmental and economic impacts that have to do with its harnessing for energy. In terms of social and economic impacts, construction of dams with reservoirs have been associated with the relocation of communities from their ancestral homes and affecting their livelihoods. In terms of environment impacts, natural vegetation are destroyed to during the dam construction and as a result of flooding after impoundment. The cost of establishing hydropower power installations is enormous and the economic viability in the short term is not lucrative (does not provide high returns in short term operations) for private sector to engage in it (Mukheibir, 2007).

The key challenge is to determine how dams are best able to contribute to African countries growth when obtaining reliable and sustainable sources of water, food and energy security, at the same time, concurrently avoiding harmful environmental impacts

and mitigating adverse impacts on the environment as far as possible (McCartney and Girma, 2012). Hydrological resources are likely to be impacted by the changing effect of temperature and precipitation in a particular location. Therefore, scientific research is required to assess the trend of hydrological and climatic processes and its impacts on power generation in the Shiroro catchement area. This will better enhance our understanding of the likely effect of climate change on hydropower generation and will further aid in the adaptation approaches to cope with its adverse effect.

1.2 Statement of the Research Problem

Energy is one of the key factors that drives development. In developing countries such as Nigeria, access to energy (such as electricity) is major constraints in their development and effort targeted to reduce poverty (Oyedepo, 2012). Demand for electricity is expected to increase in line with continuous population growth, infrastructure development and access to technology in Africa. In Nigeria, Oil and Gas, hydropower, biofuels and waste, and coal form part of the current energy sources contributing power to the National Grid and individual homes. Aside hydropower which is considered environmentally friendly, oil and gas are not environment friendly and are seen as one of the major contributors to carbon emission in most countries. Thus, making hydropower a crucial part in the country's effort to reduce carbon emission in the atmosphere as a way of climate change mitigation.

Nonetheless, the impact of climate change on hydrological resources and hydropower reservoirs has not been fully explored to reduce uncertainties on a local scale. A number of studies have attempted to enhance knowledge on the impact of climate change on hydropower and runoff both globally and on a regional scale. Hamududu and Killingtveit (2012) investigated the impact of climate change on hydropower facilities globally and

discovered that there exist variations (decrease/ increase) in predictions of hydropower generations across regions and within regions. Studies such as Mukheibir (2007), Schaefli (2007), Chaing *et al* (2013), Oyerinde *et al.* (2016) and Ravazanni *et al.* 2015 have all assessed the impact of climate on hydropower generation on a local scale worldwide. Their findings acknowledge the importance of climate change impact assessment on hydropower dam on local scale as there may exist underlying physical processes which may respond to changes in climate uniquely. The uncertainties associated with climate change impact prediction still remains a challenge for stakeholders to adequately adapt or mitigate these impacts. Currently, there are handful of research works in Nigeria which have explored impact of the changing on hydropower generation. Cervigni *et* al. (2013) assess climate change impact on dams (hydropower dams, irrigation and water supply dams) in Nigeria using historical runoff data and outputs of global circulation models (GCM) in Soil and Water Assessment Tool (SWAT) model whiles Oyerinde *et al.* (2016) also performed impact assessment on Kainji Dam Hydro-electric dam using hydromad model to estimate streamflow. There exist little or no research works on the assessment of climate change impact on Shiroro dam which this study aim to address.

The changing trends in rainfall and temperature present the challenge to determining how these changes influence hydropower generation in Nigeria. Understanding the amount of runoff that will be generated in future will be crucial in management of the dam. Physically based hydrological model when coupled with Regional Climate Models will go a long way to better help us comprehend the effect of climate change on runoff generation in river basins.

1.4 Aim and Objectives

The aim of this study is to assess the impact of climate change on the future energy generation at Shiroro dam. The specific objectives of the study are:

1. Assess the trends in climate (temperature and precipitation) of the study area.
2. Assess changes in the streamflow.
3. Assess the future power generation by modelling hydropower dam operation policy using Stochastic Dynamic Modelling.

1.5 Research Questions

1. Is climate change or variability evident in the basin?

2. What are the effects of rainfall and temperature trends from 1990 -2014 on the runoff generation in the Shiroro Catchment area?

3. What are the projected trends in the rainfall and precipitation of the river Shiroro Dam Catchment under RCPs 4.5 and 8.5?

4. What are the changes to streamflow in the Shiroro Dam Catchment as a result of these projected trends?

5. How would power generation be affected as a result of changes in streamflow?

1.5 Justification of the Study

Hydropower still remains one of the most important energy source (United State Geological Survey (USGS), 2016). Climate Change is anticipated to impact hydrological cycle and resources in the world. This will directly affect the utilisation of hydrological resources for hydropower generation in West Africa. There are varying prediction of the climate change impact on hydrological resources and hydropower generation in West

Africa and Nigeria in particular. This makes it imperative to evaluate the effect of climate change on hydropower schemes. Shiroro Hydro-Electric plant station has an installed capacity of about 600 MW with an actual generation capacity of 350 MW of power as of May 2015 (Ley *et al.,* 2015). Making it an important source of energy in Nigeria. Several researchers have stressed on the importance of applied scientific research into the evaluation of the impact of climate change on hydroelectric facilities. The importance of hydropower for power generation and contribution to Greenhouse Gas mitigation, coupled with climate change impact on its activities necessitate this study.

1.6 Scope and Limitation of Study

The study is limited to Kaduna River Basin with the Shiroro reservoir water catchment area as the main focus. The aim of this research is to assess climate change impact on hydropower dams. The data used for this research are secondary data obtained from various agencies. Climate Modelling could not be performed due to the short duration of the research period. For this reason, climate model data was obtained from CORDEX Coordinated Regional Downscaling Experiment. The research focusses on the impact of climate change on runoff generation and its contribution to energy generation. Other aspects such as impact of sediments and land use were not considered in this research due to availability of data for analysis.

1.7 Study Area

1.7.1 Kaduna River Basin

Kaduna River basin (Figure 1.1) is an important river basin in Niger State and Kaduna State as a result of its influence on agriculture activities (crop production, fisheries and animal production) water supply and electricity generation). It forms part of the lower

Niger River Basin and specifically located in the Niger Central hydrological area of Nigeria. There exist a total of eight (8) hydrological areas in Nigeria (Figure 1.2), namely Niger North, Lake Chad, Niger Central, Eastern Littoral, Western Littoral, Niger South, Upper and Lower Benue hydrological areas (Cervigni *et al.*, 2013). Subsequently, five out of these eight hydrological areas forms part of the Lower Niger Basin comprising of Niger North, Niger South, Niger Central, Lower Benue and Upper Benue hydrological areas. The River Kaduna is a tributary to the Niger River in Nigeria and it flows into the Niger River between Baro and Jebba (Grove, 1972). The source of the Kaduna River originates from northwest of Jos (Grove, 1972 and Jimoh & Ayodeji, 2003). The direction of flow of the river is westerly and south westerly after it has drained the Jos Plateau at an elevation of 1500 m passing through Kaduna Town and thereafter into the Niger River (Jimoh & Ayodeji, 2003). The tributaries to the Kaduna River are the Dinya and Sarkin River to the left side and the Tubo River on the right (Jimoh & Ayodeji, 2003).

1.7.2 Shiroro Dam and Shiroro Dam Catchment

For the purpose of this study, Shiroro dam was selected for the assessment of streamflow generation of hydropower. The dam is situated in the basin on coordinate latitude 09^0 58'N and longitude 06^0 50'E using the Geographic Coordinate System with WGS 84 datum (Suleiman & Ifabiyi, 2015). The construction of Shiroro Hydroelectric Dam was completed in 1989 (Ley *et al.*, 2015). The main purpose of the dam was for the generation of electricity. The Shiroro Hydroelectric dam was constructed at Shiroro village by the impounding of the Kaduna River at Shiroro Gorge in Niger State (Jimoh &Ayodeji, 2003). The Shiroro dam reservoir (Figure 1.1) has a lake basin area of about 320 km^2 with a maximum storage volume of 7 billion cubic metres and the maximum length of the lake is 32 km (Suleiman and Ifabiyi, 2015). The Shiroro reservoir dam has an installed

capacity of 600 MW, have four Francis turbines which contributes 150 MW each (Adie *et al.*, 2012). The part of the Kaduna River Basin contributing streamflow to the Shiroro Dam is referred to as the Shiroro catchment. Large percentage of Shiroro Catchment (Figure 1.1) area lies in Kaduna State of Nigeria with a small part in Niger State where the Shiroro Hydroelectric plant is situated.

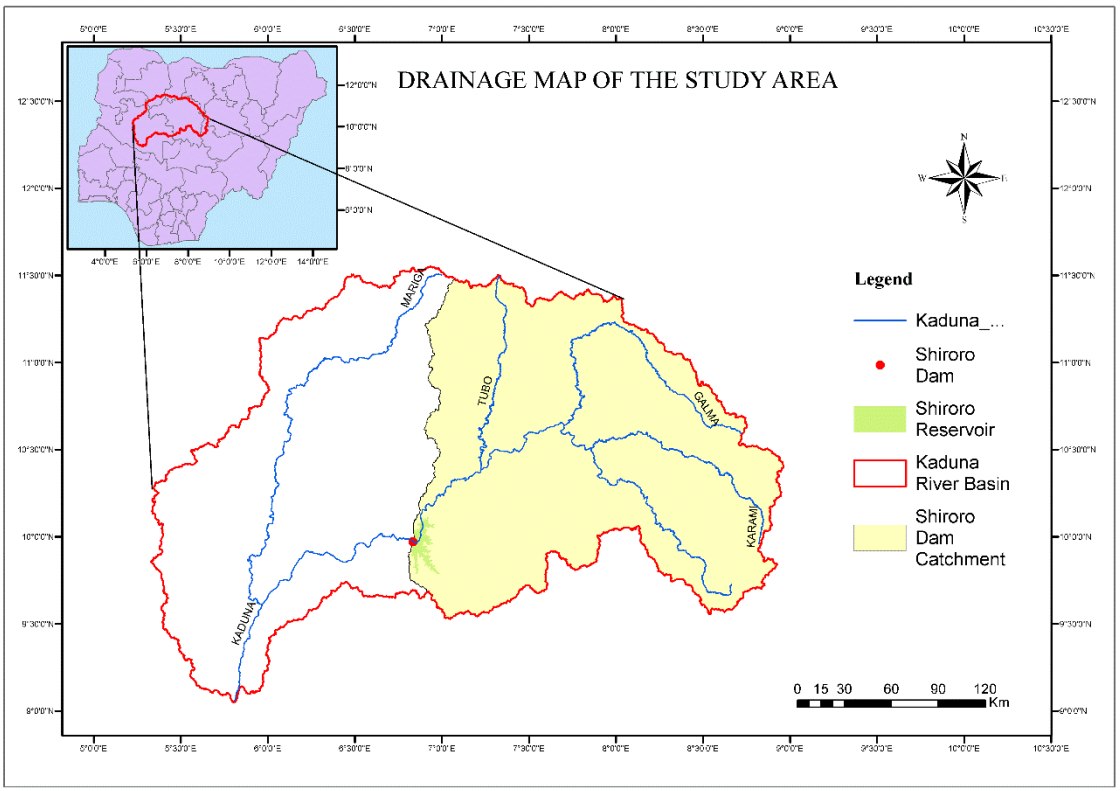

Figure 1.1. Nigeria map showing the Shiroro Catchment, Shiroro Reservoir and Kaduna River Basin

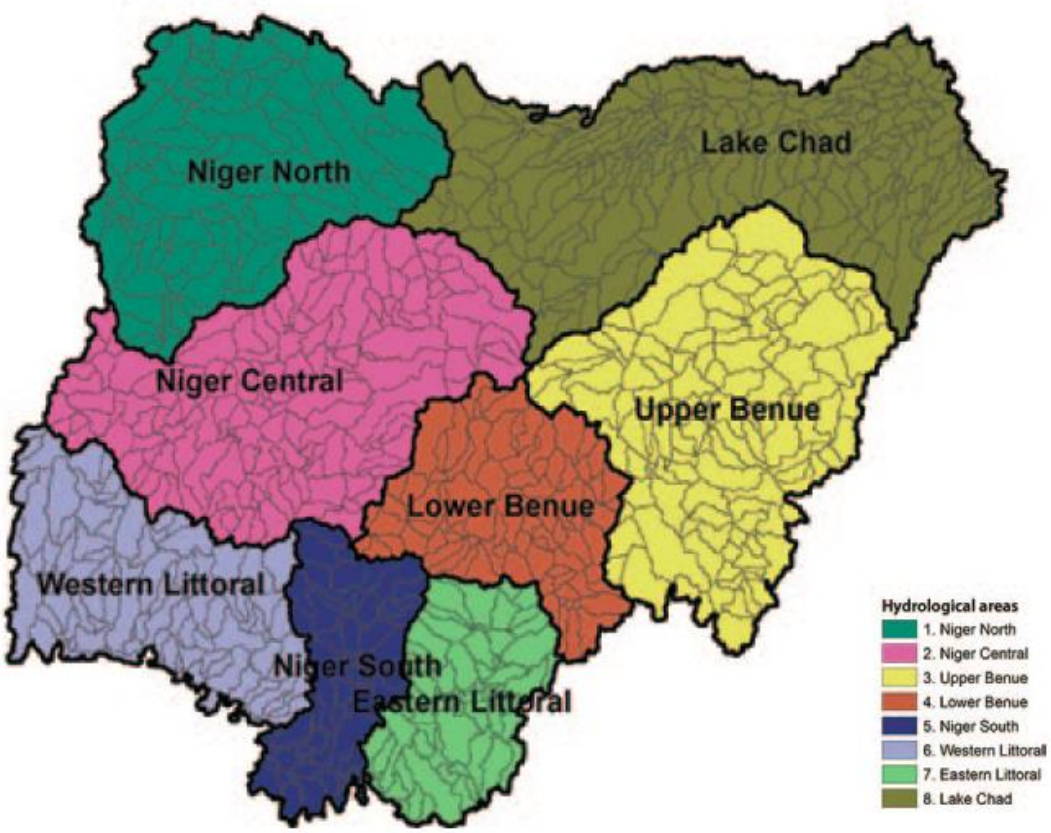

Figure 1.2. The hydrological areas of Nigeria. The study area falls in the region highlighted in pink, the Niger Central Hydrological area. (Source: Cervigni et al., 2013)

1.7.3 Climate

Shiroro is located in Niger State and the location has similar climatic condition. Niger State climatic conditions comprises of dry and wet season. Maximum average temperature in the dry season are about 38 ^{0}C as recorded between March and June (Niger State Bureau Statistics (NSBS), 2011). Niger State annual rainfall amount vary from a maximum annual amount of 1543 mm to a minimum annual rainfall of 800 mm, with the onset occurring in May and the cessation in October. Low monthly rainfall amount is recorded in March and April. The annual amount of rainfall in Kaduna ranges from 790 mm to 1658 mm with an annual average of 1210 mm for a period of 35 years from 1981 to 2015. The number of days that recorded rainfall (Rainy days) in the year ranges from

172 days to 212 days (NSBS, 2011). The dry season occurs from November to March. The lowest day recorded temperature is about 21°C. Seasonal climate event such as rainfall pattern is influence by the movement of the Intertropical Discontinuity (ITD), Tropical Easterly Jet (TEJ) and the Africa Easterly Jet (AEJ) (Omotosho and Abiodun, 2007; Akinsanola and Ogunjobi, 2014). The inland movement of the West African Monsoon (WAM) is associated with the onset of rainfall in West Africa. The hydrology of River Kaduna has only one main period of peak flow, which falls between August and September. (Adie *et al.*, 2012).

1.7.4 Vegetation and Soil

Majority of the catchment area of the Kaduna River Basin lies predominantly in Kaduna and Niger State in Nigeria. The vegetation of the entire catchment is guinea savannah (Jimoh & Ayodeji, 2003). The soils identified in the catchment are Ferric Luvisols, Gleyic Luvisols, Luvisols Arenosols, Ferric Acrisols, Orthic Acrisols, Lithosols, Lithic Ferric Luvisols, Lithic Chromic Cambisols, Luvic Arenosols and Lithic Chernozens according FAO world soil map. The predominant soils identified were Ferric Luvisols covering 74 % and Gleyic Luvisols covering 16 % of the catchment area.

1.7.5 Topography and Drainage

Niger state and Kaduna State forms part of West African belt of African Precambrian base which are underlain by Sedimentary rocks (Cretaceous-Tertiary rocks) and Basement Complex rock origins (Adelana *et al.*, 2008; Obada and Oladejo, 2013 & Omanayin and Ogunbajo, 2016). Figure 1.2 illustrate the geology of Nigeria. The Precambrian base rocks are the major rocks which underlie the North-Central area of Nigeria where the Shiroro Catchment is found including the Jos Plateau (Olugboye,

2008). These basement complex rocks comprise of ancient granite, migmatite-gneiss, quartzite (Andersen *et al.*, 2005), schists, phyllites and banded iron formations some of which are of metavolcanic or metasediments origins (Obada and Oladejo, 2013). These rock formations are characterized by limited aquifer or groundwater potential with some exceptions in weathered zones (Andersen *et al.*, 2005 and Obada and Oladejo, 2013). There also exist Jurassic younger granites present in the region of the Jos Plateau. The Jos plateau region and adjacent Plateau areas are sites where Tertiary- Volcanic Rocks which are interbedded with alluvial sediments are found (Dan-Hassan, 2016).

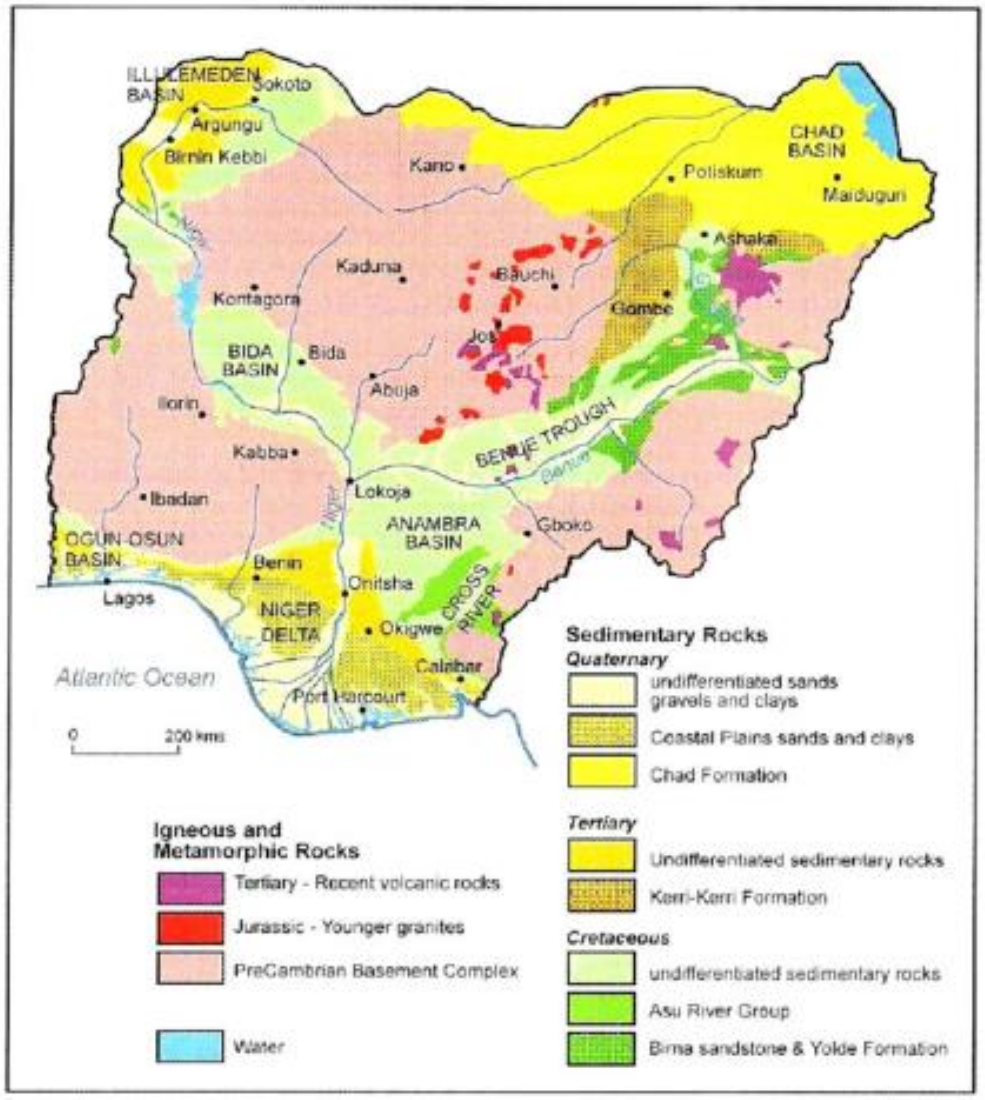

Figure 1.3. The Geologic Map of Nigeria (Sourced: Adelana *et al.*, 2008)

CHAPTER TWO

2.0 LITERATURE REVIEW

2.1 Conceptual Framework

2.1.1 Climate Change and runoff influence on Hydrological Resources

Climate defined by World Meteorological Organization (WMO) as "the measurement of the mean and variability of relevant quantities of certain variables such as precipitation, temperature or wind over a period of time from months to thousands or millions of years. Classical period accepted is 30 years" (WMO, n.d.). It defines the mean weather of a location over an extended period usually for a 30-year period. Climate change is a phenomenon which directly or indirectly affect both the socio- economic environment and the natural environment globally. Enete and Amusa (2010) acknowledged that climate change is perhaps the most crucial environmental threat thwarting efforts to achieve a world without hunger in all forms (such as extreme hunger), diseases and poverty in Africa.

Climate change is defined as "the change in the state of the climate that can be statistically tested or identified by changes in the mean and or variability of its properties that persists for an extended period typically decades or longer (Intergovernmental Panel on Climate Change" (IPCC), 2007a). Climate change results in the development of extreme weather events such as hurricanes, flooding, heatwaves and drought which are evident. National Aeronautics and Space Administration (NASA) (2016) attests to the fact that these events manifesting today had been predicted by scientist as the effect of global warming in the past. This is in agreement with (IPCC, 2007a) AR4 report which deduced that, the volume of findings of published works in general predicted that the net costs of destruction

imposed by climate change are going to be substantial and the adversely affect likely rise with time.

The impact of climate change on hydrological resources directly affects its utilization for power generation. The presence of Greenhouse gases in the atmosphere are the key drivers of climate change. Carbon dioxide concentrations have increased significantly in the past decade (Keeling *et al.,* 2005). The hydrological cycle has intimate relationship with changes in atmospheric radiation balance and temperature. The climate change effect on changes in the hydrological cycle, is estimated to affect the timing, distribution and quantity of water resources (Goulden *et al.,* 2009). Bates *et al.* (2008) confirms that climate change is going to impose increase amount of pressure on the water availability and demand in Africa. They also projected that by the year 2025 nine countries of Southern and Eastern Africa, water availability will dwindle to amounts less than 1000 m^3 per person per annum and twelve countries are exposed to limited water availability levels of 1000 m^3 – 1700 m^3 per person per annum, and the most vulnerable people at risk of water approximating to 460 million people with majority originating from Western Africa.

Risk on water resources imposed by climate change impact are without doubts crucial to the development of hydropower and hydrological resources in general. Some of these impacts rely on the changes in the quantity and period of river runs, increased reservoir and surface water bodies evaporation as a result of variation in the amount and frequency of precipitation and increase in global average temperature will affect the development of Hydropower, hydrology infrastructure installations, the management practices and the return on investments of investors in the hydro sector of economies (Kundzewicz *et al.,* 2007; Bekoe and Logah, 2013; Beilfuss and Triet, 2014). Arguably, many literatures have establish that climate change will impact water resources and undeniably the development

of hydropower sources. Many countries in Africa such as Ghana have had to ration power generated from their hydropower installations as a result of hydrological drought impact due to variation in the duration and intensity of precipitation received over a period of time (Bekoe & Logah, 2013). Eastern African countries such as Tanzania and Kenya, have also experienced electricity shortages from their hydropower installations due to hydrological drought (Mukheibir, 2007). Due to these impact, governments' dependence on coal, fossil fuel and natural gas in are on the increasing as witnessed currently in Ghana as the Akosombo dam had spells of under-operating (Gnansounou *et al.*, 2007). Changing climate has made traditional analysis of historical rainfall and river flow data for feasibility study of hydroelectric potential substantially unreliable (Milly *et al.* 2008).

Beilfuss and Triet (2014) agreed with the findings of World Commissions on Dams(2000) reports which deduced that the potential impact of climate change on global hydropower installations exist in at least these five important ways:

1. Climate change changes the reservoir inflows on a seasonal and annual basis due to reduction or increase in the runoff of the basin and altered frequency and duration of droughts conditions and affecting energy generation capacity;

2. Increase in surface evaporation as a result of increased in temperature, especially from upstream reservoirs and floodplains, reducing energy generation capacity;

3. Varied timing of wet season flows, especially delayed onset of rainy season affecting the dam operations and downstream release patterns.abuj

4. Increase in extreme flooding events (inflows) event as a result of higher rainfall intensity and more frequent intense tropical cyclones and storms, affecting dam safety and operational rule curve designed to prevent over-topping;

5. Increase in sedimentation load to reservoir, resulting from higher rainfall intensity and associated erosion resulting in reduced reservoir capacity (lifespan) and water quality.

2.1.2 Hydropower Dam

Hydropower is referred to as the energy harnessed from moving water utilising the influence of the force of gravity as water moves from higher to lower elevation usually through turbines for electricity generation (IPCC, 2007b). It also utilises the kinetic energy of water by virtue of its difference in elevation. Hydropower projects includes run-of-river, dam projects with reservoir and in-stream projects and covers a continuum of project scale (IPCC, 2011). Advancements have been in the hydropower technologies since its inception and therefore makes it a mature technology. Water utilise by hydropower installations vary temporally. However, the controllable output provided by hydropower facilities that have reservoirs can be used to meet peak electricity demands and help to balance electricity systems that have large amounts of variable Renewable Energy generation. Hydropower are utilised for supply of energy, drinking water, flood and drought control, irrigation purposes and navigation. The operation of hydropower reservoirs often reflects their multiple uses, for example, drinking water, irrigation, flood and drought control, and navigation, as well as energy supply.

Despite the significance of hydropower, Chiang *et al.* (2013) iterated that hydropower is associated with some social, environmental and economic impacts associated with its harnessing for energy. The cost of establishing hydropower power installations is enormous and the economic viability in the short term is not lucrative (does not provide high returns in short term operations) for private sector to engage in (Mukheibir, 2007).

2.1.3 Global Climate Models and Downscaling Techniques

Global climate models outputs provide an efficient and useful means in assessment and impacts studies of climate. Global Climate Models (GCMs) are numerical models which are used to simulate physical processes in the earth's atmosphere, ocean, land surface and cryosphere. These models run differential equations, laws of physics, chemistry and fluid motion which are governing the physical processes. GCMs are very important to climate change studies and impact studies as they model global climate and the response of global climate to greenhouse gas forcings. Thus GCMs are developed for the prediction of future climate changes based on greenhouse gas emission and other aerosols concentration in the atmosphere which are defined in emissions scenarios (IPCC 2000, Fiseha *et al.*, 2014). General Circulation models that simulate the earth's atmosphere are called Atmospheric General Circulation Model (AGCM) whiles Ocean General Circulation models (OGCM) simulate the processes of the ocean. Considering the long term interaction (such as the high heat capacity of the ocean and its ability to transfer heat around the Globe) between the ocean and atmosphere significance to climate, AGCM and OGCM are coupled together in assessment of climate during modelling to account for the impact of these slow ocean processes in long term simulations (Baede *et al.*, 2001). The high heat capacity of the ocean influences the hydrological cycle of the Earth's climate system through the transfer of heat and matter into the atmosphere and serves as a store for carbon dioxide, thus coupling aids in accounting for the climate system's energy budget (Baede *et al.*, 2001).

In climate change impact studies and assessment, GCMs and its output are crucial in analysing projected future climatic conditions based on scenarios such as Special Report on Emissions Scenarios (SRES), Representative Concentration Pathways (RCP) and Shared Socio-economic Pathways (SSS). Many authors (Cuo *et al.*, 2013; Pervez and

Henebry, 2014; Pervez and Henebry, 2015; Cervigni *et al.*, 2013) have utilised GCM output for climate change impact assessment on health, hydrology, hydropower, heatwaves, temperature stress on crops, droughts and flooding. GCM model outputs are coarse spatially and therefore their utilisation requires the outputs to be downscaled before employed for impact assessment on regional scale. The downscaling techniques employed are the statistical downscaling and dynamic downscaling (Lafaysse *et al.*, 2014; Willems and Lloyd-Hughes, 2016). GCM outputs comes in varieties of different spatial and temporal resolutions which fails to realistically represent variables of interest in scales suitable for hydrological models during water resources climate vulnerability and impact assessment (Layfasse *et al.*,2014). The difference in GCM models are greater than the difference between the RCM when downscaled (Beilfuss & Triet, (2014), which makes RCMs accounts for the high uncertainties in the prediction rainfall unlike GCMs in West Africa (Gbobaniyi *et al.*, 2014).

2.1.4 Hydrological Modelling

Hydrological modelling have become unarguably one of the efficient tools for assessing hydrological resources and river basin management Adeogun *et al.*,2014). Hydrological model can be considered as a mathematical representation of a hydrological cycle of an entire river basin or a part of it. According to (Cunderlik and Burn, 2003), hydrological models can be categorised in to three key categories, namely stochastic models, empirical and symbolic models. Hydrological models can also be grouped into semi-distributed or lumped.

2.1.4.1 Soil and Water Assessment Tool (SWAT) and Climate change

The Soil and Water Assessment Tool (SWAT) is a physically based semi-distributed simulation model which can simulate the effects of changes in land use and land cover (LULC) and management practices on drainage characteristics of watersheds which have variable land use, soil and management practices over extended time periods and mainly as a tactical decision planning tool (Neitsch *et al.,* 2005). The model has been utilised extensively in the world; in Africa, Asia and the United State. In Africa, SWAT has been utilised in hydrological related prediction in countries like Egypt, Sudan, South-Sudan, Ethiopia, Eritrea, Ghana, Nigeria, Uganda, Tanzania, Kenya, Burundi, Rwanda and DR Congo (Adeogun *et al.,* 2014). Studies like Schuol *et al.* (2008) utilised the SWAT model to investigate the surface and ground water changes on a regional and continental scale in Africa. The model application increased in dependability and consistency and has gained worldwide audience in its usage because of its usefulness in studying different aspects of hydrological system (Akpoti, 2016). Semi-distributed physically based models like the SWAT are well established models for studying the impact of land use practices on water, agricultural chemical yields, sediment in complex watersheds. SWAT model can be coupled with Global Climate models to make climate prediction. The model has proven useful in the impact assessment study of climate change on hydrological processes using downscaled and bias corrected data from projected Global Climate Models or Regional Climate Model outputs in studies such as (Cervigni *et al.*, 2013) where either climatic variables (such as rainfall, temperature, relative humidity, solar radiation) are utilised in the impact studies.

Modelling climate change impact on individual dams is important as spatial differences affect the magnitude of impact on hydropower (Mukheibir, 2007). This study explores

the application of bias corrected Regional Climate Model data under climate scenario forcing 4.5 as input in SWAT model to model changes in streamflow in the future.

2.2 Review of Related Studies

Mukheibir (2007) studied the potential climate change impact on large-scale hydropower schemes in Zambezi basin and Congo basin located in the Southern Africa as the authors study area. The study was based on the work and results obtained by Tadross *et al.* (2005). Tadross *et al.* (2005) downscaled a period of ten years for control and ten years for future (2070-2090) Southern Africa climatic conditions from two regional climate models (RCMs) nested in HadAM3 general circulation model and forced with A2 SRES emission scenario (climate change storyline scenarios from IPCC).

This produced results for average surface temperature and early and late summer rainfall for the periods. The author attested that by 2000 in the twenty-first century, there were 5 occurrence of years with warmer conditions in Africa since the year 1988 with the 1988 and 1995 being the years which were warmest among the 5 years with warmer conditions. The 2070 predictions for Southern Africa along the coast was showed 1 °C increase in temperature and an increase ranging from 3-5 °C inland of the coastal mountain. The result for the simulation changes for 2070 in seasonal rainfall which was predicted by the regional climate models forecast for of the sub-continent and the tropical western side indicates dryer conditions the specific months, October to November and for January to March. The RCMs show that towards the western parts of the tropics, precipitation will decrease below the baseline amount and precipitation increase towards the eastern and the south-eastern parts which were in agreement to the findings of Hewitson and Crane (2006) (Mukheibir (2007). The analysis implied that changes in precipitation and temperature poses risk to current the present hydropower installations in four (4) major

ways, such as reduction in generated runoff during droughts, losses through evaporation of surface water, and increased runoff in wet years and siltation deposits. The Congo basin was less prone to evaporation by temperature rise than the Zambezi basin since its catchment has more humidity than Zambezi basin. Flooding and rainfall in both Zambezi and Congo basin will increase leading to siltation and deposition on hydroelectricity installations. The author concluded that further investigation must be carried on to assess the potential impact on the individual catchment sites.

The study utilised RCM models which have higher resolution than Global Climate Models (GCM) and are more specific and closer to actual climate statistics of the place (African Climate Policy Centre, United Nations Economic Commission for Africa, 2011). Although the study discovered that the Congo basin will be less affected by climate change, Strzepek and McCluskey (2006) proved an adverse impact of climate in Southern Africa resulting in the reduction in streamflow.

Schaefli *et al.* (2007) sought to address the challenges of incorporating a large range of scenarios for potential climate change impacts and quantification of related modelling uncertainties on the basis of water resources. They utilised four models which were water management model, hydrological model, glacier surface evolution model and models for generation of local scale meteorological time series under climate change scenario in a simulation tool for the Swiss Alps hydropower plant that uses discharge of glacierised catchment. Meteorological time series data was obtained for 1961- 1990 as control period and future climate scenarios for period 2070-2099 using RCMs for a range of climate change scenarios for to obtain input values such as daily mean temperature, precipitation and evapotranspiration and calibration made for these values using a meteorological station in the catchment. Penman-Monteith technique was adopted in calculating daily evapotranspiration. The daily discharge was simulated by a hydrological and glacier

surface model developed by Schaefli *et al.* in 2005. They (Schaefli *et al.* in 2005) also developed a deterministic-stochastic model of water release (management model); the deterministic side dealing with release based on summer and winter demand and stochastic simulate variation in daily release based on electricity demand in the market. The modelling uncertainties of each modelling type (in each of the four model) were characterized and quantified separately. Monte Carlo simulations was used to simulate the overall modelling uncertainties of the behaviour of the system for both the control and future time periods.

The study depicted that there will be an increase of 3.4 °C in the mean daily temperature and the minimum simulated mean temperature will be -2.9 °C suggesting the future temperature was strictly higher than the temperature of the control period. The evapotranspiration simulated was higher in the future value than the control. The precipitation distribution varied with some little changes from the control over the future period (precipitation slightly decreases in the future). Thus the increase in temperature and reduced precipitation connoted increase in glacier melting and increasing in vulnerability of release (average difference between planned and actual release through turbines). The water through spillage and overtopping was negligible. The study concluded that the management system was able to handle the changes imposed by climate change. Also a consistent methodology was developed for potential impact analysis that illustrate the statistical impact of climate change are significant.

Chiang *et al.* (2013) did a similar research on the potential climate change impact on hydroelectricity generation on the Kaoping River using river discharge generation as a criteria in Taiwan. They utilised a hydrological model GWLF, while the simulated rainfall and temperature data were downscaled from four GCMs under emission scenarios A2 and B2 from IPCC. The findings portrayed that the range of discharge variations was -

10% to 82% in the wet season and -26 % to 15 % in the dry season. The researchers asserted that climate change had the potential to impact the discharge of the river. There were uncertainties in modelling as some GCM models predicted high annual rainfall whilst others predicted far less with uneven distribution of rainfall.

Bekoe & Logah, (2013) examined the effects of droughts on the operations of hydroelectricity generation in Ghana by analyzing the rainfall in the basin and lake (thus dam water levels at point of intake) water levels of the Akosombo dam and establish whether previous years of power crisis in 1943/84, 1997-98, 2003, 2006-2007 were as a result of hydrological drought. Rainfall data over a range between 1971 – 2007 from six meteorological stations in Bole, Kete-Krachi, Tamale, Yendi, Wa and Navrongo all in the Volta basin Catchment and the dam levels spanning 1970 to 2005 were collated for analysis. Analysis of rainfall, droughts and water levels were carried out to establish occasional water shortages in the crisis years and the resultant power rationing in those years was due to hydrological droughts. Thiessen polygon technique and probability of exceedance for rainfall were used in the analysis.

The study highlighted that 1983-84, 1992 and 2001 were actual drought years whilst 1977, 1988, 1993 and 2006 were nearing drought years. The year 2003 was not a drought year but proceeded after a series of drought years causing the shortfall in water in the reservoir. The studies also deduced that the return periods of droughts is 10 years and affirmed that droughts are major challenge on hydropower dams prompting power rationing.

Although the analytical approach was able to estimate the drought years as a result of the variations in the frequency and amount of rainfall received, some factors of the climatic system was not included in the analysis, such as temperature and its corresponding

evaporation effect on the catchment and the dam, the effect of wind. It appeared this method could not be used for future forecasting for evaluating scenarios of climate change in order to assess the dam's vulnerability.

Ravazzani *et al.* (2015) also examine climate change impacts on hydropower production in the Toce Alpine river basin in Italy. They sought out to quantify the influence of climate change on power generation of power plants situated in the Toce Alpine river basin. Analysis were performed using two time periods, which are 2001-2010 (past) and 2041-2050 (future). Two climate models RCMs were used, namely the REMO and RegCM3 was used for simulations of meteorological forcings and were driven by same global ocean-atmosphere-coupled model ECHAM5 using greenhouse emission scenario A1B which was the situation in 2001-2010. It used 27 nodes and 64 networks for hydropower system where nodes represented by intake and reservoirs, and further each characterized by inflow time series that described natural discharge. FEST-WB model is used to simulate continuous streamflow which computes flow routing, surface runoff, infiltration, snow and glacier dynamics and subsurface flow. Also, to evaluate how the management system and hydropower production are affected by climate change, simulations of three periods (2001-2010, 2011-2030 and 2031-2050). BPMPD solver was used in conjunction with best management value to compute the economic value.

Comparing of the findings from 2041-2050 to 2001-2010 (base year) from FEST-WB results driven by each, the REMO and that RegCM3, REMO recorded temperature rise and increased in precipitation of 1.3 K and 13 % respectfully, whilst RegCM3 recorded temperature rise and increased in precipitation of 1.1 K and 25 % suggesting an increased in evapotranspiration and discharge for all the durations of the flow curve. There was an increase in production in 2030-2050 in autumn from 2001-2010. Significant change in

the reservoir management was required deferring what Schaefli *et al.* (2007) discovered in the Swiss Alpine basin.

The catchment irrigation was not evaluated and the water utilised as drinking water was also made negligible as simulations were only steered towards power production.

Salami *et al*. (2011) investigated the influence of climate change impacts on water resources in the Kainji Hydropower Reservoir catchment. The data series collected were reservoir inflow, temperature, rainfall from the hydropower station. The researchers utilised statistical analyses techniques such as Mann-Kendall, for assessing the trend of the data reduction pattern methods and linear regression. The statistical significance was tested to determine whether the trends detected in each data series using Mann-Kendall and regression analyses were significant. The fluctuation in the each data series were examine using reduction pattern analysis over the period of analysis of the data series. Mann-Kendall test indicated a positive trends for rainfall and temperature indicating that these parameters have possibly increasing but the significance test demonstrated that only temperature was significant. The reservoir inflow had a negative but the trend was not significant indicating the possibility of reservoir inflow to reduce slightly over time and likely to be unnoticed. They concluded that infrastructure development upstream will account for the slight decrease in the reservoir inflow to the dam therefore climate change has a negative impact on hydropower generation.

Fuka *et al.* (2013) investigated the use of Climate Forecast System Analysis (CFSR) meteorological data as an alternative for conventional in situ data for hydrological watershed modelling. They examined the performance of CFSR data performance in the calibration and validation of SWAT physically based semi-distributed model against conventional in situ data which mostly does not adequately represent watershed processed

due to their low spatial resolution and may have inherent missing data values. The result indicated that CFSR (precipitation and temperature datasets) had a good performance in modelling hydrological watershed which was similar to utilising conventional In situ data for modelling the same watershed. The authors concluded that CFSR is suitable for forcing hydrological model with good performance equally as observed data or even better when ground stations are more than 10 km apart.

Oyerinde *et al.* (2016) worked to assess climate change impacts on the production of hydropower by Kainji hydroelectric dam in Niger River Basin, Nigeria and also account for uncertainties in modelling these changes. They estimated the runoff generated in the watershed which is flowing from upstream into the reservoir utilising hydrological model called Hydromad. Climatic input data of the model were obtained from a number of dynamically downscaled GCMs which are part of models used in CMIP5 by utilising a RCA regional climate model from the Rossby Centre. These data were used to simulate the inflow into the reservoir with two emission scenarios (RCP 4.5 and RCP 8.5) obtained from Africa regional downscaling experiment which are part of the CORDEX downscaling experiments. 2010-2035 and 2036-2100 was used as the near future and far future years respectively. The observed dam data from Kainji dam was utilised to generate a hydropower generation model to predict energy production of the plant in the future. IHACRES and ARMAX model were used to model the inflow to the reservoir. GCM were downscaled to a resolution of $0.45^{o} \times 0.45^{o}$ resolution with SMHI-RCA RCM within CORDEX-Africa regional downscaling experiment. Models were corrected. The study suggested that there would be increase in discharge flow to the reservoir resulting to increase in hydropower generation for most of the GCM data by both emission scenarios considered. Upstream rainfall and potential evapotranspiration will rise with reference to the base period due to climate change. Large uncertainties present in the amount of

deviations from normal conditions projected across eight downscaled general circulation models resulted from large inconsistencies related to precipitation simulations by RCMs in West Africa. However, the study did not capture other uncertainties such as the utilization and irrigation schemes and also the stochastic nature of dam operating rule.

The study was not able to include other uncertainties such utilization of the water for drinking water and irrigation. With increasing temperature, the amount of evaporation on the reservoir surface as a result of the reservoir surface area to volume ratio will affect the amount of water formed. A predictive model will be needed to predict changes in the management of the dam due to the increase discharged.

A predictive model will be needed to predict changes in the operating rule of dam due increasing or decreasing discharge due to effect of the changing climate. Furthermore, modelling climate change impact on individual dams is important as the spatial differences as a result of hydroclimatic condition of the dam location and dam design might affect the magnitude of the impact on hydropower.

Climate change future projections are based on models and their dependencies on models is important for the accuracy of the predictions. Regional models are generally accurate when used in modelling than GCMs in magnitude and even the direction of change, resulting in very low confidence in projections of future runoff for hydropower planning purposes. Multiple GCM models is required for modelling when they are primarily used or they have to be downscaled by RCMs. Prudhomme and Davies (2009) suggested that development of further high resolution RCMs is required, at the sub-basin level and reaffirming that fact that uncertainties are increases from downscaling techniques of different GCMs than RCM. Modelling climate change impact on hydropower dams should be based on individual dams as the spatial differences reflect on the magnitude of

impacts (Mukheibir, 2007) which prompts the quantifying of the potential impact of climate change on Shiroro dam.

CHAPTER THREE

3.0 MATERIALS AND METHODS

3.1 Data Collection

3.1.1 Land Use Land Cover data

The Soil and Water Assessment Tool (SWAT) model needs a Land management information such as land use data, which serve as model data for the hydrological model for simulation. Land use and cover (LULC) information is one of the essential features that influences the simulation of streamflow, surface erosion, sedimentation load and evapotranspiration in a watershed. Moderate Resolution Imaging Spectroradiometer (MODIS) annually compiled Land cover data MCD12Q1 served as the source of Land use data. The study area lies within two MODIS tiles h18v07 and h18v08. The MODIS land cover datasets were acquired for the year 2013.

3.1.2 River Discharge Gauge Data

River discharge gauge data values for inflow and outflow tributaries within the Kaduna watershed over 24 years of one gauging station was obtained from Shiroro Hydropower Station. Discharge data were divided into two parts and used for model calibration and validation purposes. Other data such as water level and dam capacity were also used to model the management response to the changes in streamflow upstream corresponding to the power generated.

3.1.3 Digital Elevation Model (DEM) Data

Digital Elevation Model (DEM) is an essential geospatial data type in the analysis and modelling of different hydrological phenomenon. A well-prepared DEM is essential for visualizing the floodplain topography and for accurate modelling of the hydrology of a

location (Kalyanapu *et al.*, 2013). Topography of the watershed were obtained from the digital elevation model that defines the height of any location in a particular region at an exact resolution spatially. DEM with a spatial resolution of 90 m by 90 m was downloaded from The Consortium for Spatial Information of the Consultative Group for International Agricultural Research (CGIARS-CSI) SRTM (Shuttle Radar Topography Mission) website which are post processed and freely distributed. The void filled SRTM data available on the CGIARS_CSI SRTM was post processed by Jarvis *et al.* (2008).

3.1.4 Soil Data of the catchment

Data required by the SWAT model includes soil data (silt, clay, loam and sand), available water content, soil texture, infiltration rate, organic carbon content, hydraulic conductivity and bulk density of the catchment area of the basin based on the varying layers of each type of soil. Soil records for the basin was acquired from Food and Agriculture Organisation's (FAO) the Digital Soil Map of the World (FAO, 2003) which was obtained from the waterbase website (http://www.waterbase.org/download_data.html). The information on the various soil property was obtained from the global soil table in the MWSWAT database.

3.1.5 Observed and GCM Climatic Data

Observed in situ daily climate data were obtained from Nigerian Meteorological Agency (NiMet). These data were essential to accomplish the requirement of the first Objective of this research. The observed climate data was used for the analysis of climate change and climate variability of the study area. The in situ data from NiMet was obtained from the year 1981 to 2015 for all the synoptic stations.

The Climate Forecast System Reanalysis data are high spatial resolution data which have application in climate and hydrological research studies (Saha *et al.*, 2010). The Climate Forecast System Reanalysis (CFSR) data served as the model input climate data which was utilised for the initial calibration of the model and also used for validation. The CFSR records are provided by the National Center for Environmental Prediction (NCEP) which is also available for download on the Texas A&M University spatial sciences website, globalweather.tamu.edu. The CFSR data were download from the year 1981 to 2013 from the SWAT global weather website since the last year (2014) of the data provided on the website was not complete. The number of weather stations (Appendix E) which were within the bounding box (coordinate bound shown in Table 3.1) of download were 72 with 17 stations actually positioned in the watershed after delineation.

The climate model output data were obtained from the output of the Coordinated Regional Downscaling Experiment (CORDEX) atmospheric model simulations. These climate change data were easily sourced from West Africa Science Service Centre on Climate Change and Adapted Land Use (WASCAL) Centre in Federal University of Technology Akure, West Africa Climate System (WACS). This data was key in the modelling of the projected river discharge into the Shiroro Dam catchment. Both historical and future scenario data (RCP 4.5 and 8.5) were obtained from the centre. Although ensemble mean data of parameters are ideal for reducing the uncertainty associated with climate model output, due to unavailability of ensemble mean, the available outputs of WRF331 RCM model driven by NCC-NorESM1-M (RCP 4.5 & 8.5) were utilised for the analysis. NCC-NorESM1-M general circulation model is a model developed by the Norwegian Climate Centre and the Weather Research and Forecasting Model (WRF) is a Regional Climate Model developed through joint efforts of the National Oceanic and Atmospheric Administration's (NOAA) National Center for Environmental Prediction, the Air Force

Weather Agency (AFWA), the Forecast Systems Laboratory (FSL) the Federal Aviation Administration, the Nava Research Laboratory and the University of Oklahoma.

Table 3.1: Climate data collected and the parameters used in the study

Data Name	Data ID	Location (degree Decimal) Lon (E)	Lat (N)	Data Used
CFSR		6.4 9.077	9.15 11.5	Temperature (Maximum and Minimum) Solar Radiation Wind Speed Relative Humidity Precipitation
NiMet	Jos Kaduna Minna Zaria	8.9 7.45 6.533 7.683	9.867 10.6 9.617 11.133	Temperature (Maximum and Minimum) Precipitation
CORDEX	AFR-44_NCC-NorESM1-M_rcp45_r1i1p1_WRF331_v4_day	6.4 9.077	9.15 11.5	Temperature (Maximum and Minimum) Precipitation
	AFR-44_NCC-NorESM1-M_rcp85_r1i1p1_WRF331_v4_day	6.4 9.077	9.15 11.5	Temperature (Maximum and Minimum) Precipitation

Source: Authors compilation, 2017.

3.2 Software Programmes used in the Study

A number of software programs were used in the conduct of this study. The Table 3.2 highlights the 8 standalone softwares adopted for the study.

Table 3.2: Software programs utilised in the study

Software	Purpose	Source
RSTUDIO	Statistical Analysis and quality Check	RStudio https://www.rstudio.com/products/rstudio/download/
RCRAN	Statistical Analysis and quality Check	R-Cran project https://cran.r-project.org/bin/windows/base/
ARCGIS	Model input Spatial data processing	ESRI http://www.esri.com/en/arcgis/products/arcgis-pro/Overview
MODIS Reprojection Tool (MRT)	Processing and reprojection of land cover product	Land Processes Distributed Active Archive Center https://lpdaac.usgs.gov/system/files/tools/MRT_download_Win.zip
MapWinGIS	Processing of Spatial data	MapWindow www.mapwindow.org
SWAT	Development and Setup of Model	Texas A&M University http://swat.tamu.edu/software/swat-executables/
CMHyd	Downscaling and Bias Correction	Hendrik Rathjens http://swat.tamu.edu/software/cmhyd/
EXCEL	Input data preparation and computation	Microsoft Corporation www.microsoft..com
WGN Excel Macros	Weather Generator file Statistics calculation	Gabrielle Boisramé http://swat.tamu.edu/media/41583/wgen-excel.zip
SWAT-CUP	Calibration, Uncertainty Analysis and Validation of Model	Neprash Technology http://www.neprashtechnology.ca/downloads/
ArcSWAT	Development of Model	Texas A&M University http://swat.tamu.edu/software/arcswat/

Source: Authors compilation, 2017.

The swat model input climate weather files were prepared using Excel and WGN Excel Macro was used to compute the weather generator parameters (WGEN statistics). The input spatial files were processed for the SWAT model using Map Window, ArcGIS and ArcSWAT. Soil and Water Assessment Tool Calibration and Uncertainty Program (SWAT-CUP) which is a stand-alone software was use for the model calibration, accounting for uncertainties and model validation. CMhyd was utilised to extract climate change data for prediction of future hydrological runoff. RStudio was used to achieve the Objective 1 by using it to detect trend in data and for other exploratory data analysis. MRT was utilised to process MODIS land cover product.

3.3 Processing Hydrometeorological Data

3.3.1 Data Quality Control

Importance of data quality in hydrological research cannot be overestimated as it can affect the results and conclusion derived. Basic data quality control was done by checking whether maximum temperature (Tmax) series where not lower than minimum temperature (Tmin) series. There were no negative values for precipitation data and replacement of missing data with -99 (which is the accepted value for the SWAT model data format) for both climatic and hydrological streamflow data (Neitsch *et al.*, 2010). Quality control was conducted using RClimDex quality control component to assess the data obtained which assist in the identification of errors such as Tmin greater than Tmax and precipitation values lesser than 0.0 mm (Wang, 2010).

3.3.2 Homogenisation

3.3.2.1 Observed Climate data

High quality and homogenous time series of climate data are important for analysing and detecting climatic trend over the study area. Often, climatic long term time series usage is hampered due to the presence of inhomogeneity in the data as a result of change in instrumentation of sites, changes in the approaches used to record the data overtime and systematic errors during data recording. The essence of trend analysis is to detect changes as a result of climatic condition, which makes a case for homogenisation of dataset where inhomogeneity exist (Wang and Feng, 2013). In this study, the Penalised Maximal *F* test and Penalised Maximal *t* test without reference series (Wang, 2008a) was used to assess homogeneity of the climate data using a package RHtestv4 developed for R statistical software environment for detecting and homogenising the Maximum and Minimum Temperature series in the in situ weather station data The RHtestV4 was also used to homogenised monthly precipitation series (Wang and Feng, 2013). The application in R was written and is maintained by Xiaolan Wang and Yang Feng from the Environment Canada and available at http://etccdi.pacificclimate.org/software.shtml which has functions utilised for detecting potential discontinuities in a base climate series (Wang and Feng, 2013). The hormogenisation of the climate data were performed without the use of metadata information from the weather stations (Wang, 2008b). In this approach, the RHTestV4 detected change points which are identified as type-1 or significant and type-0 'changepoints' which are only significant they it is in agreement with metadata at 5 % significance level. Only 'changepoints' which were type-1 was used in the homogenization process due absence of metadata.

3.3.2.1 Observed Streamflow

A number of homogenisation test such Standard Normalised Homogeneity Test (SNHT), Pettitt's Test, Von Neumann ratio test and Buishand's Range test are statistical test used popularly in hydroclimatological studies to check if hydrological time series has been obtained from a homogenous or heterogeneous records and also detect data variability and natural breaks in these data series (Seyam and Othman, 2014). Homogenization is one of the fundamental and preliminary data quality analysis applied to hydrological data series. Homogenous data series implies that the similar methodology, instrument and location of the gauge were used to obtain the data records (Kang and Yusof, 2012). These test were applied to the streamflow data series obtained from the Shiroro Hydropower Station.

3.4 Data Analysis

3.4.1 Methods for Achieving Objective 1

3.4.1.1 Observed Climate Data Analysis

Five ground observation stations were obtained from Nigerian Meteorological Agency (NiMet). A total of three stations are situated in the catchment out of the five whiles the other two are closer to the catchment. The stations positioned in the catchment were Kaduna, Zaria and Jos with Minna closer to the surroundings of the catchment. The stations obtained from the Nigerian Meteorological Agency was first tested for Normality to determine the type of statistical test to be applied whether parametric or non-parametric test. Normal distribution test. The Anderson- Darling normality test and the Shapiro-Wilks test were compared in testing the climatic (temperature, precipitation, Solar radiation and variables obtained from the weather respectively at a 95% significance level.

Anderson- Darling Test Equation

$$A_d{}^2 = -\mathrm{Np} - \mathrm{S_s} \quad (1)$$

$$S_s = \sum_{t=1}^{N} \frac{(2t-1)}{Np} [lnG(H_t) + \ln(1 - G(H_{Np1-t}))] \quad (2)$$

where Np = total number of sample, S_s = Sigma, t = the t^{th} sample of the records arranged according to ascending order and $A_d{}^2$ is known as Anderson Darling Statistics, and G is the cumulative distribution function of the specified distribution. H_i are the ordered data

3.4.1.2 Detecting Statistical Trend in Data

Trends in a random variable refers to the long term significant change demonstrated by the variable and which can be assessed through parametric and non-parametric statistics techniques (Longobardi and Villani, 2009). Nonparametric techniques such as Mann-Kendall (Mann, 1945; Kendall, 1975) has been found to have more power in detecting trend than t test in cases where a non-normal distributed variable or the variable's probability demonstrate skewness (Kundzewicz and Robson, 2000; Yue *et al.,* 2002; Önöz and Bayazit, 2003; Traore *et al.*, 2014). Autocorrelation is one of the effect that affects the detection in trend and it analysis using non-parametric tests such as Mann-Kendall. The selected stations were tested for their suitability of the application of Mann-Kendall. Positive autocorrelation can result in a type I or II error of a data during trend detection analysis (Ahmad *et al.*, 2015).

3.4.1.3 Autocorrelation

The NiMet data were tested for the presence of autocorrelation coefficient in the time series. The precipitation and temperature (maximum (Tmax) and minimum (Tmin)) for

each station were tested at 5 % significant level for autocorrelation coefficient. The Partial autocorrelation function (PACF) and the autocorrelation function (ACF) were used to calculate the autocorrelation coefficient.

Autocorrelation Equation:

The test equation for two sample autocorrelation coefficient calculations.

$$\rho = \frac{E[(m_1 - \mu_1)(m_2 - \mu_2)]}{\sigma_1 \sigma_2} = \frac{Cov(m_1, m_2)}{\sigma_1 \sigma_2} \quad (3)$$

Where E is the expectation operator, μ_1 and μ_2 are the means for m_1 and m_2 respectively. σ_1 and σ_2 are their standard deviations. For the equation which describes the test of autocorrelation for a single variable. m_1 is the original series and m_2 refers to the lag series of the original data. Sample autocorrelations of order k = 0,1,2, 3,…,n_p can be obtained from the equation below by calculating the lag variable from the original observed series m_i, i=1,2,3,…,n_p.

$$\rho(k) = \frac{\frac{1}{n_p - k}\sum_{i=k+1}^{n}(m_i - \bar{m})(m_{i-k} - \bar{m})}{\sqrt{\frac{1}{n_p}\sum_{i=1}^{n}(m_i - \bar{m})}\sqrt{\frac{1}{n_p - k}\sum_{i=k+1}^{n}(m_{i-k} - \bar{m})}} \quad (4)$$

where $\bar{m}$ refers to the average value of the variable.

Partial Correlation Equation

$$m_i = \gamma^{(u)} + \rho_1{}^{(u)} m_{i-1} + \cdots + \rho_u{}^{(u)} m_{i-u} + \varepsilon_i \quad (5)$$

The superscript "(u)" is placed on all the coefficients in regression equation 5 to show that all the coefficients, are all defined by u, which refers to the number of lags. We can

compute the sample PACF or empirical PACF, up to order U by utilising regression (5) for u = 1,…, u and retaining only the estimate $\hat{\rho}_u{}^{(u)}$½(u) for each u.

3.4.1.4 Mann Kendall and Modified Mann Kendall test

The Mann-Kendall test is one of the statistical test used to detect possible trends in observed climatic data obtained from Nigerian Meteorological Agency (NIMET) and was originally devised by Mann in 1945 as a non-parametric test for trend. Later the exact distribution of the test statistic was derived by Kendall 1975 (Akpoti, 2016). Sen's slope estimator was utilised for the estimation of the true slope of the monotonic trend in the climate data. This time series analyses were conducted on the meteorological data and using fume package (Santander Meteorology Group, 2012) in R software (R Core Team, 2017). The package and the codes used for calculating the Modified Mann-Kendall are detailed in Appendix D. Results was presented using tables and graphs. The formula for computing the Mann-Kendall test statistic (S_k) is expressed in Equation (4) (Yue, 2004).

$$S_k = \sum_{a=1}^{Nd} \sum_{b=a+1}^{Nd} \text{sgn}(X_b - X_a) \qquad (6)$$

Where X_b and X_a are monthly data values in years such that b is greater than *a* and where sgn function is expressed as:

$$\text{sgn}(X_b - X_a) = \begin{cases} 1 \text{ if } (X_b - X_a) > 0 \\ 0 \text{ if } (X_b - X_a) = 0 \\ -1 \text{ if } (X_b - X_a) < 0 \end{cases} \qquad (7)$$

Under the null hypothesis of no trend and independence of the series terms, the variance of the Mann-Kendall statistic is calculated as:

$$Var(S_k) = \frac{Nd(Nd-1)(2Nd+5) - \sum_{p=1}^{j} t_p(t_p-1)(2t_p+5)}{18} \qquad (8)$$

in which Nd refers to the sample size, j represents the number of groups which are tied and t denotes size of the *t* th group. The summation of the data series in the numerator is

employed only in situations where the data series comprises of tied values. For sample size Nd ≥ 10, the statistic S assumes normal distribution, the standard normal test statistic Z_k is computed using

$$Z_k = \begin{cases} \dfrac{S_k - 1}{\sqrt{VAR(S_k)}}, \text{for } S_k > 0 \\ 0, \quad \text{for} \quad S_k = 0 \\ \dfrac{S_k + 1}{\sqrt{VAR(S_k)}}, \quad S_k < 0 \end{cases} \tag{9}$$

The equation 9 compute the likelihood linked with this normalised statistical test. The probability density function for a Gaussian distribution with a mean value of 0 and a standard deviation of 1 is expressed by the subsequent equation:

$$f(Z_k) = \frac{1}{\sqrt{2\pi}} e^{-\frac{Z_k{}^2}{2}} \tag{10}$$

The change detected in the data series suggest a declining trend if Z_k is negative and the calculated probability is greater than the level of significance. When the Z_k is positive, it means the trend in the data series is increasing and the calculated probability is more than the level of significance. If the calculated probability is less than the level of significance, the condition of no trend is assumed.

3.4.1.5 Modified Mann Kendall Test

Autocorrelation in a data series affect the power of the as it increases the likelihood of the null hypothesis of the Mann Kendall test of no trend to be rejected (Yue *et al.* 2004).

The equation for modified Mann Kendall test with the correction factor are presented below as it appeared in Hamad and Rao (1998) and Yue (2004).

$$Var^*(S_k) = Var(S_k) \times \frac{Nd}{Nd^*} \quad (11)$$

Where Nd is the actual sample size of data (ASS), Nd^* is the effective or equivalent sample size (ESS) and $\frac{Nd}{Nd^*}$ is the correction factor for correcting the serial dependence.

For the computation of the effective sample size (ESS)

$$Nd^* = \frac{Nd}{1 + 2 \times \sum_{k=1}^{Nd-1}(1 - \frac{k}{Nd}) \times \rho_k} \quad (12)$$

For autoregressive of lag-1 process (Yue, 2004)

$$Nd^* = \frac{Nd}{1 + 2 \times \frac{\rho^{Nd+1} - Nd \times {\rho_1}^2 + (Nd + 1) \times \rho_1}{Nd(\rho_1 - 1)^2}} \quad (13)$$

With these correction factor applied to equation 6 as illustrated in equation 9, the corrected $Var^*(S_k)$ is substituted into equation 7 and the correction is translated to subsequent equations.

3.4.1.6 Theil-Sen's Slope Estimator

The Theil-Sen's slope estimator is utilised to establish the true or exact slope of data series (such as hydroclimatological data) wherever it is present in the time series. It is a robust method for fitting a line to a time series data by utilising the median of the slopes of all through pairs of two dimensional sample points. An unbiased median slope estimator approach is used to estimate the magnitude of the trend which was proposed by Sen (1968) and further modified by Hirsch *et al.* (1982).

Assuming that the trend is monotonic and linear, the Sen's slope estimation is expressed as follows:

$$b'(t) = Vt + A \quad (14)$$

Where V refers to the slope and A is the constant. With respect to the Nd pair of time series, the subsequent equation defines the slope as:

$$V_a = \frac{x_b - x_c}{b - a} \quad for\ a = 1, \ldots, \text{Nd and all c} < \text{b} \qquad (15)$$

where Va denotes the slope between data points x_b and x_c, x_b refers to data values at time b , x_c refers to data values at time c. Nd = $\frac{n(n-1)}{2}$ for single observation in each time period or Nd < $\frac{n(n-1)}{2}$, where 1<c<b<n, n refers to the total number of observations for each period. The Nd values of Va are ranked from least number to largest number and median of these N values of Va is the Sen's estimate of slope computed as:

$$V_{me} = \begin{cases} V\left[\frac{(Nd+1)}{2}\right], when\ Nd\ is\ odd \\ V\left(\frac{Nd}{2}\right) + V\left[\frac{Nd+2}{2}\right], when\ Nd\ is\ even \end{cases} \qquad (16)$$

The significance of the median V_{me} is evaluated using the two tailed test at a specified alpha value (the alpha (α) used in the analysis was 0.05). The sign of V_{me} and its value shows the direction of the trend inherent in the time series data and the steepness of the trend. Equation 11 below illustrates the confidence interval for V_{me} is calculated as.

$$C_\alpha = Z_{1-\alpha/2}\sqrt{V(S_k)} \qquad (17)$$

$V(S_k)$ representing the Mann-Kendall statistics variance is expressed in equation 8 or equation 11 when the time series is serially correlated while $Z_{k(1-\alpha/2)}$ is derived from the standard normal distribution table.

3.4.2 Methods for Achieving Objective 2

3.4.2.1 Model Description

Soil and Water Assessment Tool is a physical based semi-distributed model made for the United State Department of Agriculture subsidiary Agricultural Research Service (ARS) for the assessment of water quantity and quality (sediment and chemically yield) and complex watersheds with varying soils and land use as a result of land use practices on water resources (Arnold *et al.*, 2012). Soil and Water Assessment Tool (SWAT) model have been widely utilised worldwide for assessment of water quantity and quality issues. SWAT possess ability to model a particular watershed or a network of several watersheds which are hydrological linked in a location. The model runs on daily time step which is capable of simulating hydrology of a watershed on a continuous (long term) basis but not intended to capture detail in simulation or single-event flood routing (Neitsch *et al.*, 2010). The model comprises of eight major components namely weather, hydrology, sedimentation, soil, temperature, crop growth, pesticides, nutrients and agricultural managements.

The SWAT model divides the watershed into sub-basins (which is the first level of subdivision). The sub-basins are subdivided into Hydrological Response Units (HRU) based on the land uses, soil and slope distribution in the watershed. The HRU signifies the basic unit of the watershed which are homogenous. The water balance equation is the principle used by the SWAT model to simulate the hydrology of a watershed. The hydrology of the watershed model (Figure 3.1) can be divided into the land phase of the hydrology cycle and the water or routing of the hydrologic cycle. The land phase regulates the sediment, amount of water, pesticides and nutrients loadings of the main channel in each sub-basin. The routing phase comprises the movement of water, sediments, nutrient and pesticides through the main channel (Neitsch *et al.*, 2011). The equation below

defines the water balance:

$$SC_t = SC_o + \sum_{i=1}^{t}(P_{day} - q_s - E_d - W_s - q_g \quad (18)$$

where SC_t is the water content of the soil during the last or the final stage (mmH_2O)

SC_o is the water content of the soil during the beginning or the initial stage (mmH_2O)

P_{day} is the quantity of precipitation recorded on a day *i* (mmH_2O)

q_s refers to surface runoff amount recorded on a particular day *i* (mmH_2O)

t refers to the period (or time) (days)

E_d is the recorded evaporation amount on a day *i* (mmH_2O))

W_s refers to the quantity of water flowing into the vadose region from the soil profile on *i* th day (mmH_2O)

q_g the return flow quantity on day *i* (mmH_2O)

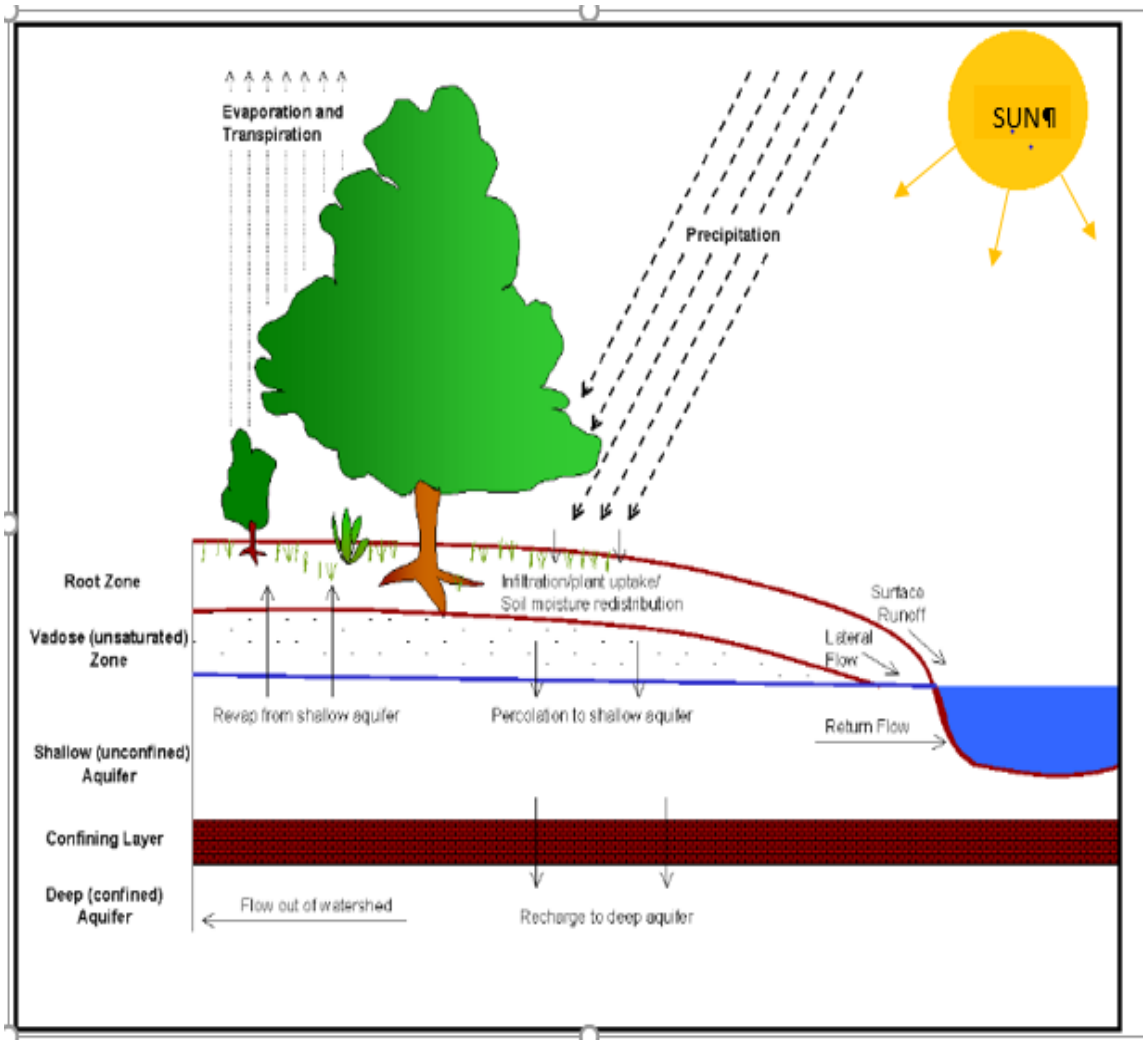

Figure 3.1. The hydrologic cycle (Source: Neitsch et al. 2010, with author's modification)

Surface runoff

Surface runoff is as a result of rate of precipitation or water application exceeding the rate of infiltration of the soil. There are two approaches provided in SWAT for the estimating surface runoff. The approaches are the Soil Conservation Service (SCS) curve number approach (SCS, 1972) and the Green and Ampt infiltration method (Green and Ampt, 1911) which are used to simulate peak rates and runoff volume in SWAT (Neitsch *et al.*, 2010).

The curve number technique employs daily time step when it is estimating the volume of the surface runoff in SWAT but it is unable account for infiltration directly. However, the quantity of water entering into the soil is calculated as the change between the amount of precipitation and the amount of surface runoff. Green and Ampt infiltration method on the other hand requires sub-daily increments data to calculate directly compute the infiltration in the mode (Neitsch *et al.*, 2011). The SCS curve number technique was employed in this research due to the daily data which were more available. The equation 19 defines the curve number equation:

$$q_s = \frac{(P_{day} - I_s)^2}{(P_{day} - I_s + S_r)} \quad (19)$$

where q_s is collected runoff (excess of precipitation) in $\mathrm{mmH_2O}$

P_{day} is the precipitation depth for the day in $\mathrm{mmH_2O}$

I_s is the initial abstraction which includes surface storage ; interception and infiltration prior to runoff

S_r is the parameter of retention ($\mathrm{mmH_2O}$) which is expressed as:

$$S_r = 25.4\left(\frac{1000}{CN} - 10\right) \quad (20)$$

where CN is the curve number for the day. *Is* is commonly given as 0.2S, hence the equation

18 is expressed as:

$$q_s = \frac{(P_{day} - 0.2S)^2}{(P_{day} + 0.8S)} \quad (21)$$

In this equation, runoff is generated when $R_{day} > I_a$. The SCS curve number is a function the permeability of the soil, land use and antecedent soil condition (Neitsch *et al.*, 2010). The soil moisture conditions are classified into four hydrological groups which are defined by their infiltration rate by the U.S. Natural Resources Conservation Service (NRCS). Group A refers to high infiltration, B for moderate infiltration, C for slow infiltration and D for very slow infiltration.

Hydrologic group refer to a group of soils similar runoff potential under similar storm and cover conditions.

3.4.2.2 SWAT Input Data Analysis

DEM Processing

CGIAR-CSI's (http://srtm.csi.cgiar.org) Digital Elevation Model (DEM) was downloaded from at a spatial resolution of 90 m by 90 m in Geographic Coordinate System with datum WGS 84. The study area lies between two tiles of DEM provided by CGIAR- CSI srtm38_10 and srtm37_10. The DEM was merged using subtraction technique in Map Window. The two DEM tiles were merged in Map Window. Using the approach illustrated in Leon (2011), a rectangular shape file was created around the study

area to clip the merged SRTM DEM file to reduce computational time. The shape file covered approximately 152 000 km^2 around the study area. The shape file served as boundary area for the study area. The clip shapefile was then projected to UTM 32 with datum WGS 84. The merged DEM was clipped using a clip shapefile in the Geographic Coordinate System (GCS) World Geodetic System 1984 (GCS WGS 84) and then projected to UTM 32 zone. The projected DEM was re-clipped using the projected clip shapefile to remove any missing values.

Land Use Processing

Land Cover data downloaded from MODIS (MCD12Q1) for the year 2013 required to be preprocessed and utilised asSWAT model input file. The MODIS data are supplied in HDF format and in Sinusoidal Coordinate System showing no datum. MODIS Reprojection Tool software (MRT) was downloaded from MODIS website for processing the land cover data. The study area was located in MODIS tile h18v07. The MRT was used to reproject the MODIS data from sinusoidal projection to GCS WGS 84 coordinate system. The International Geosphere–Biosphere Programme (IGBP) land cover tile was selected for reprojection (Table 3.3). The bounding shapefile created during the processing of the merged DEM tile was used to clip the reprojected MODIS data. The MODIS data was then processed by updating the class name found in land cover unique value in Symbology in ArcGIS. This was achieved by allocating class names to the corresponding MODIS land cover type. Sixteen (16) land cover classes (Table 3.3) were identified in the MODIS data. The sixteen land cover types of the MODIS data in IGBP classification system were reclassified in the SWAT model to the closest class in the SWAT land use classes by creating a lookup table (Table 3.4).

Table 3.3: Land cover classes of MODIS data in IGBP land cover classification

Class	IGBP (Type 1)
0	Water
1	Evergreen Needleleaf forest
2	Evergreen Broadleaf forest
3	Deciduous Needleleaf forest
4	Deciduous Broadleaf forest
5	Mixed forest
6	Closed shrublands
7	Open shrublands
8	Woody savannahs
9	Savannahs
10	Grasslands
11	Permanent wetlands
12	Croplands
13	Urban and built-up
14	Cropland/Natural vegetation mosaic
15	Snow and ice
16	Barren or sparsely vegetated
254	Unclassified
255	Fill Value

Source: Land Process Distributed Active Archive Center (http://lpdaac.usgs.gov/dataset_discovery/modis/modis_products_table/mcd12q1)

The Land Use reclassification were done for these land cover types as required by the SWAT model as illustrated by Table 3.4.

Table 3.4: Reclassification of land cover types into SWAT database land Use classes

SWAT LAND USE type	IGBP land cover type
Water	Water
Evergreen Forest	Evergreen Needleleaf and Broadleaf forest
Deciduous Forest	Deciduous Needleleaf and Broadleaf Forest
Mixed Forest	Mixed forest
Rangeland and Brush	Closed shrublands, Open shrublands, Woody savannahs,
Rangeland and grassland	Savannahs, Grasslands
Urban	Urban and built-up
Agriculture	Croplands, Cropland/Natural vegetation mosaic
Bareland	Barren or sparsely vegetated, Snow and ice
Wetland	Permanent wetlands,

Source Author's compilation, 2017.

Soil Map Processing.

The soil map contains FAO classified so maps and properties. The soil map was in GCS WGS 84 coordinate system. The soil map was subsetted by using the boundary shapefile (clip file) creating during the DEM processing and the resulting raster map reprojected to UTM 32 zone with datum WGS 84. The new soil map raster was then reclipped with the projected boundary shapefile (clip file in UTM 32 zone) to remove missing data values. In order to utilise the soil map in ArcSWAT, the new soil map had to be converted to ESRI GRID file format. The new projected soil map in UTM 32 was exported to ESRI GRID format. The ArcSWAT soil database (usersoil table) was updated with the Global Soil properties from MWSWAT database. The soil database of MWSWAT Global Soil has already incorporated FAO soil properties in their database.

Slope Classification

The study area's slope classes of was obtained by using the Slope function in ArcGIS 10.1 to define the slope classes. The slope and elevation as a topographical parameter of the watersheds were generated from the DEM using the Slope function. Five slope classes were identified in degrees. The slope classes used in the Hydrological Response Unit definition were $0^o – 2.868^o$, $2.868^o – 5.497^o$, $5.497^o – 8.844^o$, $8.844^o – 12.668^o$ and greater than 12.668^o. The highest elevation in the study area was 1582 m high, the mean elevation was 676.47 m and the lowest was 283 m above sea level.

Watershed Delineation

A new ArcSWAT project was created. Under watershed delineator menu, Automatic watershed delineator was selected and the processed DEM was loaded into the ArcSWAT project. No mask or predefined watershed shapefile was loaded. The area used was 80000 hectares for the delineation at DEM based under stream definition. The Shiroro Dam coordinates was obtained in GCS WGS 84 and projected to UTM 32 which aided in the

location of the reservoir outlet. The delineate watershed was clicked to delineate the watershed.

Hydrological Response Unit (HRU) Definition

This is the fundamental unit in the SWAT model derived from the subdivision of sub-basins based on the homogenous spatial location of slope, type of the soil and land use classification. The combination of these three (into separate HRU) controls the modelling of surface runoff in the watershed. The land use raster was loaded and reclassified using a lookup table to define the land cover into SWAT land use types as specified in Table 3.6 above. The processed soil map was loaded into the HRU menu. A lookup table was made to reclassify the soils according to the soil in the usersoils table. Slope intervals representing each slope class were inputted in to the Land Use, Soil and Slope definition menu. The SWAT model allows four types of HRU definition under the these options: the use of dominant HRU, the use of dominant land use, soil, slope, Target Number of HRUs and the use of multiple HRUs options. The multiple HRU options was used to setup the model in this study.

In order to reduce computational time and preserve detail in the HRU definition, the threshold area percentage of slope, land use and soil were set for HRU definition over sub-basin areas. The thresholds values of 10 %, 10 % and 5 % for land use classes, soil classes and slope classes respectively was set.

Weather Data Preparation

Weather data available in ArcSWAT format. SWAT model requires a weather generator file (.wgn) to run. This allows for missing weather variables to be generated statistically during modelling. WGEN file maker a Microsoft Excel macro developed by Gabrielle Boisramé, was downloaded for computing the statistics of the CFSR weather stations

required in weather generator file (.wgn). Dew point software Dew02 (Liersch, 2003) was downloaded from the SWAT website (http://swatmodel.tamu.edu/software/links-to-related-software) to compute dew point temperature from temperature (maximum and minimum) and relative humidity which one of the parameters needed for creating the wgn file. Aside the latitude, longitude and elevation values of each weather stations needed in the weather generator file, fifteen (15) statistical parameters are computed to build the weather generator file for each stations both WGEN and dew02.

The statistical parameters are:

TMPMX (monthly): average daily maximum air temperature for a month (ºC).

TMPMN (monthly): average daily minimum air temperature for a month (ºC).

RAINYRS: the number of year of maximum monthly half hour (0.5 h) precipitation data utilise to describe values for RAINHHMX (monthly).

TMPSTDMX (monthly): standard deviation for daily maximum air temperature in month (ºC).

TMPSTDMN (monthly): standard deviation for daily minimum air temperature in month (ºC).

PCPSTD (monthly): standard deviation for daily precipitation in month (mm H_2O/day).

PCPMM (monthly): average precipitation for a month (mm H_2O).

PCPSKW (monthly): skew coefficient for daily precipitation in a particular month (%).

PR_W (1, monthly): probability of wet day following a dry day in a month. Here, the wet day calculation is defined as any day with precipitation value greater than zero mm (> 0 mm).

PR_W (2, monthly): probability of wet day following a wet day in a month.

PCPD (monthly): average number of days of precipitation in a month for year of record.

RAINHHMX (monthly): maximum half hour (0.5 hour) rainfall in entire recording period in a month (mm H_2O).

SOLAVAV (monthly): average daily solar radiation for a particular month for year of record (MJ/m^2/day).

DEWPT (monthly): average dew point temperature for each month (°C).

WNDAV (monthly): average daily wind speed in particular month for all the years of record (m/s)

The values of the DEWPT monthly values were computed using the dew02 software. All the other parameters were computed using the WGEN maker Microsoft Excel macro. Thirty years of record were used to compute the CFSR stations statistics from 1981 to 2010 which was more than the minimum of 20 years recommended by (Neitsch *et al.*, 2010). RAINHHMX records are not provided as part of the CFSR data. One third of maximum daily precipitation of a month data were assumed as RAINHHMX data for all the stations based on the recommendation in the SWAT user group (https://groups.google.com/forumswatuser/kpZMCke3BvU).

3.4.2.3 Sensitivity, calibration, Uncertainty analysis and validation

Parameter Sensitivity analysis

Parameters of SWAT model are calibrated either manually or automatically. The sensitivity analysis is carried out to identify the most influential parameters in the SWAT model for streamflow simulation before calibration takes place (Griensven *et al.*, 2006).

This is because there are numerous parameters in ArcSWAT and not all of them are significant to the contribution of streamflow. Sensitivity analysis helps to identify the important parameters and reduces the number of parameters used in calibration and improve precision of a parameter the sensitivity analysis were done in two ways. Parameters selection were also based on parameters sensitive to streamflow in Abbaspour *et al.* (2004), other parameters likely to influence streamflow, Schuol *et al.* (2008) and Akpoti *et al.* (2016), with the latter two working in similar climatic zone as the study area. The Global Sensitivity Analysis (where all parameters were varying simultaneously) was used to analyse the sensitivity of the parameters used in the calibration process. Fourteen (14) parameters were used in the calibration process. The Global Sensitivity employs multiple regression systems that regresses Latin hypercube generated parameters against the objective function (Abbaspour, 2015). The relative significance of each parameter is determined by using the statistical test *t*-test. The sensitivities values obtain give average changes in objective function derived from changes in parameter while all other parameters are simultaneously changing. The *t*-stats refers to the coefficients of the parameter divided by the standard error and is the extent of the precision to which the coefficient of regression is measured, hence the larger the values in absolute and the smaller the p-value (less than 0.05), the more sensitive the parameter (Abbaspour, 2015). Thus, there exist a 95 % chance of being correct about the sensitivity of the parameters based on the *t*-stats and the p-value (at 0.05). The parameters used in the calibration are illustrated in Table 3.5 below.

Table 3.5: Parameters used in the calibration of the SWAT model of the Study area

H	Definition	Absolute SWAT values
r__SOL_K().sol	Saturated hydraulic conductivity	0 – 2000
v__ALPHA_BF.gw	Baseflow alpha factor (days)	0 – 1
r__CN2.mgt	SCS runoff curve number f	35 – 98
v__CH_N2.rte	Manning's "n" value for the main channel	-0.01 – 0.3
v__ESCO.hru	Soil evaporation compensation factor	0 – 1
v__CH_K2.rte	Main channel's effective hydraulic conductivity alluvium	-0.01 – 500
r__SOL_BD().sol	Moist bulk density	0.9 – 2.5
v__GW_REVAP.gw	Groundwater "revap" coefficient	0.02 – 0.2
v__OV_N.hru	Manning's "n" value for overland flow	0.01 – 30
v__CANMX.hru	Maximum canopy storage	0 – 100
v__RCHRG_DP.gw	Deep aquifer percolation fraction	0 – 1
v__GWHT.gw	Initial groundwater height (m).	0 – 25
v__GWQMN.gw	Threshold depth of water in the shallow aquifer required for return flow to occur (mm)	0 – 5000
r__SOL_AWC().sol	Water capacity available to the soil based on the soil layer.	0 – 1

Source: Authors compilation, 2017.

The model codes r_, v_ and a_ refers to the type of changes applied to the parameters. r_ refers to the value of the current parameter is multiplied by (1+ a given value), v_ means the default parameter value is substituted by a particular value and a_ means a specified amount is added to the default value Abbaspour, 2015). r_ is normally preferred for spatial parameters such as .mgt and .sol parameters.

Performance Evaluation

The SWAT model performance is evaluated after the calibration and validation on the initial model simulation run. The model is evaluated by performance on its ability to simulate and project flow by using primarily three objective functions known as the Nash-Sutcliffe Efficiency (NSE), coefficient of determination (R^2) and Percent Bias (PBIAS) (Abbaspour *et al.*, 2015). These statistics of goodness of fit were employed to assess the performance of the model. The equations (19) to (21) define these statistical objective functions.

$$R^2 = \frac{\left[\sum_{i=1}^{n}(X_{obs,i} - \bar{X}_{obs})(X_{sim,i} - \bar{X}_{sim})\right]^2}{\sum_{i=1}^{n}(X_{obs,i} - \bar{X}_{obs})^2 \sum_{i=1}^{n}(X_{sim,i} - \bar{X}_{sim})^2} \quad (19)$$

$$NSE = 1 - \frac{\sum_{i=1}^{n}(X_{sim,i} - X_{obs,i})^2}{\sum_{i=1}^{n}(X_{obs,i} - X_{obs})^2} \quad (20)$$

$$PBIAS = 100 \times \frac{\sum_{i=1}^{n}(X_{obs} - X_{sim})_i}{\sum_{i=1}^{n} X_{obs,i}} \quad (21)$$

where:

$X_{obs,i}$ is the observed flow at time i (m^3/s)

$X_{sim,i}$ is the simulated flow at time i (m^3/s)

X_{obs} is the measured variable (m^3/s)

X_{sim} is the simulated variable (m^3/s)

i is the i^{th} measured or simulated data

$\bar{X}_{obs}$ is the average or mean of the measured variable

$\bar{X}_{sim}$ is the average or mean of the simulated variable

n is the total number of data points to be matched.

Table 3.6: Performance and interpretation of the values of objective functions used for Monthly time step calibration

Objective Function	Performance			
	Very Good	Good	Satisfactory	Unsatisfactory
R^2	>0.85	$0.75 < R^2 \leq 0.85$	$0.6 < R^2 \leq 0.75$	$R^2 \leq 0.6$
NSE	0.8 <NSE ≤ 1.0	0.7 < NSE ≤ 0.8	0.5 <NSE≤ 0.7	NSE ≤ 0.5
PBIAS	0 ≤ ± 5	± 5 <PBIAS< ± 10	±10 < PBIAS< ± 15	PBIAS ≥ ± 15

The goodness of fit values for objection functions are based on recommendations by Moriasi *et al.* (2015).

Calibration, Validation and Uncertainty Analysis

The SWAT simulation methodology consisted of an initial calibration and validation phase proceeded by another phase whereby the impact of variations in climatic inputs are assessed for the hydrology of Kaduna River basin. Based on the approached of Abbaspour *et al.* (2015) more half (approximately 65 %) of the streamflow records from the gauging station at the Shiroro dam was utilised for calibration and the rest used for the model validation. The SWAT model tries to mimics physical processes in reality. The Soil and Water Assessment Tool – Calibration and Uncertainty Programs (SWAT-CUP) which is a standalone program was used for the calibration and validation of the SWAT model. The model is initially run for the calibration between the periods 1990 – 2005 and for validation period from 2006 – 2013 in the SWAT-CUP program. The SUFI-2 algorithm was used for the calibration. The calibration are based on improvement of the goodness fit after every iteration made. The process of calibration ends when a goodness of fit statistics stops (normally after 3 iterations are recommend) improving with iterations. Under the SUFI-2 approach, 200 runs were done for each iterations and each parameters updated automatically, the new values fall within the Absolute Swat values range of parameters in the SWAT-CUP program. More iterations are performed to improve the statistics of the goodness of fit of the model. In this study, five iterations were performed and the best solution selected from them.

Downscaling and Bias Correction of Climate model data

In order evaluate the effect of the different climate change scenarios on the hydrological processes in the watershed, the two scenarios collected were downscaled and bias corrected using the observed climate data (CFSR). The CMhyd software was used for extracting point station projected scenarios and bias correction of temperature (maximum and minimum temperature) and precipitation. The Distribution Mapping bias correction

method were used for both temperature and precipitation downscaled values. This approach used in the CMhyd program are well illustrated in Teutschbein and Serbert (2012). The Figure 3.2 illustrates the schematic approach used in the bias correction approach and utilisation of the data in the model.

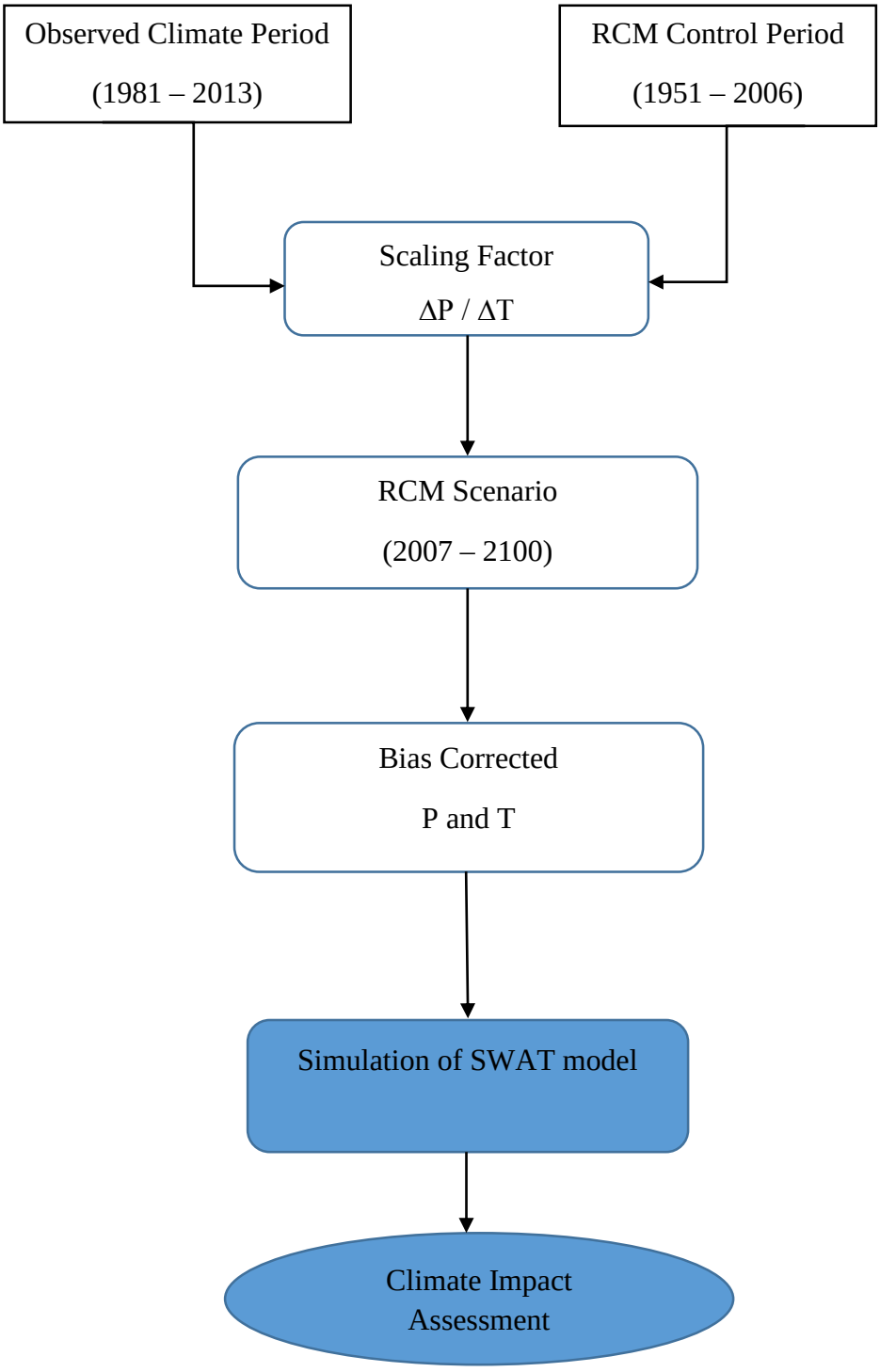

Figure 3.2. A simple flow chart to use bias corrected RCM outputs in SWAT model.

(Source: Fiseha *et al*., 2014, with author's modification)

3.4.3 Methods for Achieving Objective 3

3.4.3.1 Modelling of Hydropower dam data.

Stochastic Dynamic Programming was used to model the dam optimization efficiency due to the unpredictable management policy of the dam. An existing power model utilised in the Jimoh (2008) and Cervigni *et al.* (2013).

In expressing the objective function of fig. 9 which illustrate a hydropower power reservoir systems, equation 22 is used which is expressed below:

$$O_i = A_i + A_{i-1} + \ldots + A_I + O_{I+1} \qquad (22)$$

where:

A_i refers to the water return at stage i that is as a result of the release R given the final and initial storages, and the water value at the end of stage I is represented by O_{I+1} is the last stage in the twelve (12) month planning periods. These benefit is to exploit fully the area under the energy generated. In previous studies (Jimoh, 2008 & Cervigni *et al.*, 2013) the model has been utilised, first for the objective criteria used were to maximise production of energy at a price of ₦12 /KWh (kilowatt hour) for firm power, a penalty for deficit power at ₦12 /KWh and a ₦6 /KWh secondary price for any extra power above the firm power (secondary power) produced. The second objective is to decrease water spill (as part of flood control measures) whiles ensuring water use and demand downstream are satisfied.

The Bellman's optimization principle was used for the analysis which begin from a time T and moves backward (from final state to initial state and decisions). The Bellman's state that "an optimal policy has the property that whatever the initial state and initial

decisions are, the remaining decisions must constitute optimal policy for the state resulting from the first decision".

The following equations 23 to 29 illustrate the operation of the hydropower and Figure 3.3 highlights the schematic diagram of the hydropower plant.

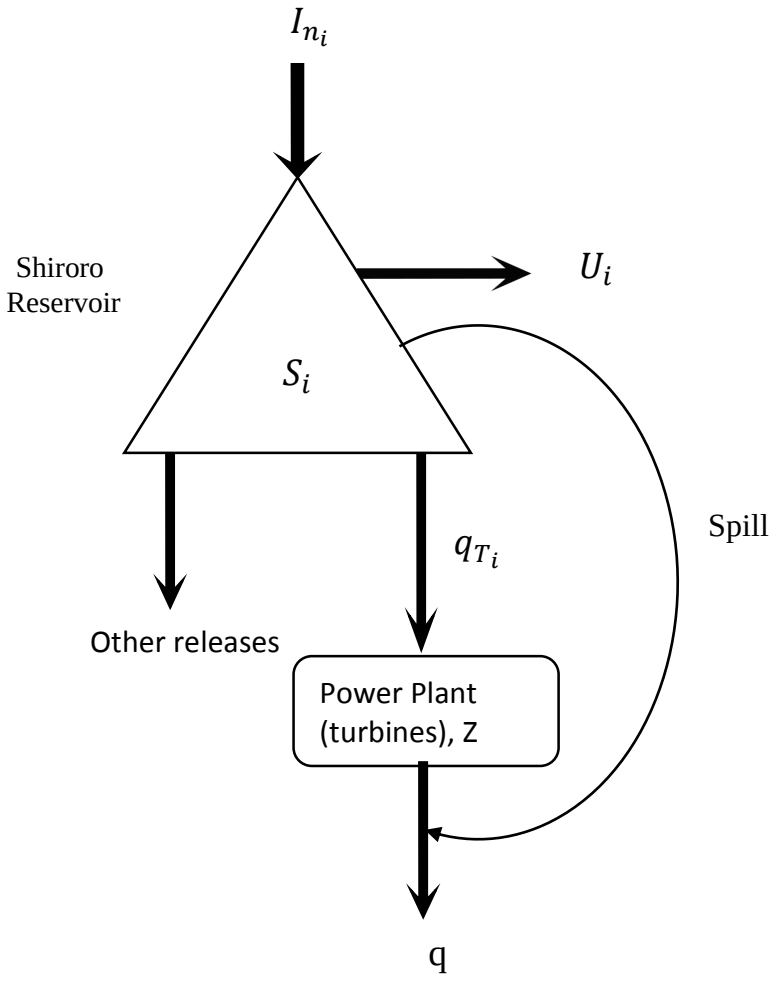

Figure 3.3. The schematic diagram of Hydropower generating plant. S is the storage, I_{n_i} is the inflow to the reservoir, U is the losses from evaporation and seepage, q is the release and q_{T_i} is the discharge through the turbines and *i* represents time (Jimoh, 2008)

Continuity equation:

$$S_{i-1} + I_{ni} - U_i - q_i = S_i \quad (23)$$

Where q_i refers to the outflow from the reservoir at time i, U_i is the loss from the reservoir at time i, I_{ni} is the reservoir inflow at time I and S_i is the reservoir storage (Figure 3.3)

Storage Constraints:

$$S_{dead} < S_i < S_{max_i} \quad (24)$$

$$S_{i+1} \leq S_{max_i} \quad (25)$$

The S_{dead} is the reservoir dead capacity storage also known as the minimum storage. S_{max_i} refers to the maximum water storage at time i.

Release Control:

$$q_i \geq maxq_o \quad (26)$$

Where q_o defined the fixed water requirement at time i required to be released to support water supply, ecology and irrigation schemes downstream (minimum demand) from the reservoir. $maxq_o$ refers to the maximum mandatory water requirement for satisfying demand of water at downstream.

Power production Equation

$$E_{C_i} = f \times q_T \times H_{aT} \times \eta \quad (27)$$

Where E_{C_i} is the energy production capacity, f is the electrical energy conversion potential factor and H_{aT} is the average head over the turbine. q_T refers to the flow going to the turbine and η is the efficiency of the power plant.

There exist restriction on the energy to be produced by the power plant which is dependent on the available number of hours for production of energy (h_n) and the plant capacity (P_c). This implies that, the maximum peak power produced P_{MP} can be expressed as:

$$P_{MP_i} = P_{C_i} \times \eta \times h_{ni} \quad (28)$$

Therefore, at any time *i*, the power produced is defined as:

$$P_{Z_i} = \min(P_{T_i}, P_{MP_i}) \quad (29)$$

P_{Z_i} is the peak power produced, P_{T_i} is the total power produced at a specific time *i.*

The stochastic dynamic programming power model facilitated the determination of the reservoir's monthly release policy for where the reservoir storage is the state variable S_i at the beginning of a stage and the release from the reservoir is the decision variable. The solution derived from equation 22 by working from the end of the decision horizon for a period of 12 months. There are a number of discretisation of storage for the reservoir on a monthly scale. Equation 27, 28 and 29 was used to compute the power produced for each month. The hydropower reliability of the power plant is examined using the energy produced and the release policy. Reliability can be defined as the number of successful times the monthly power goal is achieved against the number of operational months (Jimoh, 2008).

CHAPTER FOUR

4.0 RESULTS AND DISCUSSION

4.1 Normality

The normality test is one of the basic statistical techniques applied to the data series. These test determine the appropriate of a statistical technique to be applied on the data series. The normality test conducted on the monthly temperature (maximum and minimum), rainfall and streamflow indicates that all the data series does not exhibit Gaussian distribution when the Anderson-Darling normality test was applied to all the data series. Table 4.1(a, b and c) illustrate the test results of the Anderson Darling Test.

Table 4.1a: Anderson-Darling test for normality of the temperature and rainfall data

Weather Stations	Maximum Temperature		Minimum Temperature		Precipitation	
	A^2	p-value	A^2	p-value	A^2	p-value
Jos	42.251	2.2×10^{-16}	301.34	2.2×10^{-16}	2676.7	$\mathbf{2.2 \times 10^{-16}}$
Kaduna	39.371	2.2×10^{-16}	132.65	2.2×10^{-16}	2928.5	$\mathbf{2.2 \times 10^{-16}}$
Minna	82.966	2.2×10^{-16}	68.597	2.2×10^{-16}	3001.1	$\mathbf{2.2 \times 10^{-16}}$
Zaria	42.633	2.2×10^{-16}	173.88	2.2×10^{-16}	3161.5	$\mathbf{2.2 \times 10^{-16}}$

Source: Authors compilation, 2017.A^2 is the Anderson-Darling test statistics. W is the Shapiro-Wilk test statistics.

Table 4.1b: Anderson-Darling and Shapiro-Wilk tests for normality for monthly streamflow from 1990 to 2014 at the Shiroro Dam

Anderson-Darling	Result	Shapiro-Wilk	Results
A^2	29.9297	W	0.7482
P-value	< 0.00010	P-value	< 0.00010
Alpha	0.05	Alpha	0.05

Source: Authors compilation, 2017.A^2 is the Anderson-Darling test statistics. W is the Shapiro-Wilk test statistics.

Table 4.1c: Shapiro-Wilk test for normality of the temperature and rainfall data

Weather Stations	Maximum Temperature		Minimum Temperature		Precipitation	
	W	**p-value**	**W**	**p-value**	**W**	**p-value**
Jos	0.9289	6.73×10^{-13}	0.9289	3.06×10^{-13}	0.8528	$\mathbf{2.2 \times 10^{-16}}$
Kaduna	0.9738	7.22×10^{-7}	0.9322	6.94×10^{-13}	0.8176	$\mathbf{2.2 \times 10^{-16}}$
Minna	0.9466	3.63×10^{-11}	0.9882	0.001738	0.8514	$\mathbf{2.2 \times 10^{-16}}$
Zaria	0.9636	1.07×10^{-8}	0.9339	1.09×10^{-12}	0.8016	$\mathbf{2.2 \times 10^{-16}}$

Source: Authors compilation, 2017.A^2 is the Anderson-Darling test statistics. W is the Shapiro-Wilk test statistics.

The Null hypothesis H_0 of the Anderson-Darling test and the Shapiro-Wilk states that the variable in the sample belong to population which is a normal distribution. The Null hypothesis of the Shapiro-Wilk test is rejected and the alternative accepted for all the data series, which is also same as the Anderson-Darling. The test for the data series were performed at a significance level of $p \leq 0.05$, implying that any p-value below the significance means the H_0 of the Anderson-Darling test which state that the data follows a specified distribution is rejected and the alternative accepted. A non-parametric test approach is therefore suitable to analyse these data series.

4.2 Homogeneity of Data

The Table 4.2a shows the result of the homogenization test using the RHtestv4 software. The maximum and minimum series of Kaduna was homogenous. The homogeneity test results for maximum temperature displayed that Kaduna, Jos, Minna and Zaria were homogenous. The RHtestV4 homogenisation technique were also applied to minimum temperature series from Jos, Minna and Zaria except Kaduna which was homogenous.

Table 4.2a: Homogeneity test and homogenisation of Temperature (maximum and minimum) and rainfall for the weather stations

Weather Stations	Maximum Temperature		Minimum Temperature		Precipitation	
	H	HG	H	HG	H	HG
Jos	Yes	No	No	Yes	No	Yes
Kaduna	Yes	No	Yes	No	No	Yes
Minna	Yes	No	No	Yes	No	Yes
Zaria	Yes	No	No	Yes	No	Yes

Source: Authors compilation, 2017. H means homogenous (if dataset was homogenous), HG refers to Homogenised series (if dataset was homogenised).

Table 4.2b: Homogeneity test and of Streamflow data from Shiroro Dam

Homogenisation Test	Shiroro Flow Station		
	Test	T	p-value
Standardised Normal Homogenisation Test	T0=2.6078	7/1/2009	0.8769
Pettitt's Test	K=1835.0000	5/1/2009	0.8038
Von Neumann's Test	N=0.6329		< 0.0001
Buishand's Test	Q=11.5424	7/1/2009	0.7159

Source: Authors computation, 2017.

Homogenisation test on precipitation for Kaduna proved otherwise from the result on temperature series. The precipitation data from Kaduna was not homogenous when the RHtestV4 was applied to the monthly series of the data. Monthly precipitation data from the other stations such as Jos, Minna and Zaria were also not homogenous and thereby required homogenisation.

Homogenisation test for streamflow was performed using statistical test which have been applied to streamflow. Four statistical test were used to test the Homogeneity of the streamflow data obtained from Shiroro dam. Results obtained from three of these test (Buishand's test, Standardised Normal Homogeneity test and Pettitt's test) for monthly streamflow data exhibited that the data was homogenous and were drawn from similar technique of flow recording and instruments. Table 4.2b shows the results of The Von Neumann's test statistics pointed out that the p-value obtained was lesser than the significant level indicating that the data is in homogenous. The data was classified as being homogenous without any further homogenisation techniques applied to it since three out of the four test affirm this conclusion.

4.3 Trend Analysis

4.3.1 Autocorrelation

The data series from the weather stations (maximum and minimum temperature and precipitation) and the Shiroro dam (streamflow) were tested for serial correlation. This prior test is to ensure the data series are drawn from independent series. Figure 4.1, 4.2 and 4.3 illustrate the test of autocorrelation using autocorrelation function for annual averaged maximum temperature, minimum temperature, and annual summed precipitation and streamflow for the weather stations and the Shiroro dam respectively. Figure 4.4, 4.5 and 4.6 shows the partial correlation test for the maximum temperature,

minimum temperature, and precipitation and streamflow for the weather stations and the Shiroro dam respectively. The autocorrelation or partial correlation which are present at any lag will exceed the confidence bound (blue lines) on the plots which are obtained from a 95% confidence level.

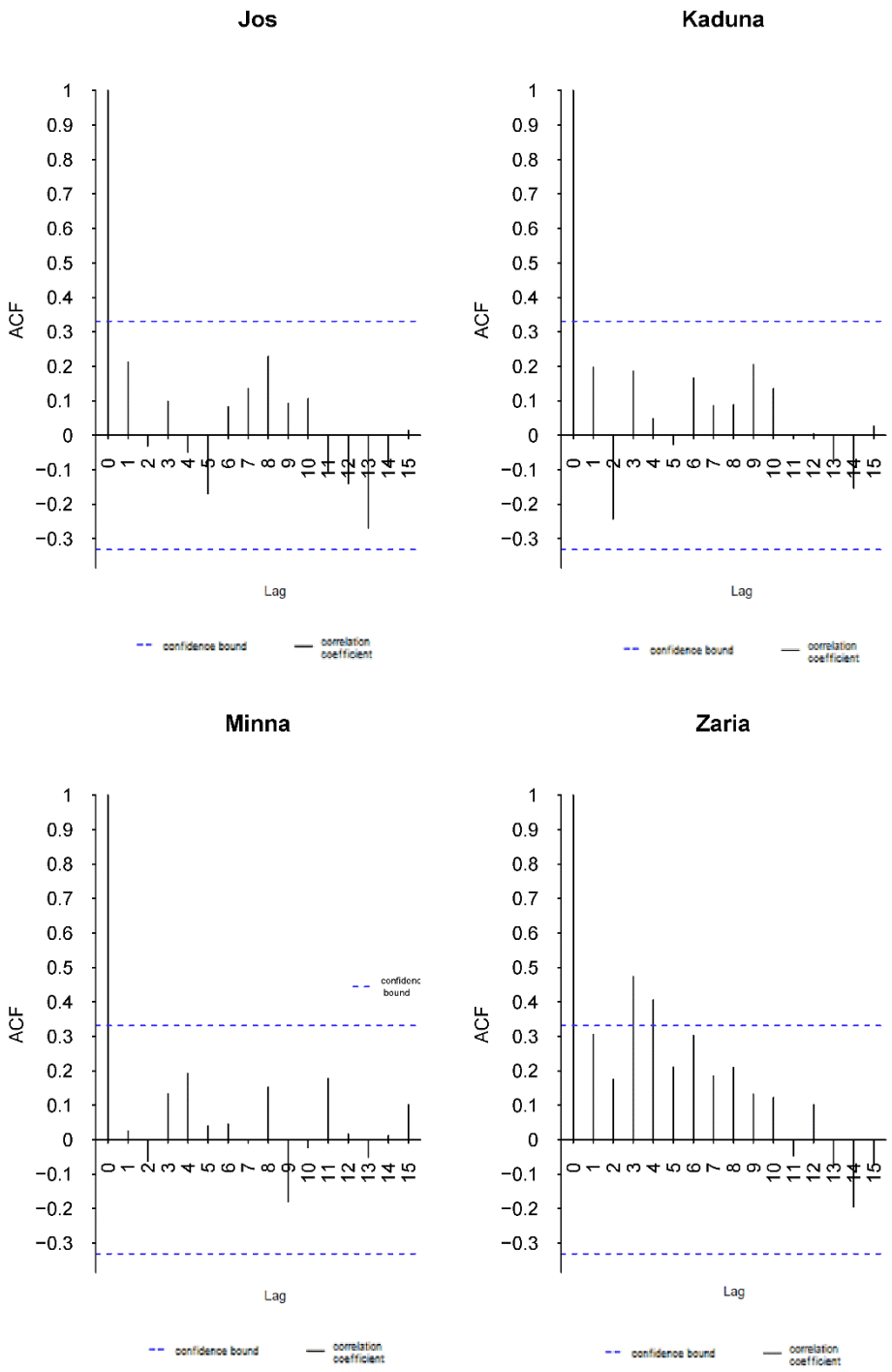

Figure 4.1. Autocorrelation plot of Maximum Temperature for the weather stations

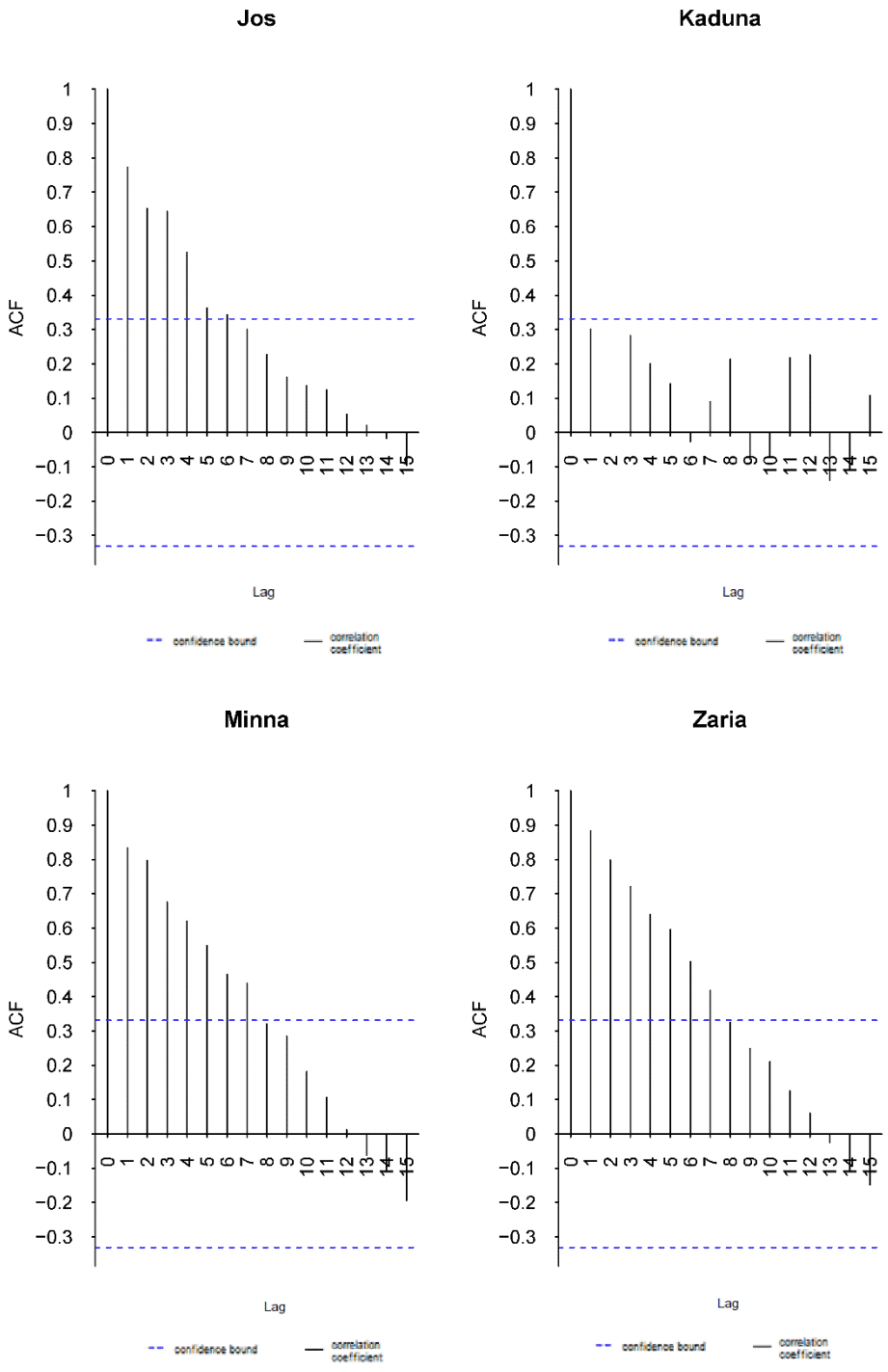

Figure 4.2. Autocorrelation plot of Minimum Temperature for the weather stations

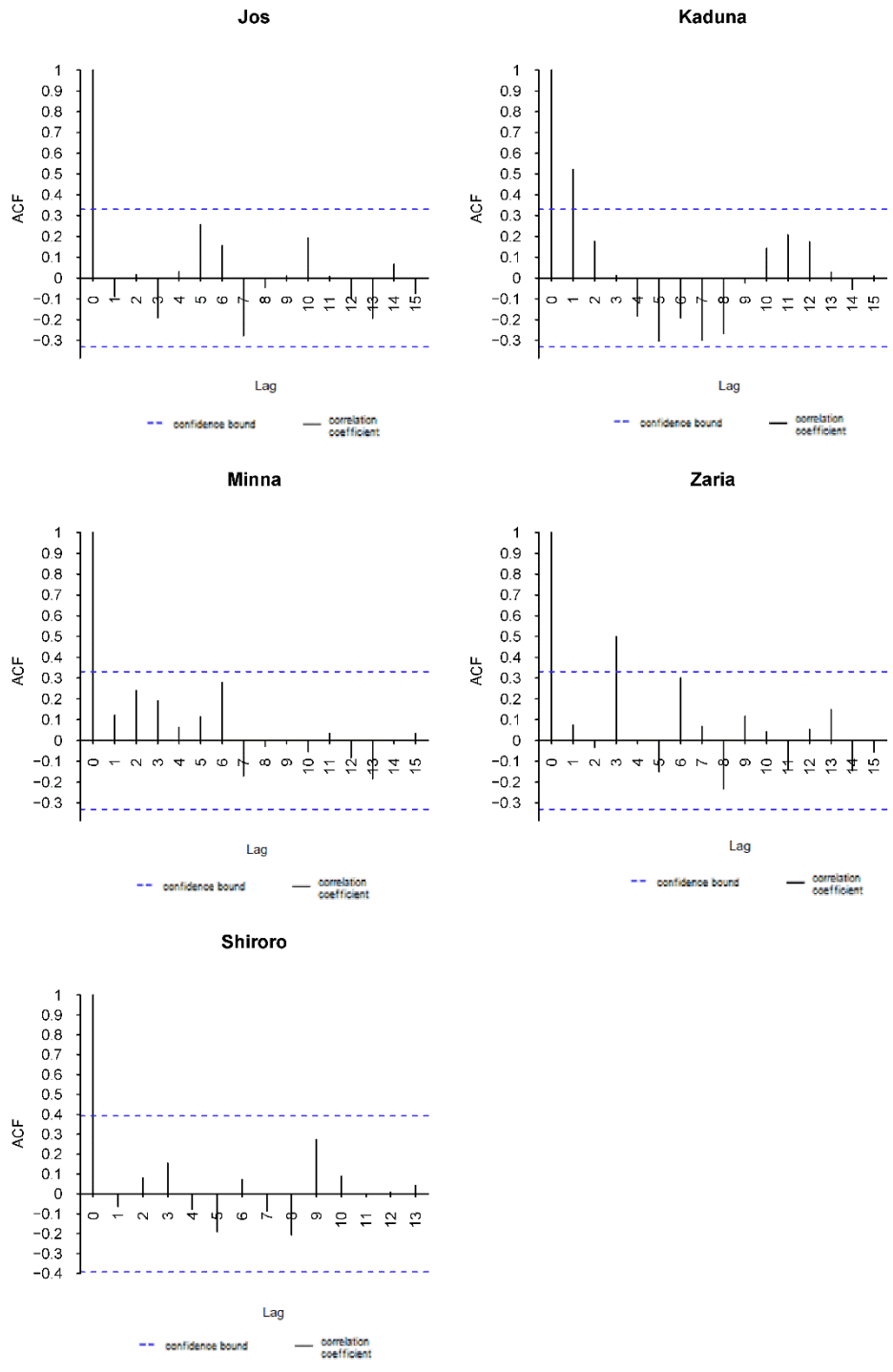

Figure 4.3. Autocorrelation plot of Precipitation for the weather stations and Shiroro Dam streamflow

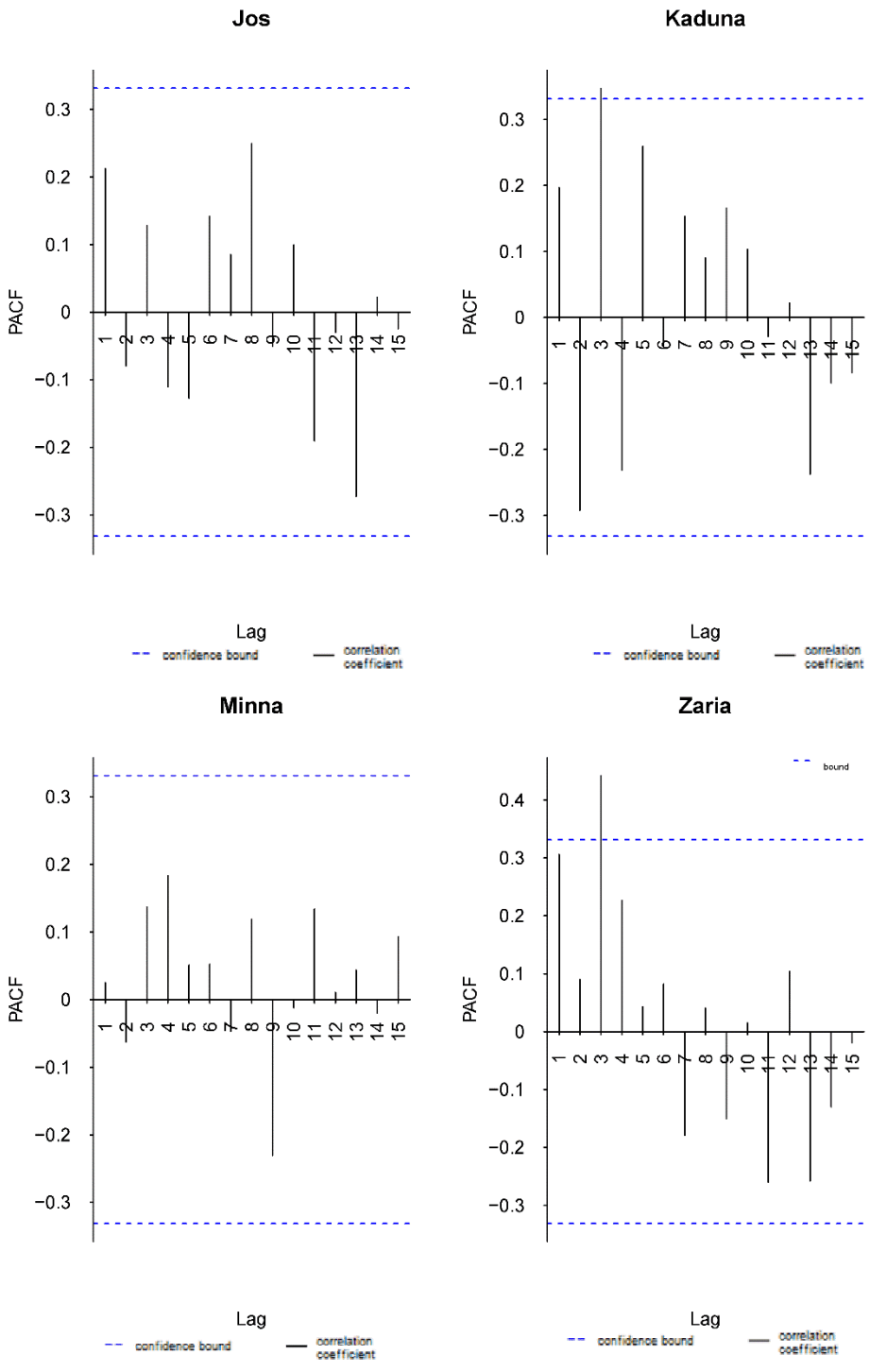

Figure 4.4. Partial autocorrelation plot of Maximum temperature for the weather stations

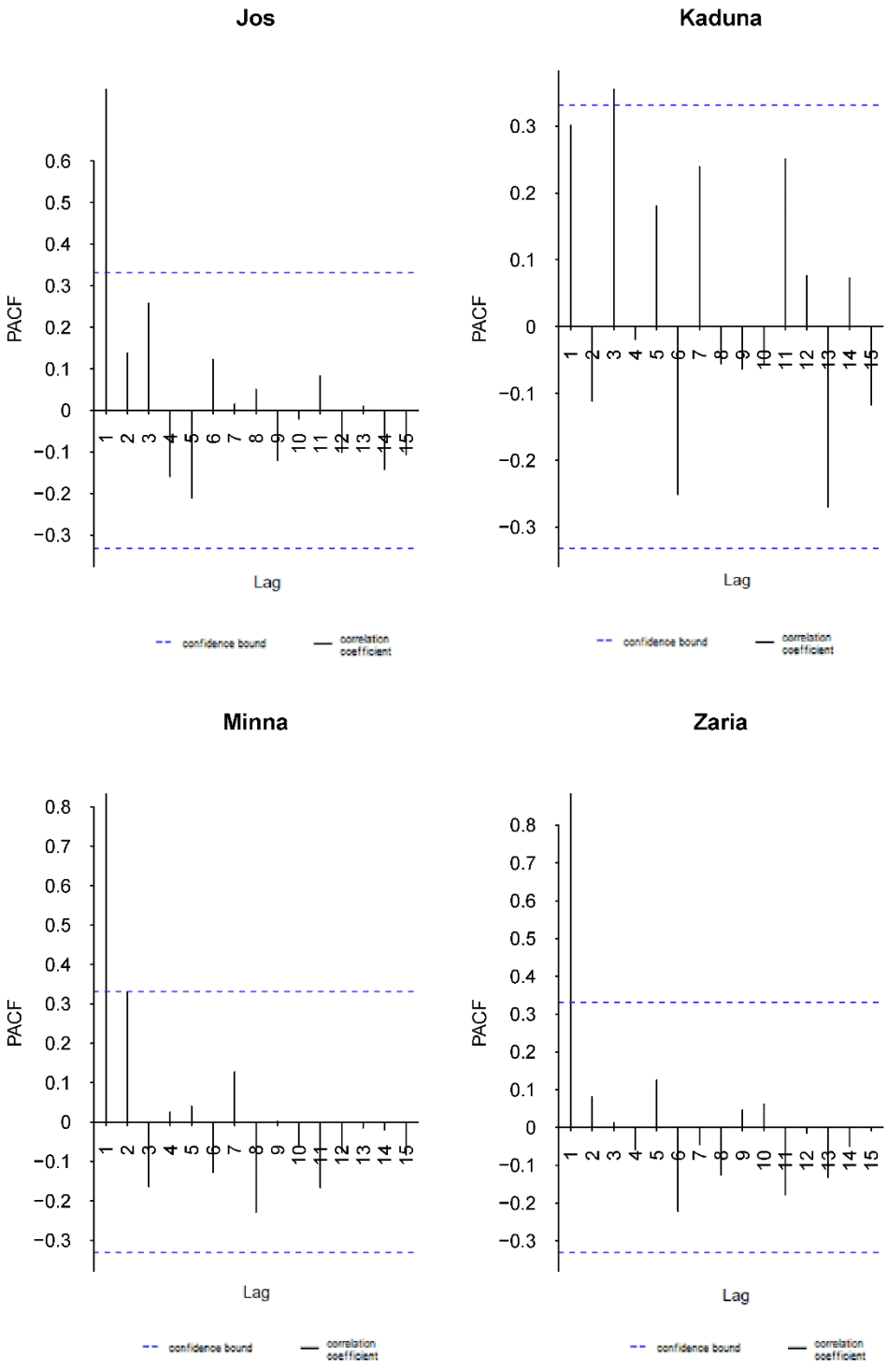

Figure 4.5. Partial autocorrelation plot of Minimum temperature for the weather stations

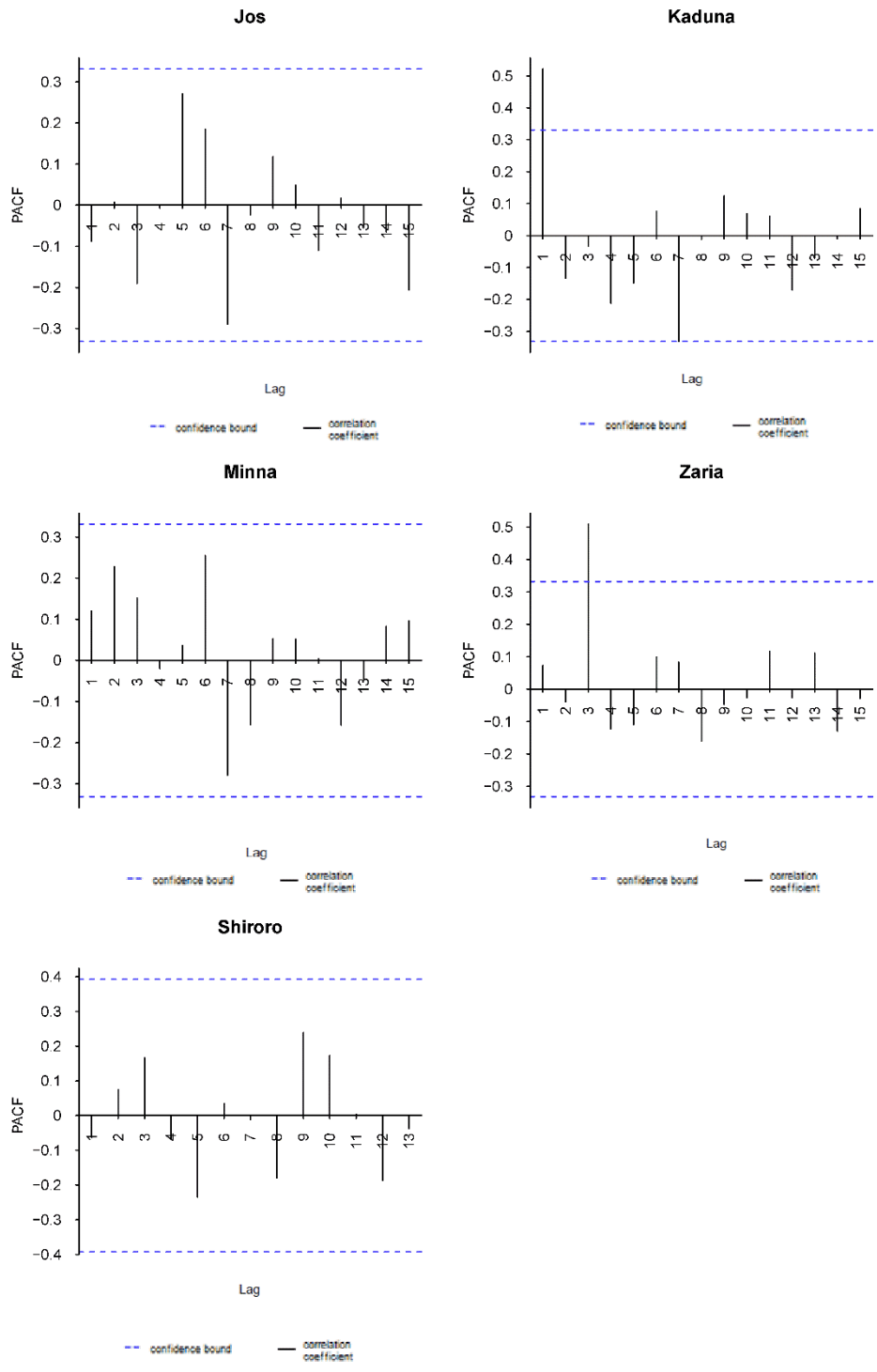

Figure 4.6. Partial autocorrelation plot of Precipitation for the weather stations and streamflow at Shiroro Dam

All the stations evaluated reported no autocorrelation at lag 1 in the maximum temperature series. Minimum temperature series test of autocorrelation for each stations at lag 1 as shown in Figure` 4.2 and 4.5 demonstrated the presence of autocorrelation in Jos, Kaduna and Zaria series. Precipitation series from each stations outlined the presence of autocorrelation at lag 1 in Kaduna series. Streamflow data had no autocorrelation at lag 1. These results affirmed the importance of utilising the modified Mann-Kendall test to analyse the trend of the series.

4.3.2 Mann-Kendall trend test

4.3.2.1 Temperature

Figures 4.7 and 4.8 illustrate the plot 12 months average observed maximum and minimum temperature of the stations within Shiroro catchment basin and and its surroundings, beginning from the year 1981 to 2015. The station in Minna is located outside the Shiroro catchment whiles Jos, Kaduna and Zaria are located in the basin.

The Mann-Kendall test was applied to the maximum temperature values of each stations at a confidence level of 95 %. The results are shown in Table 4.3 for the annual time series, the p-value was set at 0.05, implying that any station statistics that produces a p-value less than the set significance level (α) of 0.05 will lead to the H_0 being rejected. This implies that a trend is present in the data series and that trend is significant statistically. On the other hand, where the p-value obtained was more than the level of significance (α), the H_0 of no trend is accepted.

Maximum and Minimum Temperature

The Mann-Kendall test shows interesting result for the stations analysed for the maximum and minimum temperature, average annual temperature and seasonal maximum and minimum temperature.

The result of the Mann Kendall test for the annual time series shows that maximum temperature of the stations in Kaduna, Jos, Minna and Zaria was increasing. Amongst these stations, Kaduna, Jos and Zaria stations showed that the positive trend in maximum temperature were statistically significant, thereby suggesting that H_0 can be rejected whilst the trend of maximum temperature in Minna was statistically not significant. Zaria time series recorded the second highest S of 295 but the τ = 0.4957983 was poor indicating a weak trend. Jos, Kaduna and Minna also displayed τ values less than 0.5 indicating a weak strength of the trend. The Sen's slope suggested that the annual maximum temperature of Kaduna, Jos, Minna and Zaria which had increasing trends having slope magnitude of 0.0161 °C/annum, 0.0122 °C/annum, 0.0162 °C/annum and 0.0280 °C/annum respectively. Zaria recorded the highest increase in maximum temperature among all the stations.

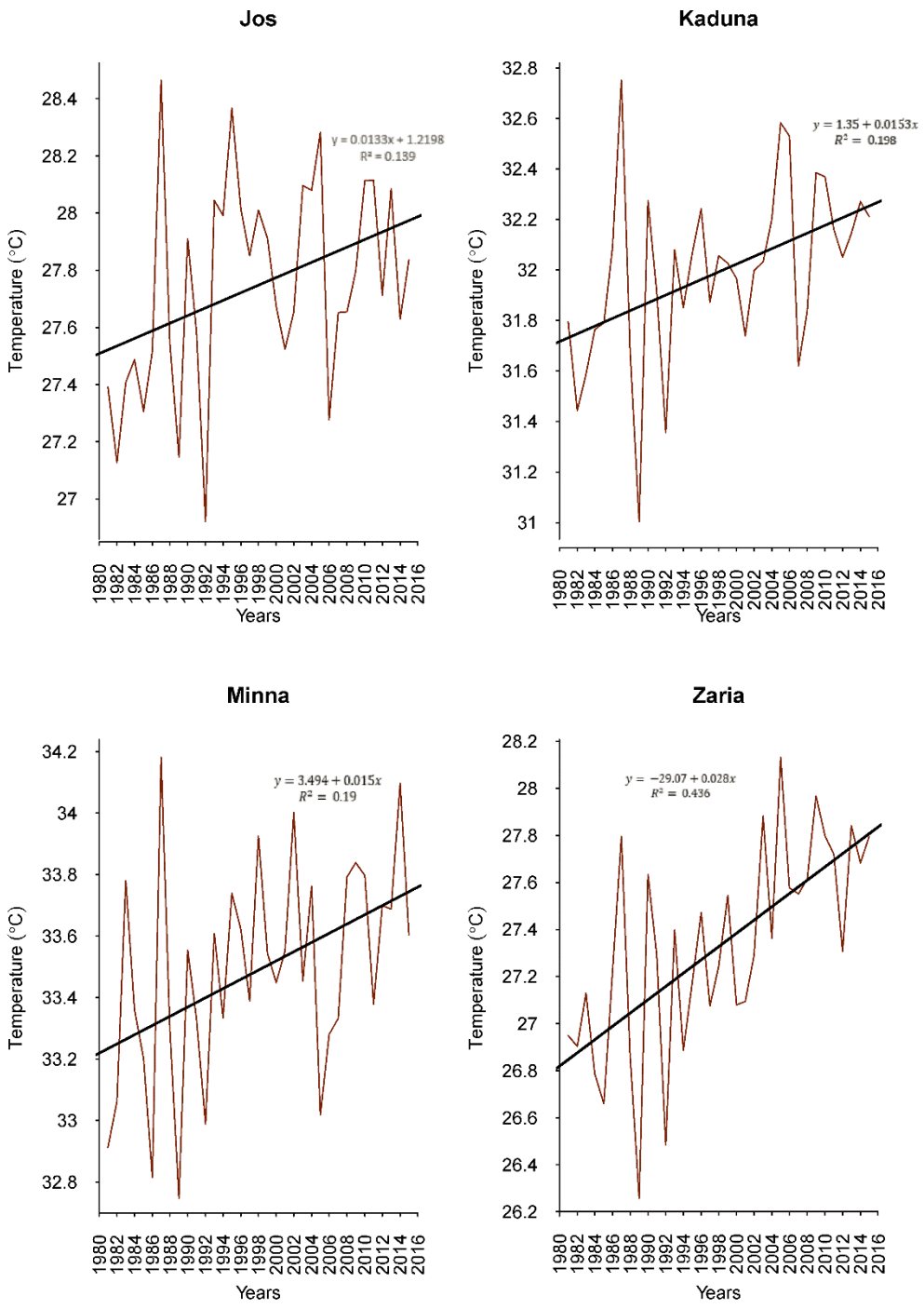

Figure 4.7. Plot of the Maximum Temperature averages of the Stations (Kaduna, Jos, Minna and Zaria)

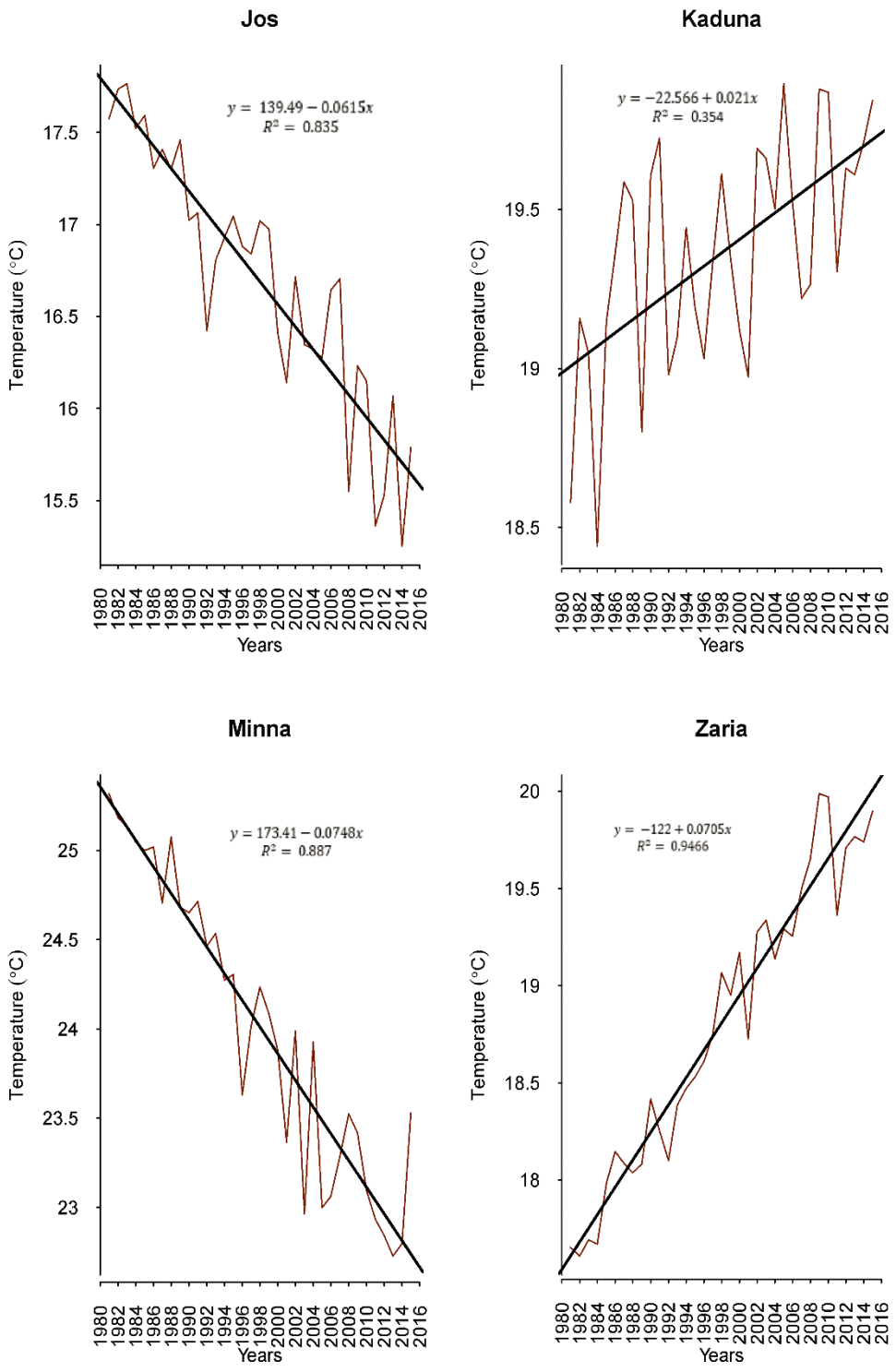

Figure 4.8. Plot of the Minimum Temperature averages of the Stations (Kaduna, Jos, Minna and Zaria)

Table 4.3: Mann-Kendall test result for the annual Maximum Temperature time series (from 1981 to 2015)

Mann-Kendall Test	**Stations**			
	Kaduna	**Jos**	**Minna**	**Zaria**
Mann-Kendall Score (S)	197.0	173.00	187.0	295.00
Kendall's Tau	0.33109	0.29076	0.31429	0.49580
Var (S)	4958.33	4958.33	4958.33	4958.33
Z	2.78348	2.44265	2.64147	4.17522
p-value (two tailed test)	0.00538	0.01458	0.00825	2.98×10^{-5}
Var*(S)	1565.603	4958.333	4958.33	4958.33
Corrected Z	4.95354	2.44265	2.64147	4.17522
N/N*	0.31575	1	1	1
Sen's Slope	0.01609	0.01216	0.01617	0.02801
Corrected p-value	7.2877×10^{-7}	0.01458	0.00825	2.98×10^{-5}
Alpha (α)	0.05	0.05	0.05	0.05
Test Interpretation	Reject H_0	Reject H_0	Reject H_0	Reject H_0

Source: Authors compilation, 2017.

The Mann-Kendall was applied to the annual minimum temperature series from the stations between the time period of 1981 to. Table 4.4 illlustrate the result of the Mann Kendall test statistics for all the stations that were investigated. Jos and Minna exhibit a decreasing trend in minimum temperature series over the period. The trend exhibited by these stations were statistically significant. Kaduna and Zaria also recorded positive trends in the observed period wich were also statistically significant. The Thiel Sen's slope results suggest that the minimum temperature in Kaduna and Zaria are increasing annually at a magnitude of 0.018958 °C/annum and 0.07012 °C/annum respectively whilst Jos and Minna were decreasing with an annual magnitude of -0.0600 °C/annum and -0.07704 °C/annum respectively. The change in minimum temperature in Jos was the highest among the stations investigated.

Table 4.4: Mann-Kendall test result for the annual Minimum Temperature time series (from 1981 to 2015)

Mann-Kendall Test	**Stations**			
	Kaduna	Jos	Minna	Zaria
Mann-Kendall Score (S)	241	-471	-485.0	519
Kendall's Tau	0.40504	-0.79160	-0.815	0.872
Var (S)	4958.333	4958.333	4958.33	4958.333
Z	3.40834	-6.67467	-6.87349	7.35634
p-value (two tailed test)	0.00065	2.4778×10^{-11}	6.2649×10^{-12}	1.89×10^{-13}
$Var^{*}(S)$	1702.61	2887.1505	4958.33	4958.333
Corrected Z	5.81639	-8.74708	-6.87349	7.35634
N/N*	0.34338	0.58228	1	1
Sen's Slope	0.01895	-0.0600	-0.07704	0.07012
Corrected p-value	6.01×10^{-9}	2.1894×10^{-18}	6.2649×10^{-12}	1.89×10^{-13}
Alpha (α)	0.05	0.05	0.05	0.05
Test Interpretation	Reject H_0	Reject H_0	Reject H_0	Reject H_0

Source: Authors compilation, 2017.

Annual Temperature

The annual temperature were obtained by finding the average between the annual maximum and minimum temperature series for each station. Mann Kendall test on the average temperature of each station depicted the presence of significant trend in the temperature series. Jos and Minna revealed genarally decreasing trend in mean annual temperature with annual rate of -0.06 °C, -0.02 °C and -0.03 °C respectively. The statistics obtained from Jos was in agreement with Akinosola and Ogunjobi (2014) with the decreasing trend of Minna contrasting their findings. These decrease in temperature are far below the global annual increase of 0.25 °C to 0.27 °C per decade. Kaduna and Zaria which are found in the northern part of the catcment has an increasing trend in average temperature with magnitude of 0.018 °C and 0.049 °C per annum respectfully. Kaduna rate of annual temperature change were similar to the findings of Okpara *et al.* (2013) of change in the Lower Niger of 0.0163 °C whilst Zaria rate of change was above their average obtained and lower than the global mean temperature change from 2001 to 2005 (IPCC, 2007c). The mean annual temperature and the minimum temperature trend decrease of Jos and Minna were in agreement whiles their maximum temperature indicated an increasing trend. Kaduna and Zaria mean, maximum and minimum annual temperature were in agreement connoting an increasing trend.

Table 4.5: Mann-Kendall test result for the annual Average Temperature time series (from 1981 to 2015)

Mann-Kendall Test	Stations			
	Kaduna	**Jos**	**Minna**	**Zaria**
Mann-Kendall Score (S)	259	-341	-375	445
Kendall's Tau	0.435	-0.573	-0.63	0.748
Var (S)	4958.333	4958.333	4958.333	4958.333
Z	3.66397	-4.82849	-5.31134	6.30544
p-value (two tailed test)	0.00025	1.3757×10^{-6}	1.0882×10^{-7}	2.874×10^{-10}
Var*(S)	1494.206	4181.963	4958.333	4958.333
Corrected Z	6.67443	-5.25767	-5.31133	6.30543
N/N*	0.30135	0.84340	1	1
Sen's Slope	0.01809	-0.02132	-0.03042	0.04915
Corrected p-value	2.4819×10^{-11}	1.4589×10^{-7}	1.0882×10^{-7}	2.874×10^{-10}
Alpha (α)	0.05	0.05	0.05	0.05
Test Interpretation	Reject H_0	Reject H_0	Reject H_0	Reject H_0

Source: Authors compilation, 2017.

4.3.2.4 Total Annual Precipitation

Total annual precipitation for all the stations were tested for presence of trend by employing the Mann-Kendall trend test and Sen's slope. Table 4.6 illustrates the test statistics obtained from the Mann-Kendall trend test. All the precipitation data from all the stations unveils the presence of positive trend in the dataStations that indicated significant positive trend were Kaduna, Minna and Zaria with magnitude of 6.81 mm per annum, 5.378 mm per annum and 7.983 mm per annum respectively.

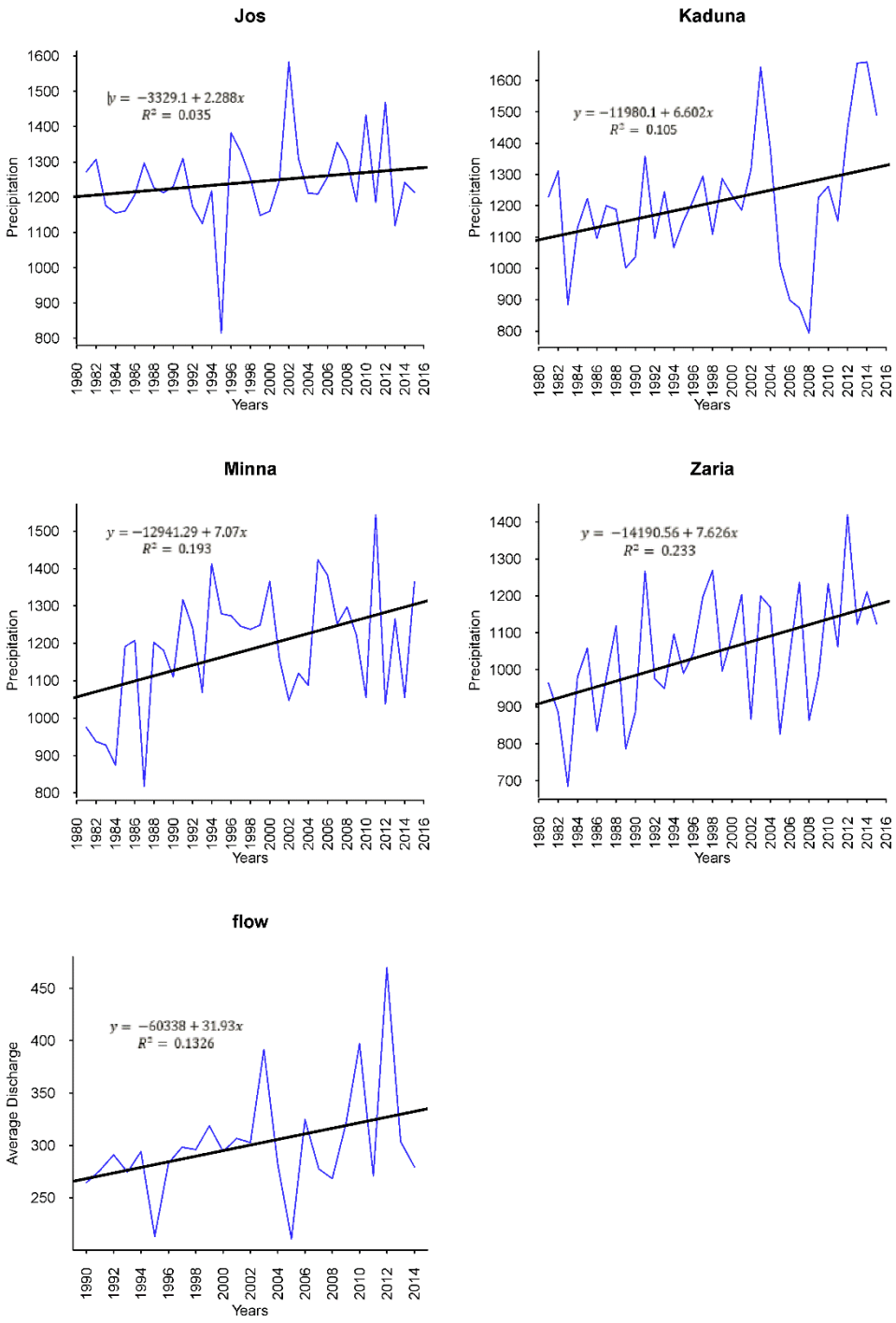

Figure 4.9: Plot of the Precipitation of the stations (Kaduna, Jos, Minna and Zaria) and averages discharge from the Shiroro Dam

Table 4.6: Mann-Kendall test result for the annual precipitation time series (from 1981 to 2015)

Mann-Kendall Test	Stations			
	Kaduna	**Jos**	**Minna**	**Zaria**
Mann-Kendall Score (S)	129	63	151	205
Kendall's Tau	0.22	0.11	0.25	0.345
Var (S)	4958.333	4958.333	4958.333	4958.333
Z	1.8178	0.8805	2.1302	2.8971
p-value (two tailed test)	0.069	0.3786	0.0332	0.0037
Var*(S)	3472.321	1417.587	4958.333	3127.221
Corrected Z	2.1722	1.6467	2.1302	3.6479
N/N*	0.7003	0.2859	1	0.6307
Sen's Slope	6.81	1.75	5.378	7.983
Corrected p-value	0.0298	0.0996	0.0332	0.00026
Alpha (α)	0.05	0.05	0.05	0.05
Test Interpretation	Reject H_0	Accept H_0	Reject H_0	Reject H_0

Source: Authors compilation, 2017.

4.3.2.5 Streamflow and evaporation trend at Shiroro dam

Mann-Kendall trend test was applied on streamflow data spanning 25 years from the year 1990 to 2015. The results as illustrated in Table 4.7 show the presence of positive trend in the time series but the trend was statistically not significant having computed the p-value of 0.0721 which is greater than the significant value of 0.05. Evaporation data (Figure 4.10) at the dam site reveal a negative trend which was in agreement with the temperature trends in Minna situated downstream of the dam. The statistics of climate from the surrounding stations (Minna) demonstrates decreasing temperature trends years whilst there are no significant trends in precipitation.

Table 4.7: Mann-Kendall test result for the annual Streamflow series (from 1981 to 2015) for the Shiroro Dam

Mann-Kendall Test	Shiroro Station
	Streamflow
Mann-Kendall Score (S)	78
Kendall's Tau	0.26
Var (S)	1833.333
Z	1.7983
p-value (two tailed test)	0.0721
Var*(S)	1833.333
Corrected Z	1.7983
N/N*	1
Sen's Slope	20.74
Corrected p-value	0.0721
Alpha (α)	0.05
Test Interpretation	Accept H_0

Source: Authors compilation, 2017.

In summary, there exist climate variability existence in the Shiroro catchment supported by statistics from Zaria, Kaduna, Jos and Minna. Kaduna stations stations reveal a positive trend in maximum temperature values with a low Tau value of 0.33 implying lower strength of the trend which is significant, minimum temperature has a positive trend with a Tau value of 0.4 indicating low strength of the trend inherrent in the data. Precipitation also shows an increasing trend with a Tau value of 0.22. The same situation occurs in the precipitation time series with a positive trend but a low Tau value. Similarly, the Zaria time series of maximum temperature, minimum temperature average air temperature and

precipitation all record an increasing trends with Tau values of 0.495, 0.872, 0.748 and 0.345 respectively. The maximum daytime temperature and night time (minimum) temperature in the Zaria and Kaduna station indicates increasing trend which agrees with the average temperature time series which could suggest an increase occurence of hotter days and hotter nights. The evaporation is likely to increase with increasing temperature whilst the trends in precpitation shows lower strength in magnitude will not be enough to compensate for water losses from surfaces. Jos stations shows a lower strength of positive trend in maximum temperature, minimum temperature records a strong negative trend with Tau values of -0.74. Thus, implying more rapid lower temperature and hotter temperatures. The average air temperature had strong negative trend with Tau value of 0.748. Precipitation showed positive trend which was not siginificant. Stations surrounding the catchment such as Minna had strong negative trends in average air temperature with Tau values of -0.883 and -0.63 respectively. Precipitation in Minna had low strength. Night time temperature in Minna experiences a cooling trend whilst daytime temperature is increasing with low strength in the trend compared to minimum temperature. Streamflow data shows positive trend in the period observed but was not significant.

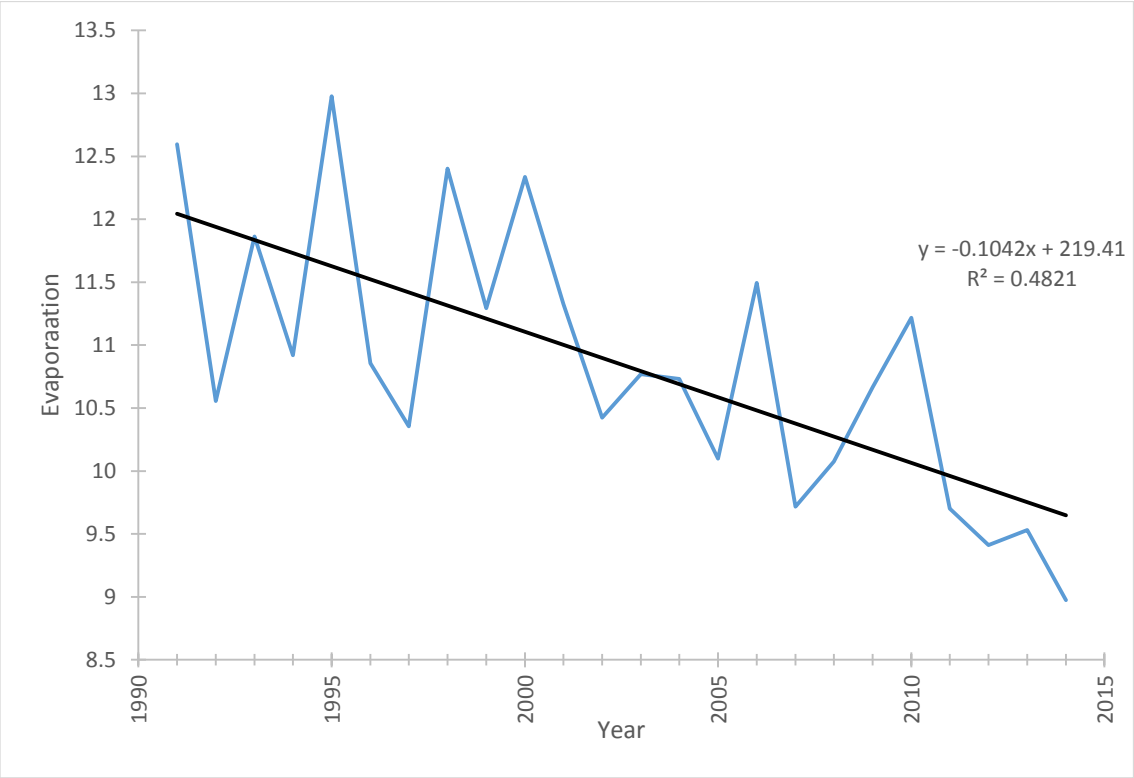

Figure 4.10. Evaporation Trend at Shiroro Dam (from 1991 to 2014) (source: Author)

4.4 Soil and Water Assessment Tool Setup, Calibration and Validation Analysis

4.4.1 Model Setup

The characteristic soil map, slope map and land use maps reclassified during the model setup are shown in Figure 4.11 – 4.13. The total Shiroro dam catchment area delineated is 3468410.2514 ha (34684.102514 km) with 21 subbasins and 109 hydrologic response units. The dominant land use in the catchment is agricultural comprising 86.43% of the total catchment area, 12.46 % of the area are covered by range and grasses, with minor land uses such as residential, forest (mixed and deciduous), range and brush, barren land and wetlands account for 0.52 %, 0.02 %, 0.11 %, 0.1 % and 0.05 % respectively. Table 4.8 shows the dominant soil in the catchment.

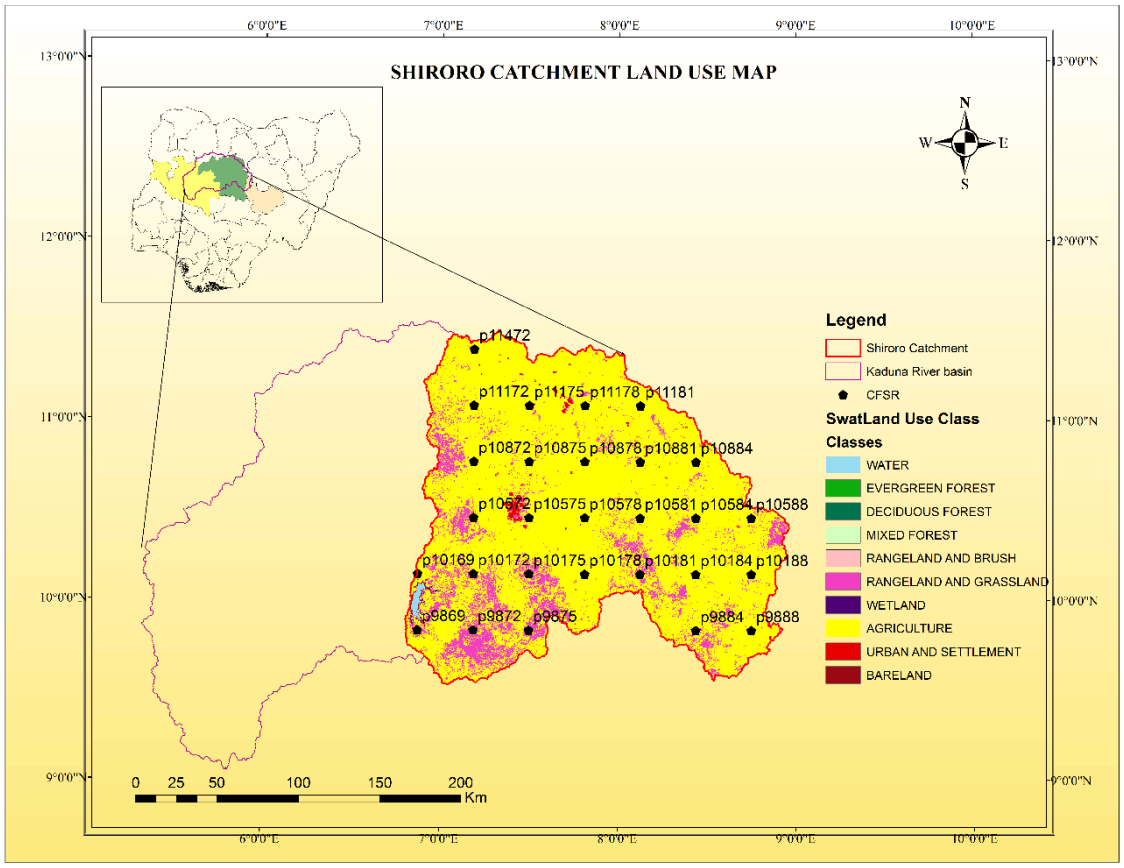

Figure 4.11. Shiroro Catchment Map showing the land use and the Kaduna River Basin

Table 4.8: Soil types, textural class and hydrologic groups found the Shiroro catchment

Dominant Soil Name	Soil classification	Hydrologic Group	TEXTURE	Watershed Area %
Lithosols	I-60	C	LOAM	0.76
Lithosols	I-c-99	C	LOAM	0.46
Ferric Acrisols	Af12-2b-1020	D	SANDY_CLAY_LOAM	1.54
Orthic Acrisols	Ao43-1b-1056	C	LOAMY_SAND	1.56
Lithosols	I-Lf-1255	C	SANDY_CLAY_LOAM	1.46
Lithosols	I-bc-1324	C	LOAM	0.42
Ferric Luvisols	Lf1-1420	C	SANDY_CLAY_LOAM	0.02
Ferric Luvisols	Lf41-1-2a-1468	C	SANDY_LOAM	0.98
Ferric Luvisols	Lf42-1a-1470	C	SANDY_LOAM	11.77
Ferric Luvisols	Lf49-1a-1476	C	SANDY_LOAM	39.1
Ferric Luvisols	Lf53-1480	C	SANDY_CLAY_LOAM	0.61
Ferric Luvisols	Lf8-1493	C	SANDY_CLAY_LOAM	24.71
Gleyic Luvisols	Lg26-2a-1511	C	SANDY_CLAY_LOAM	16.25
Luvic Arenosols	Ql5-1632	C	SANDY_LOAM	0.37

Source: Authors compilation, 2017.

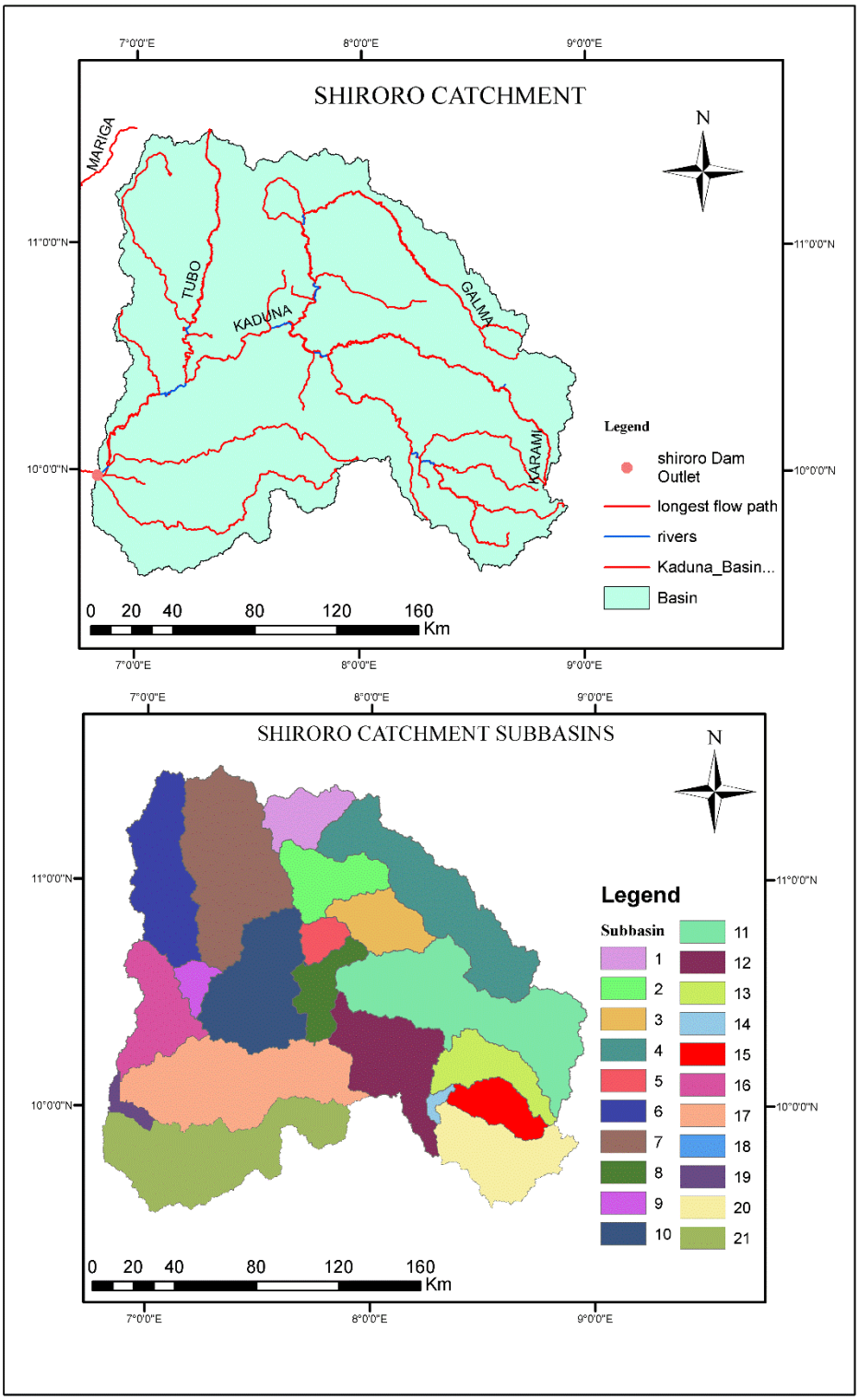

Figure 4.12. Catchment map of Shiroro Dam showing River network and the outlet (top map) and the Subbasins (bottom map)

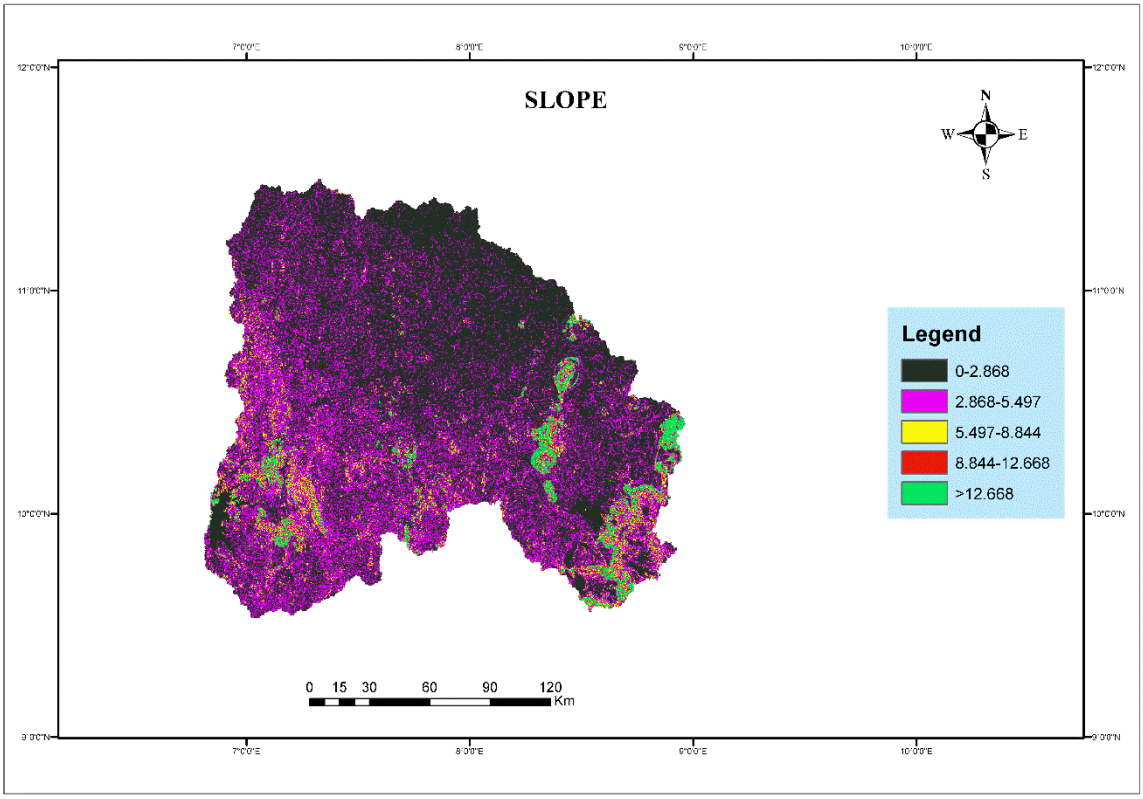

Figure 4.13. Catchment map of Shiroro Dam showing the slope classification

Luvisols forms a greater part of the catchment with a total percentage of 93.44 % of the total catchment. Other soil types are Lithosols and Acrisols having 3.1 % area each in the catchment with Arenosols being the least present soil having a catchment area percentage of 0.37 %. The slope class with the highest percentage in the subbasin is 0° – 2.868° accounting for 61.31 % of the catchment area indication that majority of the land surface of the catchment is near flat surface (near level lands). 30.15 % of the catchment have a slope class between 2.868° – 5.497° which can be classified as gentle sloping land. 5.497° – 8.844° (moderate slope) which is 3.97 % of the total catchment area, 8.844° - 12.668° % (strong slope) which is 1.50 % of the total catchment area and 12.668° - 9999° or > 12.668° (strong slope to very steep). These interpretation of slopes are based on the classification of slopes by the Barcelona Field Studies Centre.

4.4.2 Sensitivity Analysis

Soil Water Assessment integrates several parameters which are used for the calibration of models. Some of these parameters are location specific (Temperate regions and Tropical Regions) and also differs in sensitivity in different watersheds and even sub-watersheds during the calibration process of the model. The Global Sensitivity analysis was used to identify most sensitive parameters for the model calibration. This approach varies parameters simultaneously and thereby nullifies the issues associated with One at a Time sensitivity analysis (OAT). The most sensitive parameters during the calibration stage are illustrated in Table 4.9. Four parameters were sensitive out of the fourteen parameters used for the calibration of the model.

Table 4.9: Parameters Most Sensitive to flow in the Shiroro catchment

Parameter Name	t-stat	p-value	Min value	Max value	Fitted Value
R__CN2.mgt	4.94	0.000002	-0.209959	0.063959	-0.113403
V__GW_REVAP.gw	4.86	0.000003	0.073671	0.221329	0.197335
V__GWQMN.gw	4.12	0.000057	1041.76599	3683.23413	3452.1055
V__ESCO.hru	3.10	0.002255	0.480847	0.64066	1.0

Source: Authors compilation, 2017.

SUFI-2 algorithm fitted these parameters as sensitive with values having absolute t-stats values and lower p-value less than 0.05 significant level. The most sensitive parameter was the CN2 and least sensitive among the parameters was the ESCO.

4.4.3 Calibration and Validation of the Model

The SWAT model was initially setup using daily values of precipitation, relative humidity, solar radiation, maximum and minimum temperature, and wind in ArcSWAT. During the calibration, monthly values of streamflow data were used for the calibration of the model in the SWAT-CUP. Nash-Sutcliffe Efficiency was the objective function employed during the calibration of the model. A Nash-Sutcliffe objective function ranges between negative infinity (-∞) to one (1) (Abbaspour, 2015). Table 4.10 indicates the

results of calibration from the five iterations with 200 simulations using SUFI-2 algorithm.

Table 4.10: Calibration results for 200 simulations for each iterations

Iteration	Summary Statistics					
	NSE	***R^2***	***PBIAS***	**P-factor**	**r-factor**	**Mean Sim (mean Obs value)**
1st	0.38	0.49	2.9	0.92	2.80	277.77 (286.01)
2nd	0.43	0.51	-0.2	0.79	1.27	286.64 (286.01)
3rd	0.46	0.55	17.8	0.67	0.80	235.08 (286.01)
4th	0.47	0.55	13.9	0.56	0.50	246.32 (286.01)
5th	0.22	0.47	-14.4	0.82	1.52	327.14 (286.01)

Source: Author's compilation, 2017. Sim refers to the simulation values obtained and Obs is the observed values measured.

Based on Moriasi *et al.* (2015), the results of NSE and R^2 from the five iteration were unsatisfactory for monthly scale calibrations whilst the PBIAS for the 1st and 2nd iteration could be said to be very good. PBIAS of the 3rd iteration was unsatisfactory whilst those of the 4th and the 5th iteration suggest a satisfactory results for the calibration. Although an NSE value of one represents the models simulated streamflow values having perfect agreement with the observed streamflow values, values of NSE higher than zero of a model is considered acceptable performance level and a less than or equal to zero value shows that the average of the observed data is a better at prediction than the model (Dile and Srinivasan, 2014). The 2nd iteration simulated streamflow average (286.64 m^3/s) value was the closest the observed average streamflow value of 286.01 for the calibration

period also indicating an overestimation. The 1st iteration simulated average streamflow (277.77 m^3/s (underestimation)) was the next in good estimate closer to average observed streamflow, other iterations such as 4th iteration (246.32 m^3/s (underestimation)), 5th iteration (327.14 m^3/s (overestimation)) and 3rd iteration (235.08 m^3/s (underestimation)) follow in the order of difference of simulated streamflow values from the observed streamflow values. In accounting for uncertainty in the calibration of the model, all the p-factor representing the amount of observed streamflow values enclosed by the 95PPU band were all greater than 0.5 for all iterations revealing that higher amount of observed streamflow were bracketed. The r-factor being the depth of the enclosed 95PPU band bracketing the observed data were also good except for the value obtained in the 1st iteration which was rather large.

In selecting the goodness of fit iteration for as the best solution out of these results, the recommendations of Abbaspour *et al*. (2015) based on uncertainty analysis. They recommended a p-factor greater than 0.7 and r-factor less than 1.5. Therefore, the 2nd iteration was selected as a good fit using this criteria. The 2nd iterations had the best average simulated streamflow to average observed streamflow in prediction. The value of PBIAS of -0.2 was significantly good even though the negative sign suggested an overestimation of the simulated streamflow to the observed streamflow. The NSE value obtained during calibration range was in agreement with the range stipulated in the results of Schuol *et al.* (2008) in the basin. Figure 4.14 shows the plot of the simulated and observed streamflow obtained in the calibration.

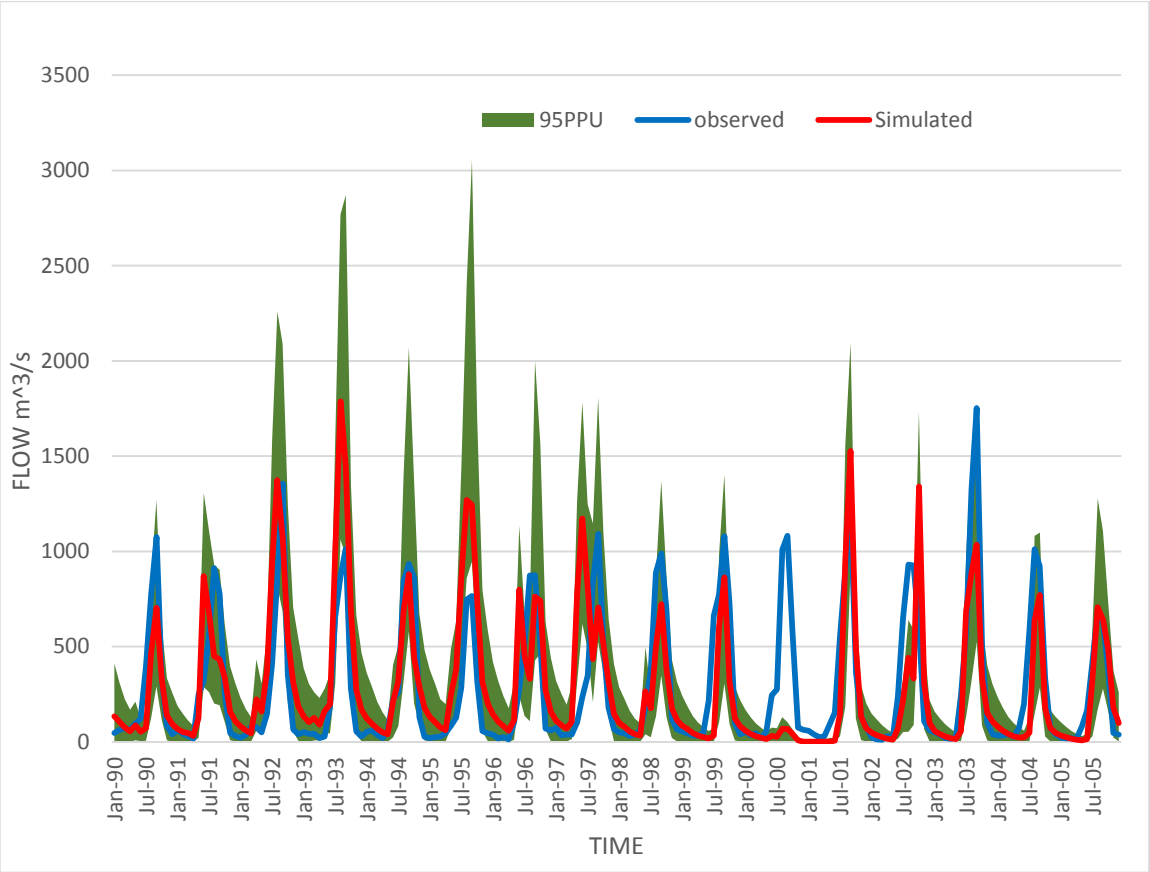

Figure 4.14. Calibration of model from the year 1990 to 2005

The calibrated model was able to simulate flow peaks at similar periods as the observed peak flow but the simulated discharge reveals patterns of underestimation and overestimation of flow in a number of the years. The periods June 1990 to Dec 1990, July 1998 to January 1999, July 1999 to January 2000, July 2003 to January 2004 and July 2004 to January 2005 indicates the period where underestimation of simulated peak flow by the calibrated model. The model overestimate peak flow between July 1993 to January 1994, July 1995 to January 1996 and July 2002 to January 2003. There is a record of a drought year by the simulated flow between the periods of June 2000 to January 2001 where peak flow recorded in the simulated flow as against the observed flow for that period was extremely low. This is as a result of the precipitation data used in modelling (Srinivasan, 2013). During that period NCEP CFSR precipitation data from all the stations recorded very low rainfall. Applying an assumption that closer weather stations

of CFSR to an in-situ weather station should have similar climatic features, in- situ observed weather stations' (located in the Shiroro catchment) monthly precipitation series were compared with CFSR weather station points close-by to investigate the low peak recorded between the periods of June 2000 to January 2001. Figure 4.15 illustrates the monthly precipitation values of the weather stations of observed in-situ stations and nearby CFSR weather stations. From the plot Figure 4.15 and 4.16 the CFSR peak precipitation records fall below the observed in-situ peak precipitation average amount by about 150 mm for both Kaduna and Zaria stations. Figure 4.17 reveal not much of significant difference between the periods. The annual precipitation of the CFSR stations in close proximity to Zaria, Kaduna and Jos were compared with annual precipitation of these stations. CFSR (p11175 (330.12 mm) and p11178 (347.67 mm)) stations close to Zaria weather station (1089.9 mm) were less than the annual precipitation of the observed records by a range of 742.23 mm to 759.78 mm (0.68 % to 0.0.69 % of the observed annual precipitation) in the year 2000. Also, CFSR stations (p10572 (321.39 mm), p10575 (451.32 mm) and p10875 (423.27 mm) in close proximity to Kaduna (1232.8 mm) weather station were less than the annual precipitation of the observed records by a range of 781.48 mm to 911.41 mm (0.63 % to 0.74 % of the observed annual precipitation) in the year 2000. Finally, CFSR stations (p9888 (672.56 mm), p9891 (705.39 mm) and p10188 (415.28 mm) near Jos (1160 mm) weather station were less than the annual precipitation of the observed records by a range of 454.61 mm to 744.72 mm (0.39 % to 0.64 % of the observed annual precipitation). These deficits in annual precipitation amount in the year 2000 may account for the low prediction in the model during the calibration stage.

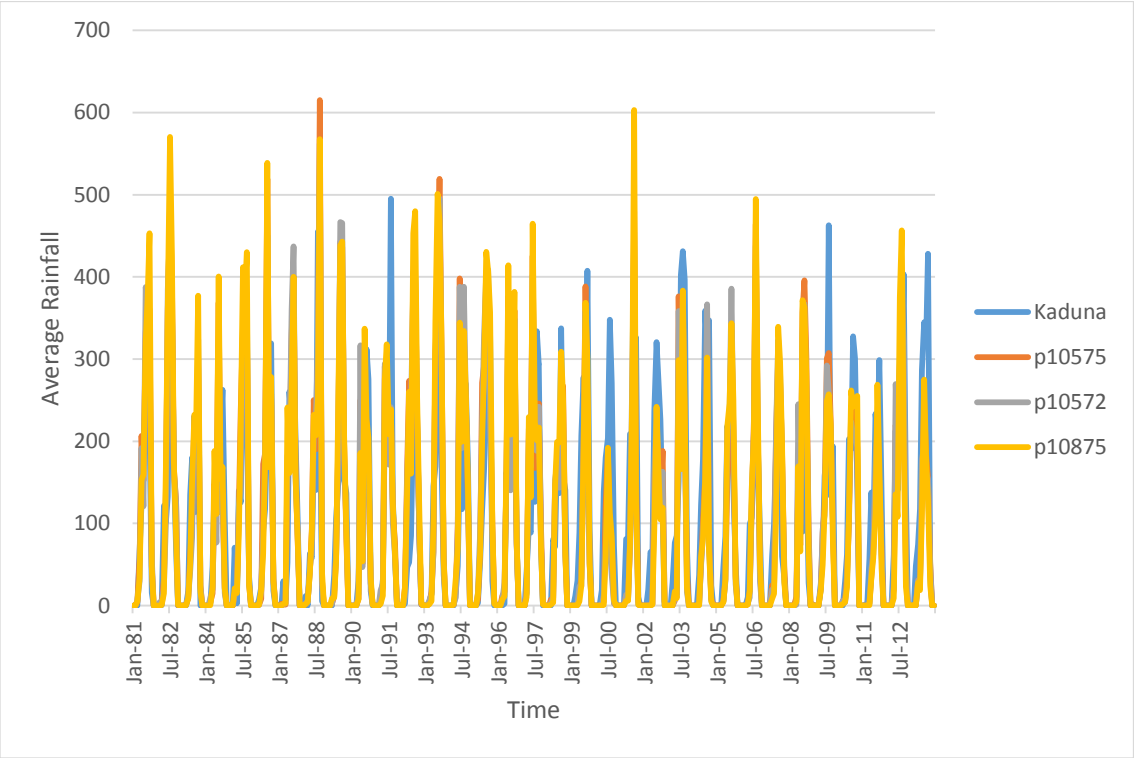

Figure 4.15. Monthly precipitation of Kaduna Station and nearby CFSR weather stations in the Catchment

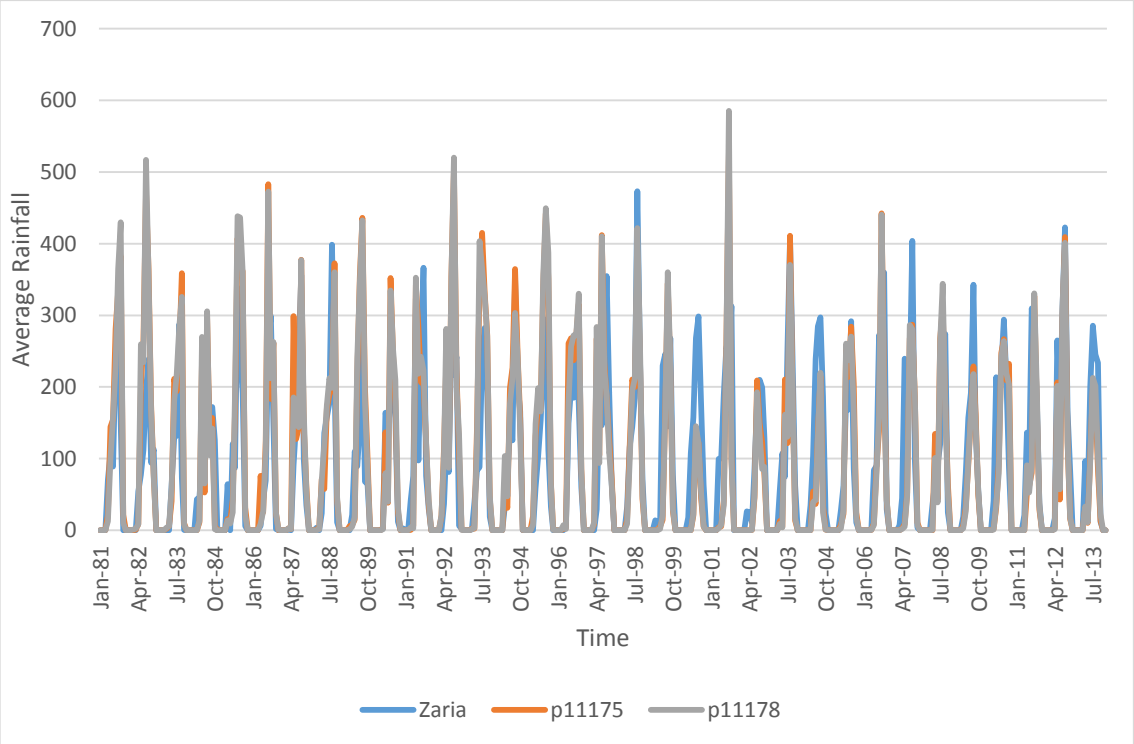

Figure 4.16. Monthly precipitation of Zaria Station and nearby CFSR weather stations in the Catchment

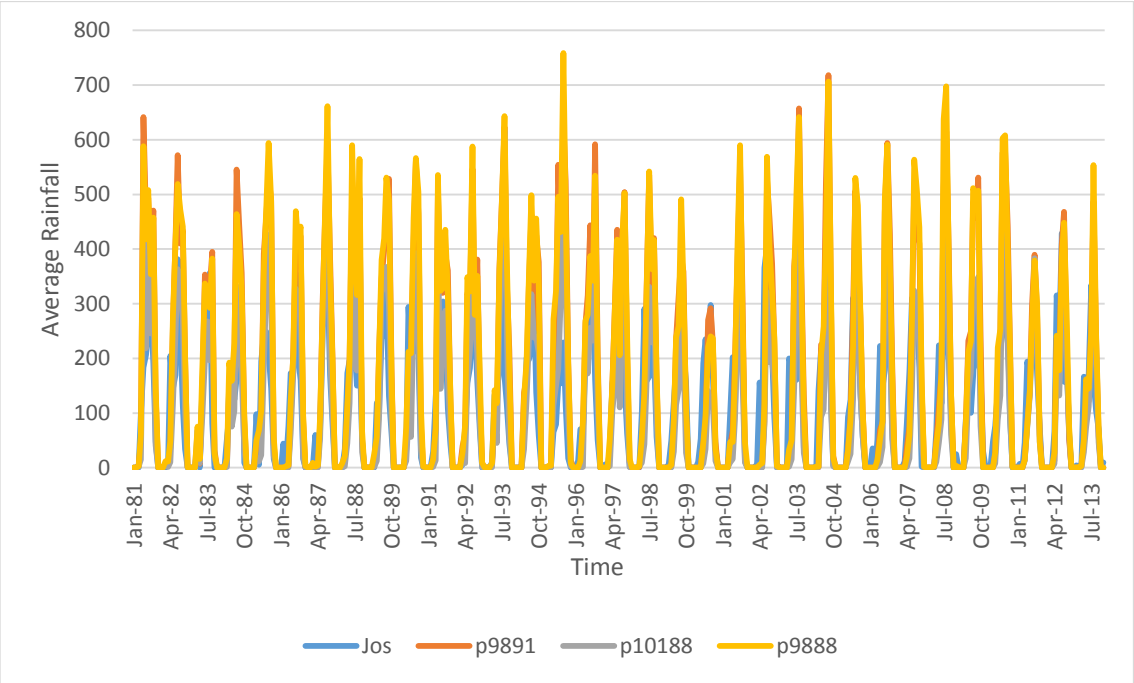

Figure 4.17. Monthly precipitation of Jos Station and nearby CFSR weather stations in the Catchment

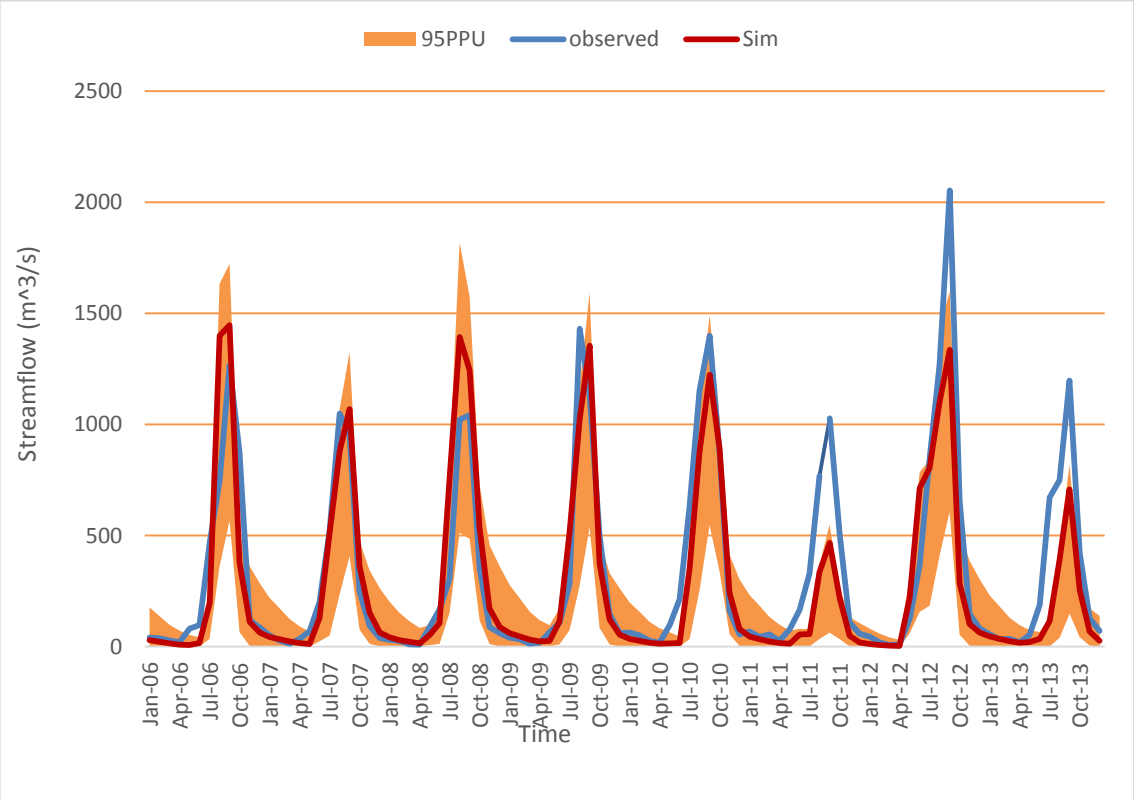

Figure 4.18. Validation of model from the year 2006 to 2013

During the validation stage of the model (Figure 4.18), the statistical results from the validation of the model reveal improved values of NSE and R^2 compared to the calibration period. The NSE value for the validation period was 0.77, R^2 was 0.79 and PBIAS was 8.3. According to Moriasi *et al.* (2015), these values obtained for all the performance evaluation criteria are classified as good during the evaluation period. The p-factor of 0.77 and the r-factor of 0.77 values were within the recommended range of p-factor > 0.7 and r-factor < 1.5. The average simulated streamflow values was 278.35 m^3/s whiles the observed streamflow values was 327.65 m^3/s indicating underestimation by the model during the validation period. The Most sensitive parameters during the calibration period are edited in the ArcSWAT project and the model run from the base years to the projected future scenario of 2100 for both RCP 4.5 and 8.5.

4.4.3.1 Projected Trends in HydroClimatic Parameters

Changes in the hydroclimatic variables were analysed for the base year and the three projected periods of 2021 to 2045 (near future period), 2046 to 2070 (mid future period) and 2071 to 2095 (far future period). Average 25-year records of these future periods for the RCP 4.5 and RCP 8.5 were compared against 25-year period of the observed base period (1990 to 2014). The average annual changes in the hydroclimatic variables such as streamflow, potential evapotranspiration (PET), temperature (maximum and minimum) in the catchment were assessed relative the baseline period from 1990 – 2013 (Table 4.11). The average maximum temperature, minimum temperature, potential evapotranspiration, streamflow and precipitation for the baseline period were 29.12 °C, 18.32 °C, 208 mm, 299.02 m^3/s and 1286.094 mm respectively. Maximum temperature values based on the simulation of the downscaled NCC-NorESM1-M with WRF331 model depicts an increase in the near future (NF) of 9.79 %, a further increase of 10.77 % in the Mid Future period and 12.89 % towards the end of the 21st century (Far Future)

under RCP 4.5 representing an increase of 2.85 °C for NF, 3.13 °C for MF and 3.40 for FF. The RCP 8.5 predicts 9.94 % increase in maximum temperature in the immediate future (NF), 12.88 % increase in the mid future and a drastic increase of 16.22 % towards the turn of the century which indicated an increase of 2.89 °C, 3.75 °C and 4.17 °C respectively for NF, MF and FF. Minimum temperature projection followed the same trend as the maximum temperature under both RCP4.5 and 8.5 but had lower percentage of increase relative to the baseline period (Table 4.11). In the near future, minimum temperature rose by 4.85 %, 6.15 % in the mid future period and 8.18 % under RCP 4.5 which represents an increase of 0.89 °C, 1.13 °C and 1.5 °C in the NF, MF and FF respectively. Under RCP 8.5, minimum temperature values showed an increase of 4.81 % in the near future, 9.89 % in the mid future (actually showing a decline from the initial increase) and 15.17 % towards the end of the century (Table 4.11). Precipitation in both RCP 4.5 and 8.5 shows an initial increase of 21.12 % and 22.13 % in the near future (NF) respectively, 19.10 % and 18.89 % in the mid future (MF) respectively and 18.25 % and 6.77 % respectively towards the end of the century (Table 4.11). Precipitation projection is observed to decrease drastically towards the year 2100 but it is still higher than the baseline average. These increase in precipitation can be as a result of inability of Regional Climate Models to simulate precipitation in West Africa and uncertainties inherent in the models (Sylla *et al.*, 2008, Oyerinde *et al.*, 2016). Streamflow will increase in the near future and mid future and reduce towards the end of the 21st century under RCP 8.5 in line with the decreasing precipitation. The reduction in the streamflow towards the year 2100 exceeded that of the baseline streamflow average. Generally, the increase in temperature, precipitation, streamflow, PET and temperature values in RCP 8.5 were higher than in RCP 4.5 projections. Nevertheless, the increase in streamflow are

characterised by extreme events of precipitation which resulted in high streamflow within particular years. This also resulted in intermittent streamflow generation by the model.

Table 4.11: Percentage hydroclimatic trends in the near future (NF, 2021-2045), mid future (MF, 2046- 2070) and far future (FF, 2071-2095) comparative to the historical (1990-2014)

Hydroclimatic variables	RCP 4.5			RCP 8.5		
	NF	MF	FF	NF	MF	FF
Streamflow (%)	38.01	39.83	48.49	43.02	67.77	14.57
Precipitation (%)	21.12	19.10	18.25	22.13	18.89	6.77
Potential Evaporation (%)	26.47	28.56	28.44	28.44	30.51	33.58
Maximum Temperature (%)	9.79	10.77	11.70	9.95	12.89	16.24
Minimum Temperature (%)	4.85	6.15	8.18	4.81	9.89	15.17

Source: Authors compilation, 2017.NF is near future (2021 – 2045), MF is mid future (2046 – 2070) and FF is Far Future (2071 – 2095). RCP is Representative Concentration Pathways.

4.5 Energy Projections

The annual energy generation from the dam were analysed under RCP 4.5 and RCP 8.5 scenarios. The hydropower generation outputs were modelled by assuming an ideal situation where the plant is capable of operating at full capacity without occurrence of malfunctioning units (or scenario of timely maintenance practices) in the years modelled. The output of the model for all the scenarios and time period under observation are represented in appendix A, B and C for Near future (2021 – 2045), Mid future (2046 – 2070) and Far future (2071 – 2095) respectively.

4.5.1 Energy Analysis in the Near Future (2021 – 2045)

The annual projected streamflow magnitude in RCP 8.5 were slightly higher than those in RCP 4.5 (Figure 4.19) which directly correlates with the energy production (Figure 4.20) in the near future period. Under RCP 4.5, average annual flow in the near future was lower than the average annual flow in RCP 8.5 by 3.63 % but total energy produced in RCP 4.5 was slightly greater than in RCP 8.5 in the near future by 0.17 %. Contrarily, the total revenue produced is projected to be 1.4 % (5.6 billion Naira) more under RCP 8.5 scenario than in RCP 4.5 scenario for the entire near future period. The increase in revenue under RCP 8.5 scenario can be attributed to the seasonality in flow where a high annual flow could be a result of high intermittent flow within the year as against an average flow thoughout the year. Intermittent flow with dry spells or month with low flowmight result in low power generation as against steady mean flow. Thereby suggesting that the reliability of the plant in the near future under RCP 4.5 was slightly lower than under RCP 8.5 (Table 4.12). Maximum energy produced under each scenario above 2000 GWh/year were produced in the years 2030, 2034, 2039 and 2040 under RCP

8.5 scenario whilst under RCP 4.5 scenario, it was produced in the years 2027, 2029, 2033, 2038 and 2039 under RCP 4.5 scenario.

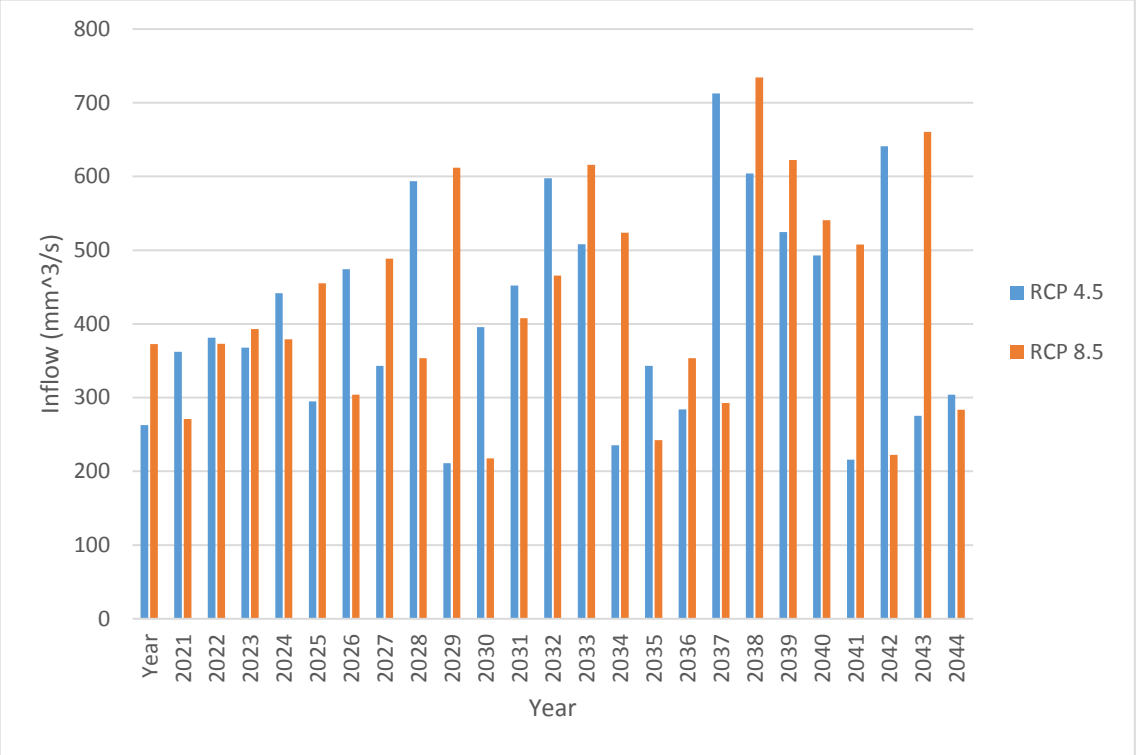

Figure 4.19. Annual average streamflow in the Near Future for both RCP 4.5 and RCP 8.5 scenario

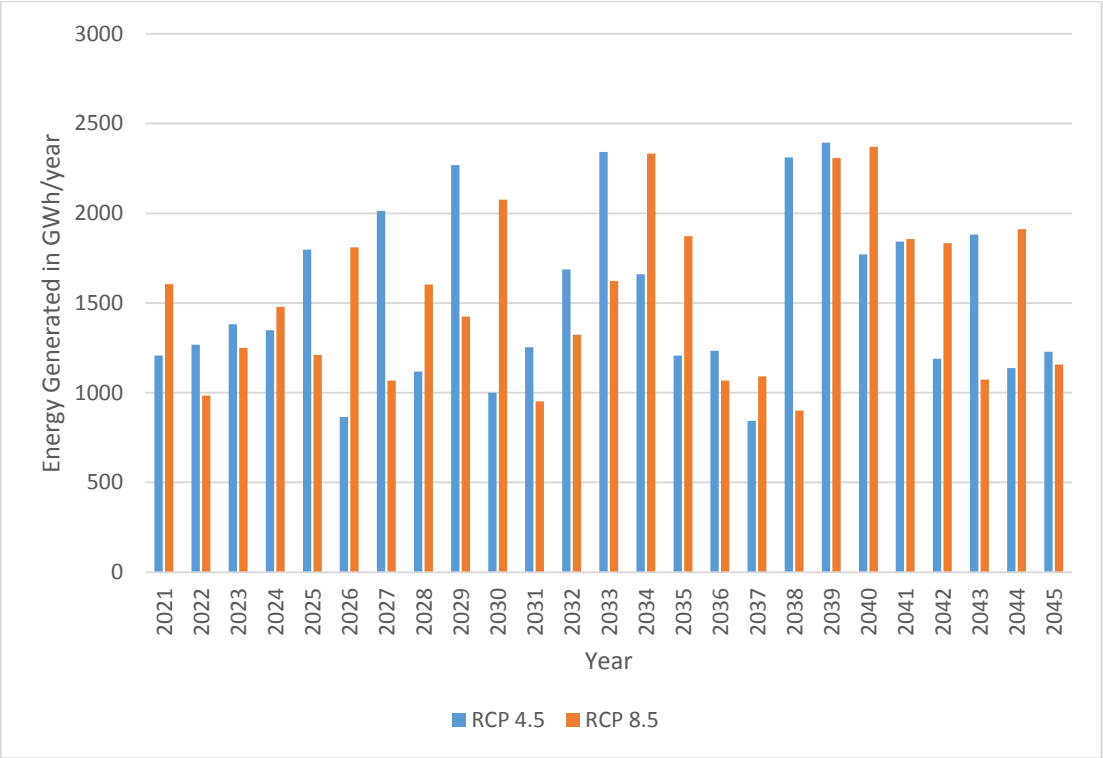

Figure 4.20. Annual Energy generation under both RCP 4.5 and 8.5 scenarios in the Near Future

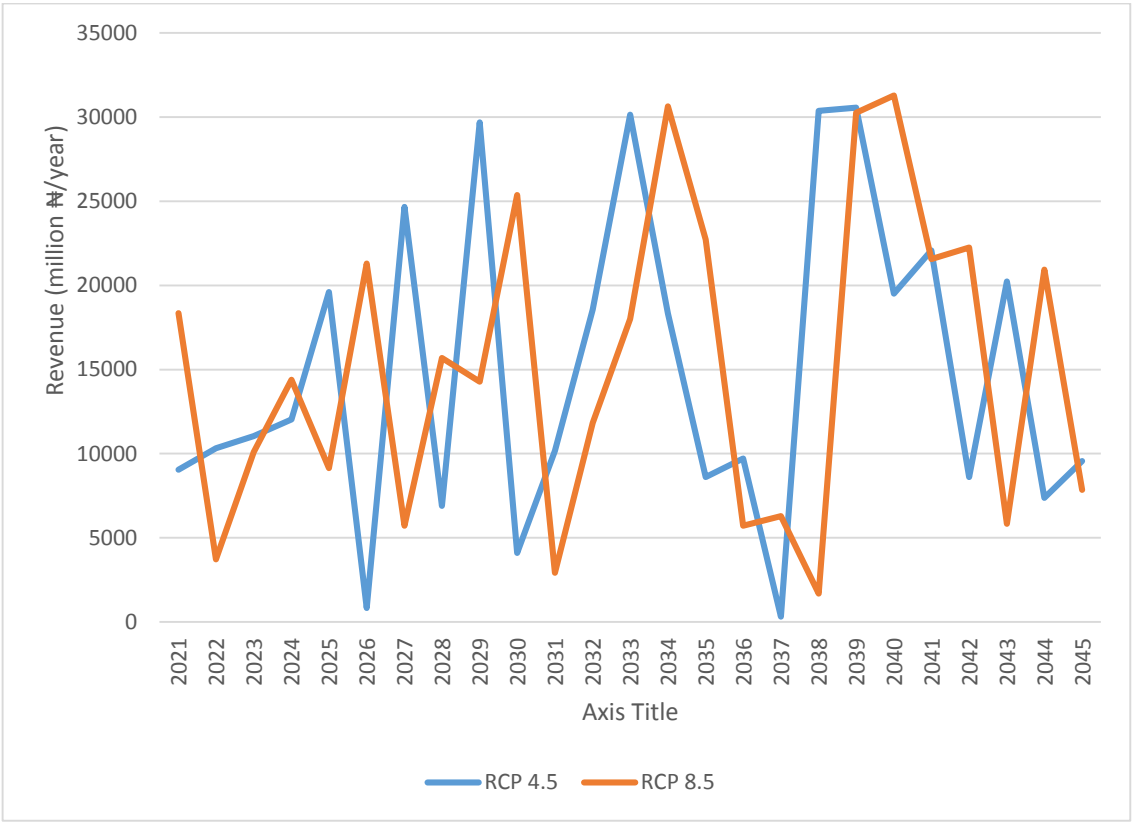

Figure 4.21. Annual Revenue in Millions Naira in the Near future

Revenue generated in millions of Naira (Figure 4.21) also shows considerable benefits of the power plant under RCP 8.5 scenario with more than 50 % of the years reporting benefits of 1 billion Naira or more. Lowest amount of revenue generated is likely to occur under RCP 4.5.

4.5.2 Energy Analysis in the Mid Future (2046 – 2070)

In the Mid future, the magnitude of the annual average streamflow under RCP 8.5 remains higher than those in RCP 4.5 (Figure 4.22) which directly correlates with the energy production (Figure 4.23) in the mid future period similar to the near future. Maximum energy of 2000 GWh/year and above were produced in the years 2024, 2028, 2031 to 2050, 2055, 2056, 2061, 2067 and 2068 under RCP 8.5 scenario whilst its was produced in the years 2046, 2054, 2055, 2060, 2066 and 2067 under RCP 4.5 scenario.

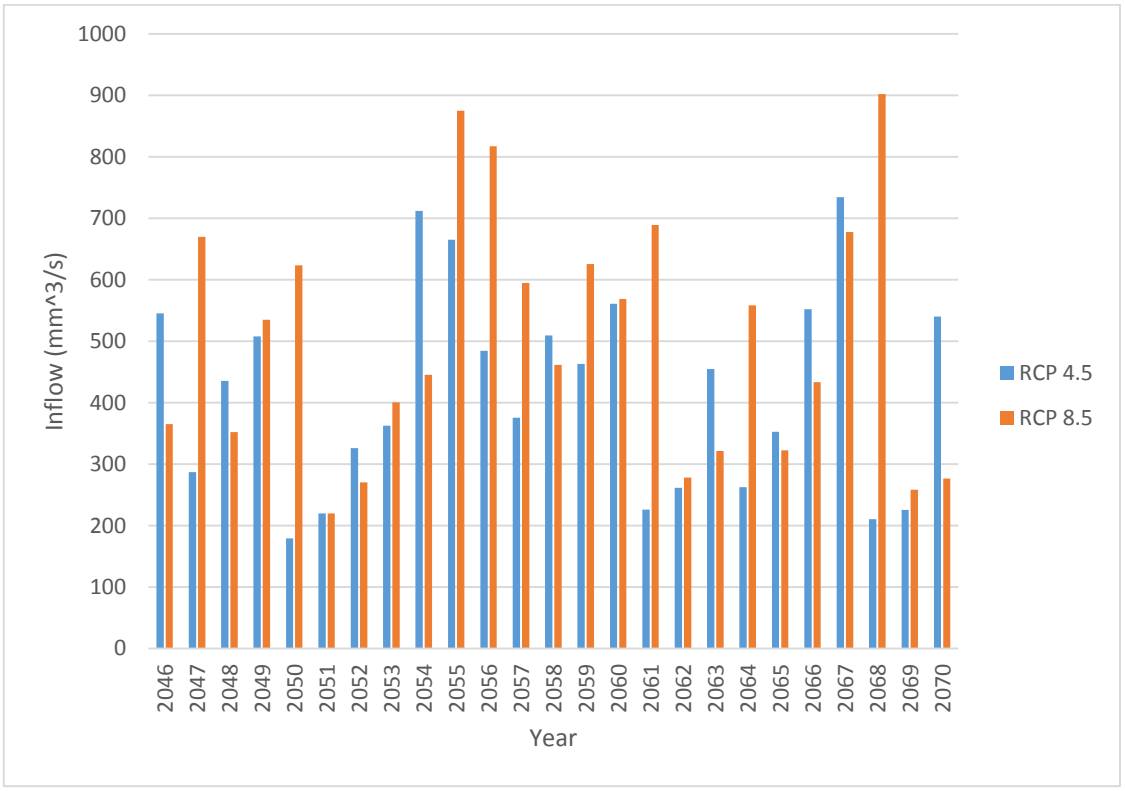

Figure 4.22. Annual average streamflow in the Mid Future under both RCP 4.5 and RCP 8.5 scenario

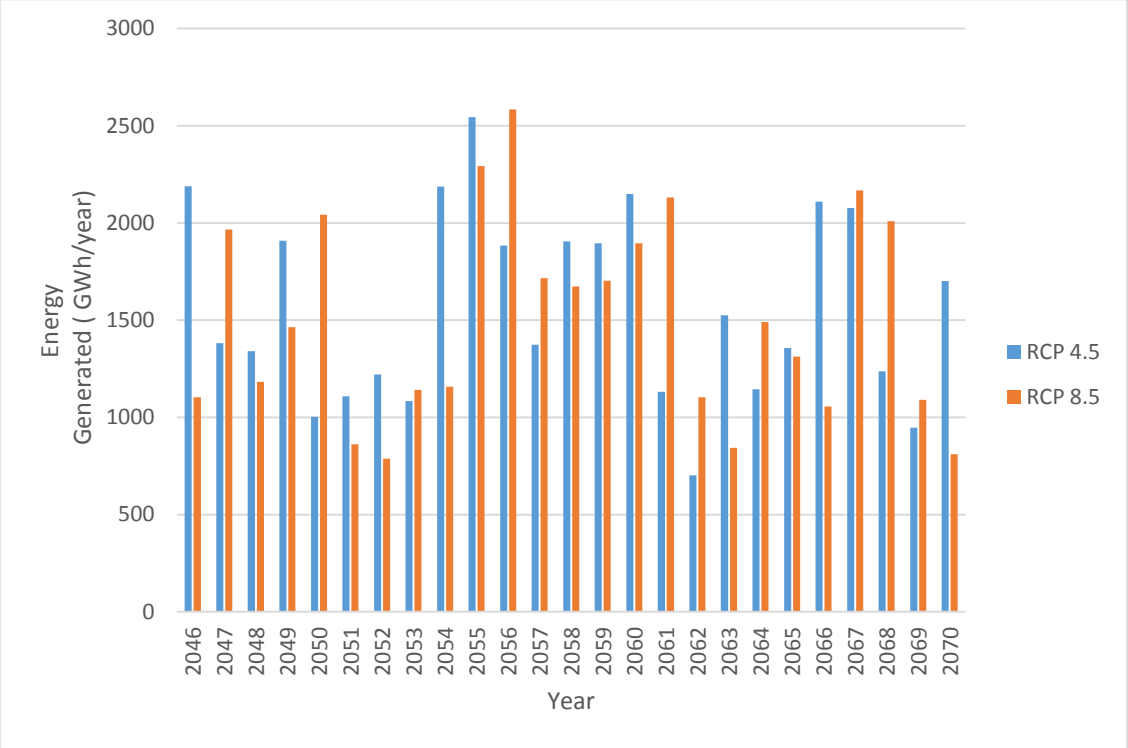

Figure 4.23. Total Annual Energy generation under both RCP 4.5 and 8.5 scenarios in the Mid Future

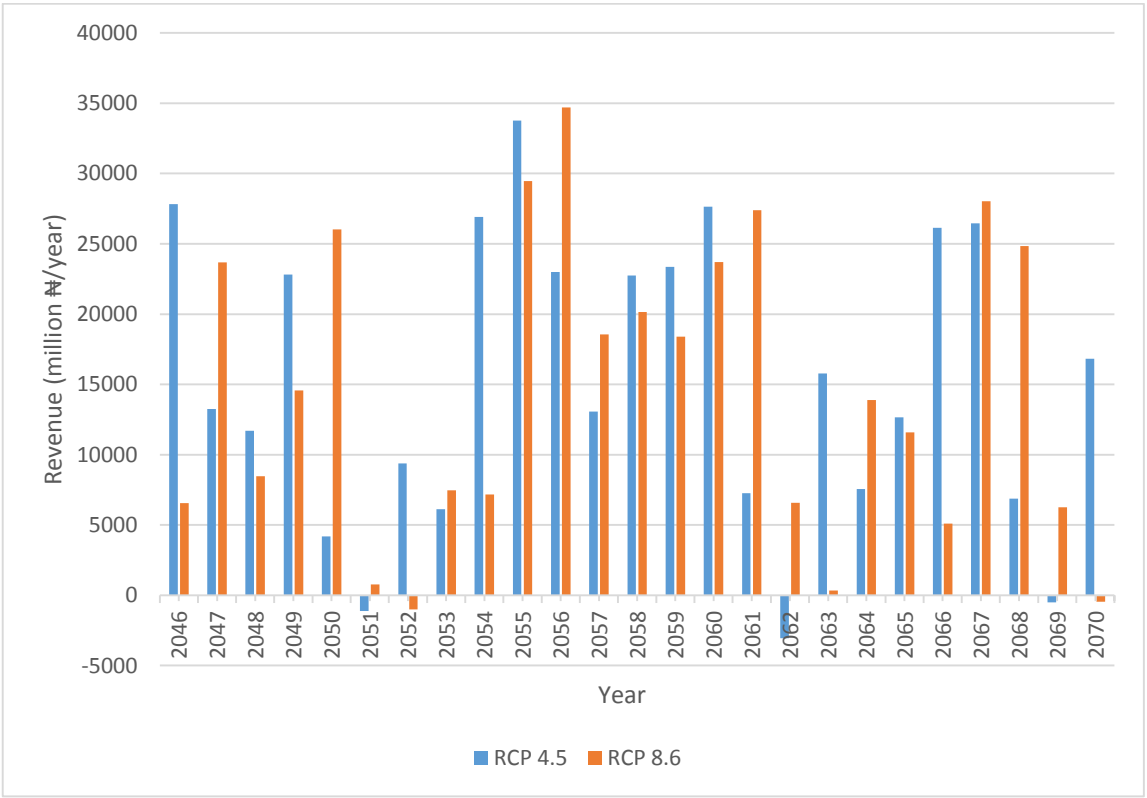

Figure 4.24. Total Annual Revenue in Millions Naira in the mid future

Energy generated under RCP 4.5 was slightly higher than energy generated under RCP 8.5 even though streamflow under RCP 8.5 was slightly higher than RCP 4.5. This disparity can be accounted in the additional sale of secondary power after the target has been achieved. Revenue margins in Millions of Naira (Figure 4.24) reveal a projected loss made by the power plant under both RCP 4.5 and RCP 8.5 scenarios in the years 2051 (1.1 billion Naira), 2062 (3.1 billion Naira) and 2069 (507.37 million Naira) under RCP 4.5 scenario and 2052 (1.02 billion Naira) and 2070 (460.09 million Naira). Also, benefits in the years 2051 and 2063 under RCP 8.5 scenario are very low and below 800 million Naira per annum. These net losses are as a result of the power plant inability to produce power to achieve the target (firm power) when the penalty rule is applied for each month in a particular year. The relationship between power generated and revenue is not linear when the power generated is below the target. Thus, months that reached firm power mimic increasing linear curve whilst the contrary is also true.

4.5.3 Energy Analysis in the Far Future (2071 – 2095)

The projected annual average streamflow magnitude (Appendix C) in RCP 4.5 were slightly higher than those in RCP 8.5 (Figure 4.25) which directly correlates with the energy production (Figure 4.26) in the far future (FF) period. Under RCP 4.5, average annual flow in the near future was marginally higher than the average annual flow under RCP 8.5 scenario by 22.8 % of average annual streamflow under RCP 4.5 scenario. Also, total energy produced under RCP 8.5 scenario was slightly more than under RCP 4.5 in the far future by 0.69 % of total annual energy generated under RCP4.5 scenario. Comparatively, the total revenue produced is projected to be 0.7 % (3.1 billion Naira) more under RCP 8.5 scenario than in RCP 4.5 scenario for the entire far future period. Though the streamflow under RCP 4.5 increased more than streamflow simulated under

RCP 8.5, the power production were based on constraints highlighted in equation 23 – 26 and are stochastic in nature. The increase in revenue under RCP 8.5 are as a result consistent average flow in a year as against intermittent high flow under RCP 4.5 is going to affect energy production as explained earlier and reliability of the plant in months with dry spells (Figure 4.26). The reliability of the plant in a particular month affects the pricing of the energy.

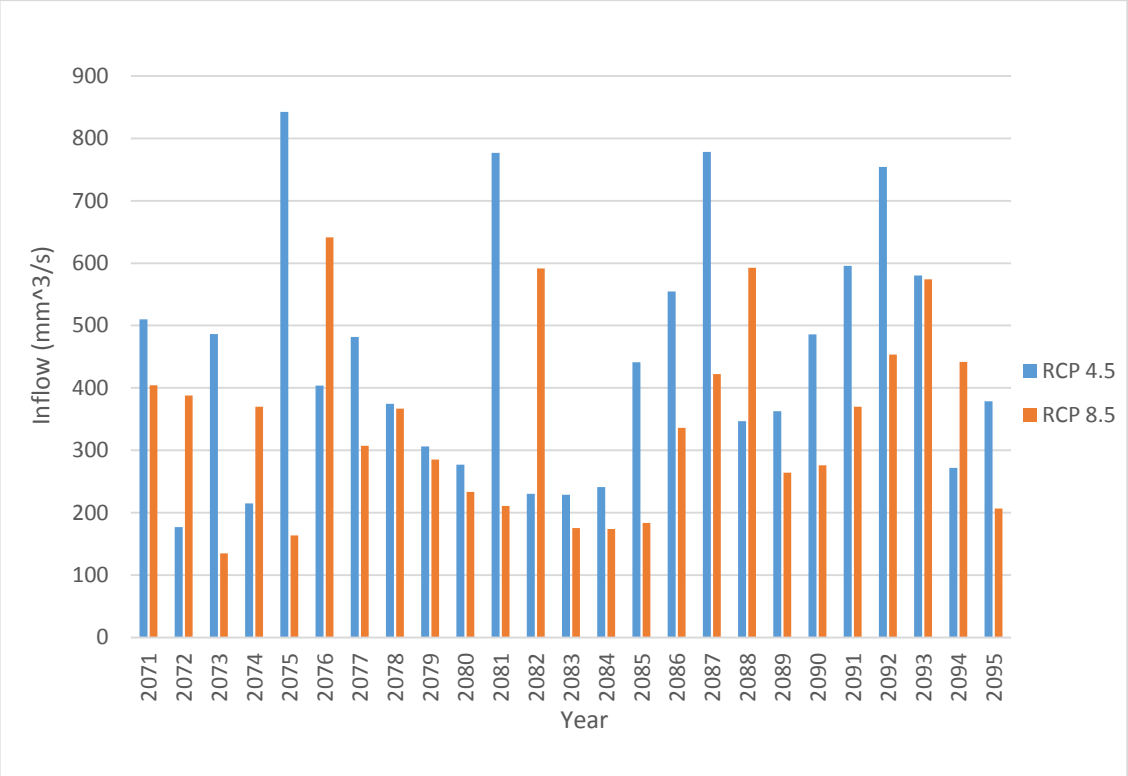

Figure 4.25. Annual average streamflow in the Far Future under both RCP 4.5 and RCP 8.5 scenario

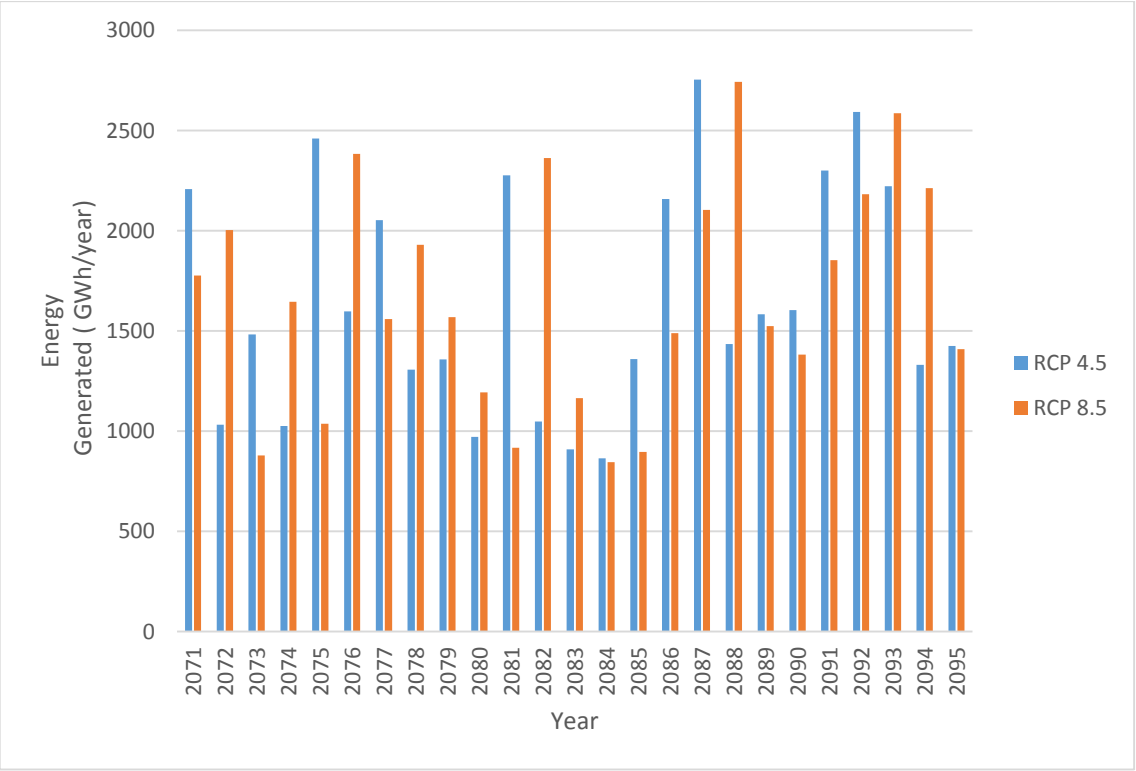

Figure 4.26. Annual Energy generation under both RCP 4.5 and 8.5 scenarios in the Far Future

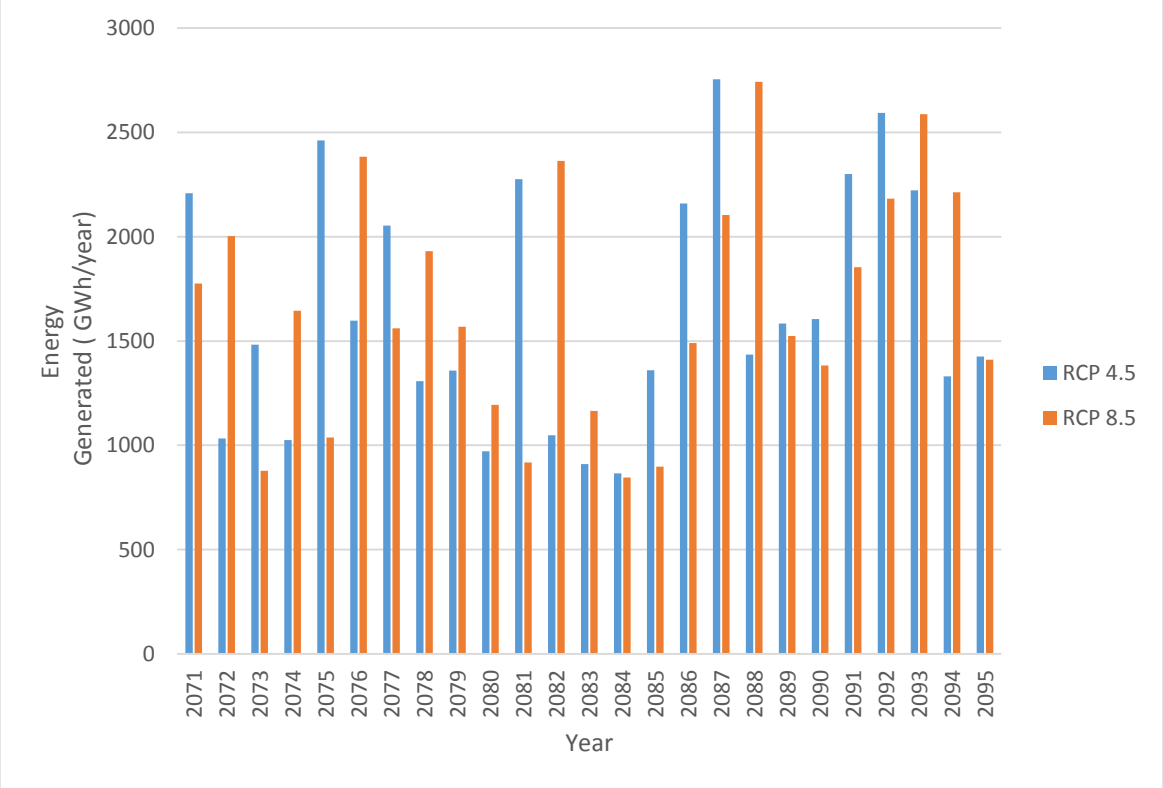

Figure 4.27. Annual Revenue in Millions Naira in the Far future

The revenue generated in millions of Naira (Figure 4.27) reveal a projected revenue of the power plant in the far future made by the power plant under both RCP 4.5 and RCP 8.5 scenarios. In the far future period, the plant is projected to record revenue with minimum revenue (benefits) of 800 million Naira in both RCP 4.5 and 8.5 scenario. There are no losses reported in any particular for both the scenarios.

4.5.4 Reliability of Hydropower plant

In modelling the monthly power generation using the dynamic stochastic model, the reliability of the plants was based on the ability of plant to reach the target which was the firm power set at 138 KWh/month. The reliability of the power plant in the various scenarios under RCP 4.5 and 8.5 for all the future periods (NF, MF and FF) are illustrated in Table 4.12.

Table 4.12: Reliability and Revenue for the possible future periods under both climate change scenarios

	RCP 4.5			**RCP 8.5**		
Period	**NF**	**MF**	**FF**	**NF**	**MF**	**FF**
Reliability (%)	0.68	0.64	0.7	0.7	0.69	0.72
Revenue (million Naira)	372294.9	380614.5	434167.5	377858.2	362179	437273.9

Source: Authors compilation, 2017.NF is near future (2021 – 2045), MF is mid future (2046 – 2070) and FF is Far Future (2071 – 2095). RCP is Representative Concentration Pathways.

The reliability of the power plant was evaluated under each scenario and periods in the future and revenue generated (Table 4.12). Under RCP 4.5, the reliability of the power plant was 0.68 % in the near future (2021 – 2045), reduced in the mid future (2046 – 2070) at 0.64 % and increased in the far future at 0.7. Similar results are projected by RCP 8.5 scenario with 0.7 % reliability factor of the plant in the near future, reducing to 0.69 in the mid future and 0.72 in the far future period. Comparing these reliability factors obtained in another study by Cervigni *et al.* (2013), the report an initial reliability factor of 0.68 % to 1 % in the year 2020 and an increase 0.89 % to 1 % in the 2050. The results in the near future (2021 – 2045) similar to their observation in the 2020 whilst the mid future reliability differs from their reliability they obtained at the end of the year 2050. The reliability of the plant in scenario RCP 8.5 were higher than in scenario RCP 4.5 during the period under consideration (Table 4.12) but lower than the acceptable value of 0.75 implying that climate change will have severe impact on the plant. With the projected average annual streamflow being higher than the baseline in both scenarios, the occurrence of extreme precipitation events will force operators to spill water in order to protect the dam which can likely result in flooding downstream of the dam in periods where very high flow is occur.

CHAPTER FIVE

5.0 CONCLUSION AND RECOMMENDATIONS

5.1 Conclusion

The first objectives of this study was to investigate the trends in hydroclimatic variables of stations situated in the Shiroro catchment and its immediate surroundings using Mann-Kendall statistical techniques. The findings from the variables of the stations were significant at 95 % confidence level. Kaduna, Jos and Zaria indicated an increasing trend in the maximum temperature series whilst only Jos had a decreasing minimum temperature trend with Kaduna and Zaria illustrating positive trends in their minimum temperature. Average temperature in Kaduna and Zaria had positive trends. On the contrary, Jos average temperature suggested a decreasing trend. Minna recorded negative trends for the average temperature series. Precipitation analysis showed no significant trend in Jos whilst positive weak trends were found in Kaduna, Minna and Zaria for the period under investigation. Streamflow time series showed the presence of trend which was not significant after statistical evaluation of data. Among the hydroclimatic variables analysed, there was high variation in the period observed for temperature time series. Thus, all the findings from each station indicating the presence of high climate variability in the catchment. Based on the findings of Okpara *et al.* (2013) in similar locations, these gradual changes can be associated with evidence of climate change occurring in the catchment.

The second objectives were to assess the changes in streamflow in the catchment. The Soil and Water Assessment Tool (SWAT) was utilised to quantify changes in streamflow of the catchment. The Soil and Water Assessment Tool was used to setup a model for the Shiroro catchment and calibrated from the period of 1990 to 2005 and validated from 2006 to 2013 on monthly time steps. The calibration results based on criteria

recommended by Moriasi *et al.* (2015) were unsatisfactory which was related to underestimation of rainfall by the CFSR precipitation datasets during the year 1999 and 2000. Nevertheless, the best solution of the calibrated model was selected by utilising uncertainty fitting criteria recommended by Abbaspour *et al.* (2015). During the validation process, the validation statistics were adjudged good for the calibrated model.

Streamflow was projected to increase under both RCP 4.5 and RCP 8.5 in the near future, mid future and far future more than the baseline. The streamflow under RCP 8.5 scenarios reduced towards the turn of the century but still remain higher than the baseline average streamflow value. These changes correlated with projected changes in precipitation at the dam sites. Temperature values rose gradually from near future, mid future and far future under both scenarios.

In the assessment of the future power generation in the possible future, a stochastic dynamic model was utilised to assess impact of changes in streamflow on hydropower generation. Generally increase in streamflow correlated with the increase in energy generated. In the application of the optimisation operation rule constraints, increase in energy production does directly infer to generation of revenue as the ability of the energy generation of plant to achieve firm power influences the pricing of energy. The reliability of the plant of the plant from the near future reduces from 0.68 to 0.64 in the mid future and increases to 0.7 in the far future under RCP 4.5 scenario. Similarly, the reliability of the plant reduces from 0.7 in the near future to 0.69 in mid future and then increases to 0.72 in the far future under RCP 8.5 scenario. Revenue under RCP 8.5 were in agreement with the changes in the reliability of the plant. Under RCP 4.5, revenue increases gradually from the near future to far future despite the dip in reliability during the mid future. The sale of secondary power in wet years may have accounted for the revenue increase even though reliability reduced in the mid future. Reliability obtained from all

the scenarios were below the acceptable value of 0.75 suggesting that the optimum benefit to be derived from the plant will be impacted by climate change as a result of occurrence of intermittent flow regimes in the catchment. Inter-basin water transfers such as Gurara Basin transfer to Shiroro are will be key in improving hydropower generation in the catchment.

5.2 Recommendations

From the findings of this work, it was observed that intermittent flow as result of climate change are likely to occur in the catchment.

As a result of intermittent flow in the catchment, operators of the dam should adopt optimisation policy that will maintain water especially during periods of high inflow to protect the environment downstream of the dam.

The spatial resolution of hydrological model input data affect the prediction of streamflow, we recommend that the application of other rainfall reanalysis and satellite products such as Climate Hazards Group InfraRed Precipitation with Stations (CHIRPS), Tropical Applications of Meteorology using SATellite (TAMSAT), Tropical Rainfall Measuring Mission (TRMM), Era Interim Reanalysis data, Modern-Era Retrospective analysis for Research and Applications version 2 (MERRA-2), Precipitation Estimation from Remotely Sensed Information using Artificial Neural Networks (PERSIANN) and Global Precipitation Climatology Project (GPCP) to improve streamflow modelling of the catchment. Other spatial datasets such as HydroSHEDS, Advanced Spaceborne Thermal Emission and Reflection Radiometer (ASTER GDEM), European Space Agency (ESA) CCI Land Cover product.

Multiple GCMs output and ensemble mean from GCM outputs should be used in future to study the climate change impact on the hydrology and hydropower generation in the catchment. This will reduce the uncertainties associated in applying only one GCM.

Inter-basin Transfer should be explored and manage effectively to help improve the reliability of the hydropower plant in the Shiroro Dam Catchment expecially in periods of low flow of water into the reservoir.

Finally, climate change impact on sediments in both the present and future scenarios and their effect on power generations should be investigated.

REFERENCES

Abbaspour, K. C., Johnson, C. A., & Van Genuchten, M. T. (2004). Estimating uncertain flow and transport parameters using a sequential uncertainty fitting procedure. Vadose Zone Journal, 3(4), 1340-1352.

Abbaspour, K. (2015). SWAT-Calibration and uncertainty programs (CUP)-User Manual. Swiss Federal Institute of Aquatic Science and Technology, Eawag, Duebendorf, 1-100.

Abbaspour, K. C., Rouholahnejad, E., Vaghefi, S., Srinivasan, R., Yang, H., & Kløve, B. (2015). A continental-scale hydrology and water quality model for Europe: Calibration and uncertainty of a high-resolution large-scale SWAT model. Journal of Hydrology, 524, 733-752.

Adelana, S. M. A., Olasehinde, P. I., Bale, R. B., Vrbka, P., Edet, A. E., and Goni, I. B., (2008). An overview of the geology and hydrogeology of Nigeria: In: Chapter 11 in Adelana, S. and McDonald, A. (Eds). Applied groundwater studies in Africa: IAH Selected Papers on Hydrogeology, 13. pp 171-198. CRC press Taylor & Francis group.

Adeogun, A. G., Sule, B. F., Salami, A. W., & Okeola, O. G. (2014). GIS-Based Hydrological Modelling using SWAT: Case study of upstream watershed of Jebba reservoir in Nigeria. *Nigerian Journal of Technology*, 33(3), 351-358.

Adie, D. B., Ismail, A., Muhammad, M. M., & Aliyu, U. B. (2012). Analysis of the water resources potential and useful life of the Shiroro Dam, Nigeria. Nigerian Journal of Basic and Applied Sciences, 20(4), 341-348.

African Climate Policy Centre- United Nations Economic Commission for Africa (2011). Climate Change and Water in Africa: Analysis of Knowledge Gaps and Needs. United Nations Economic Commission for Africa.

Ahmad I, Tang D, Wang T, Wang M, Wagan B (2015). Precipitation Trends over Time Using Mann-Kendall and Spearman's rho Tests in Swat River Basin, Pakistan. *Adv. Meteorol.* P 15. doi:10.1155/2015/431860

Akinsonola, A. A. & Ogunjobi, K. O (2014). Analysis of Rainfal and Temperature Variability over Nigeria. *Global journal of Human Social Science: Geography, Geo-Sciences, Environmental Disaster Management,* 14(3). Online ISSN: 2249-460x & Print ISSN: 0975-587X.

Akpoti K., Antwi E. O. & Kabo-Bah A. T. (2016). Impact of Rainfalll Variability, Land Use and Land Cover Change on Streamflow of Black Volta Basin, West Africa. *Hydrology*, 3, 26. doi: 10.3390/hydrology3030026

Andersen, I., Ousmane, D., Jarosewich-Holder, M., Olivry, J.-C. & Golitzen, K. G. (2005). The Niger River Basin: A Vision for Sustainable Management. Directions in Development. Washington, DC: World Bank. © World Bank. https://openknowledge.worldbank.org/bitstream/handle/10986/7397/345180PAPER0NR1Basin01OFFICIAL0USE1.pdf?sequence=1&isAllowed=y, License: CC BY 3.0 IGO

Arnold, J. G., Moriasi, D. N., Gassman, P. W., Abbaspour, K. C., White, M. J., Srinivasan, R., & Kannan, N. (2012). SWAT: Model use, calibration, and validation.

Transactions of the ASABE, 55(4), 1491-1508.

Baede, A.P.M., E. Ahlonsou, Y. Ding, & D. Schimel. (2001). The climate system: an overview. Ch.1 in Climate change 2001: the scientific basis: contribution of Working Group I to the third assessment report of the Intergovernmental Panel on Climate Change. Cambridge, U.K.; New York: Cambridge University Press. Retrived from https://www.ipcc.ch/ipccreports/tar/wg1/pdf/TAR-01.PDF

Barcelona Field Studies Centre (n.d.). Measuring Slope Steepness. Retrieved from https://geographyfieldwork.com/SlopeSteepnessIndex.htm

Bates, B. C., Kundzewicz, S. W. & Palutikof, J. P. (2008). Climate change and water. *Technical paper of the Intergovernmental Panel on Climate Change*. Geneva: IPCC Secretariat.

Beilfuss, R., & Triet, T. (2014). A scoping study on Climate change and hydropower in the Mekong River Basin: a synthesis of research. *Deutsche Gesellschaft für Internationale Zusammenarbeit (GIZ) GmbH*. Retrieved from https://www.giz.de/en/downloads/giz2014-en-study-climate-change-hydropower-mekong.pdf

Bekoe, E. O., & Logah, F. Y. (2013). The Impact of Droughts and Climate Change on Electricity Generation in Ghana. *Environmental Sciences*, 1(1), 13–24.

Cervigni, R., Riccardo, V., and Monia, S., eds. (2013). Toward Climate-Resilient Development in Nigeria. Directions in Development. Washington, DC: World Bank. doi:10.1596/978-0-8213-9923-1. License: Creative Commons Attribution CC BY 3.0.

Chiang, J.-L., Yang, H.-C., Chen, Y.-R., & Lee, M.-H. (2013). Potential Impact of Climate Change on Hydropower Generation in Southern Taiwan. *Energy Procedia*, 40, 34–37. http://doi.org/10.1016/j.egypro.2013.08.005

Cunderlik, J. M., & Burn, D. H. (2003). Non-stationary pooled flood frequency analysis. Journal of Hydrology, 276(1), 210-223.

Cuo, L., Zhang, Y., Gao, Y., Hao, Z., & Cairang, L. (2013). The impacts of climate change and land cover/use transition on the hydrology in the upper Yellow River Basin, China. Journal of Hydrology, 502, 37-52.

Dan-Hassan, M. (2016). Preliminary pages, ASPECT OF HYDRO OF FCT.

Dile, Y. T. & Srinivasan, R. (2014). Evaluation of CFSR climate data for hydrologic prediction in data–scarce watersheds: An application in the Blue Nile River basin. *Journal of American Water Resources Association (JAWRA)*, 1-16. DOI: 10.1111/jawr.12182

Enete, A., & Amusa, T. (2010). Challenges of Agricultural Adaptation to Climate Change in Nigeria: a Synthesis from the Literature. Fact Reports, 4(8), 0–8. Retrieved from http://factsreports.revues.org/678

Fiseha, B. M., Setegn, S. G., Melesse, A. M., Volpi, E., & Fiori, A. (2014). Impact of Climate Change on the Hydrology of Upper Tiber River Basin Using Bias Corrected Regional Climate Model. http://doi.org/10.1007/s11269-014-0546-x.

Food and Agriculture Organization of the United Nations (FAO) (2003). Digital Soil Map

of the World (DSMW): based on the FAO/UNESCO Soil Map of the World, Original Scale 1:5 000 000. FAO-AGL (Land and Water Development Division), Rome.

Fuka, D. R., Walter, M. T., MacAlister, C., Degaetano, A. T., Steenhuis, T. S., & Easton, Z. M. (2013). Using the Climate Forecast System Reanalysis as weather input data for watershed models. *Hydrol. Process.*, DOI: 10.1002/hyp.10073

Gbobaniyi, E., Sarr, A., Sylla, M. B., Diallo, I., Lennard, C., Dosio, A., Dhiédiou, A., Kamga, A, Klutse, N. A. B., Hewitson, B., Nikulin, G. & Lamptey, B. (2014). Climatology, annual cycle and interannual variability of precipitation and temperature in CORDEX simulations over West Africa. International Journal of Climatology, 34(7), 2241-2257. DOI: 10.1002/joc.3834

Gnansounou, E.; Bayem, H.; Bednyagin, D.; Dong, J. (2007). Strategies for regional integration of electricity supply in West Africa. *Energy Policy*, 35, 4142–4153.

Goulden, M., Conway, D., & Persechino, A. (2009). Adaptation to climate change in international river basins in Africa: a review. *Hydrological Science Journal*, 54(5) 805-828.

Griensven, A.V., Meixner, T., Grunwald, S., Bishop, T., Diluzio, M., Srinivasan, R. (2006). A global sensitivity analysis tool for the parameters of multi-variable catchment models. *Journal of Hydrology*, 324, 10–23.

Grove T. (1972). The dissolved and solid load carried by some West African Rivers: Senegal, Niger, Benue and Shari. *Journal of Hydrology*, 16, 277-300.

Gyau-Boakye, P. (2001). Environmental impacts of the Akosombo dam and effects of climate change on the lake levels. *Environment, Development and Sustainability*, 3(1), 17–29. http://doi.org/10.1023/A:1011402116047

Hamed, K. H., & Rao, R. A. (1998). A modified Mann-Kendall trend test for autocorrelated data. *Journal of Hydrology*, 204, 182 – 196.

Hirsch, R. M., Slack, J. R., & Smith, R. A. (1982). Techniques of trend analysis for monthly water quality data. Water resources research, 18(1), 107-121

Intergovernmental Panel on Climate Change (IPCC) (2000). Special Report on Emission Scenarios (Sres): A Special Report of Working Group II of the Intergovernmental Panel on Climate Change. Cambridge University Press, Cambridge

Intergovernmental Panel on Climate Change. (2007a). Observed changes in climate and their effects. AR4 SYR Synthesis Report -1. Retrieved October 5, 2016, from https://www.ipcc.ch/publications_and_data/ar4/syr/en/mains1.html

Intergovernmental Panel on Climate Change IPCC. (2007b). Magnitudes of impact - AR4 WGII Summary for Policymakers. Retrieved October 8, 2016, from https://www.ipcc.ch/publications_and_data/ar4/wg2/en/spmsspm-c-15-magnitudes-of.html

Intergovernmental Panel on Climate Chang (IPCC) (2007c). Climate Change 2007: The Physical Science Basis. Contribution of Working Group I to the Fourth Assessment Report of the Intergovernmental Panel on Climate Change [Solomon, S., D. Qin, M. Manning, Z. Chen, M. Marquis, K.B. Averyt, M.Tignor and H.L. Miller (eds.)]. Cambridge University Press, Cambridge, United Kingdom and New York, NY,

USA.

Intergovernmental Panel on Climate Change, IPCC (2011). Summary for Policymakers. In: IPCC Special Report on Renewable Energy Sources and Climate Change Mitigation [O. Edenhofer, R. Pichs-Madruga, Y. Sokona, K. Seyboth, P. Matschoss, S. Kadner, T. Zwickel, P. Eickemeier, G. Hansen, S. Schlömer, C. von Stechow (eds)], *Cambridge University Press*, Cambridge, United Kingdom and New York, NY, USA. http://doi.org/10.5860/CHOICE.49-6309

IRENA. (2015). Rethinking Energy (IRENA flagship report) - 2015 Edition. Irena, 344. Retrieved from www.irena.org/publications. http://doi.org/10.1002/9781119994381

Jarvis, A., Reuter, H.I., Nelson, A. & Guevara, E. (2008). Hole-filled SRTM for the globe Version 4, available from the CGIAR-CSI SRTM 90m Database (http://srtm.csi.cgiar.org).

Jimoh, O. D., & Ayodeji, O. S. (2003). Impact of the Gurara River (Nigeria) interbasin water transfer scheme on the Kaduna River at Shiroro Dam. Proceedings of Symposium IUGG2003- Hydrological Risk Management and Development, IAHS Publication, Saporo 281:277-286.

Jimoh, O. D. (2008). Optimized operation of Kainji reservoir. *J. Technol*, 12, 34-42.

Kalyanapu, A. J., Hossain, A. A. K. M., Kim, J., Yigzaw, W., Hossain, F., & Shum, C. K. (2013). Toward a Methodology to investigate the downstream flood hazards on the American River due to effects of artificial reservoir size and Land- Use/ Land Cover Patterns. *Earth Interactions,* 17(24), 1-24.

Kang, H. M., & Yusof, F. (2012). Homogeneity tests on daily rainfall series in Peninsular Malaysia. *Int. J. Contemp. Math. Sciences*, 7(1), 9-22.

Keeling C.D. et al. (2005) Atmospheric C_2O and $^{13}C_2O$ Exchange with the Terrestrial Biosphere and Oceans from 1978 to 2000: Observations and Carbon Cycle Implications. In: Baldwin, I. *et al.* (eds) A History of Atmospheric CO2 and Its Effects on Plants, Animals, and Ecosystems. Ecological Studies (Analysis and Synthesis), vol 177. Springer, New York, NY

Kendall, M. (1975). Multivariate analysis. Charles Griffin.

Kundzewicz, Z. W., & Robson, A. (2000). Detecting trend and other changes in hydrological data. World Meteorological Organization.

Kundzewicz, Z.W., Mata, L.J., Arnell, N.W., Döll, P., Kabat, P., Jiménez, B., Miller, K.A., Oki, T., Sen, Z., and I.A. Shiklomanov. (2007). Freshwater resources and their management. Climate Change: Impacts, Adaptation and Vulnerability. Contribution of Working Group II to the Fourth Assessment Report of the Intergovernmental Panel on Climate Change, M.L. Parry, O.F. Canziani, J.P. Palutikof, P.J. van der Linden and C.E. Hanson, Eds. *Cambridge University Press,* Cambridge. UK. 173-210

Lafaysse, M., B. Hingray, A. Mezghani,J. Gailhard, and L. Terray (2014). Internal variability and model uncertainty components in future hydrometeorological projections: The Alpine Durance basin, Water Resource. Res., 50, doi:10.1002/2013WR014897

Leon, F. L. (2011). Step by step geo-processing and set-up of the required watershed data

for MWSWAT (MapWindow SWAT) version 2. Accessed online at http://www.waterbase.org

Ley, K., Gaines, J., & Ghatikar, A. (2015). The Nigerian energy sector – an overview with special emphasis on renewable energy, energy efficiency and rural electrification. Retrieved from Deutsche Gesellschaft für Internationale Zusammenarbeit (GIZ) GmbH Website: https://giz.de/en/downloads/giz2015-en-nigerian-energy-sector.pdf

Liersch, S. (2003). The programs dew.exe and dew02, exe user's manual.

Longobardi, A. & Villani, P. (2010). Trend analysis of annual and seasonal rainfall time series in the Mediterranean area. *Int. J. Climatol,* 30:1538-1546. doi: 10.1002/joc.2001

Mann, H. B. (1945). Nonparametric tests against trend. Econometrica: Journal of the Econometric Society, 245–259.

McCartney, M. P., & Girma, M. M. (2012). Evaluating the downstream implications of planned water resource development in the Ethiopian portion of the Blue Nile River. *Water International*, 37:4, 362-397, https://dx.doi.org/10.1080/02508060.2012.706384

Milly, P.C.D., Betancourt, J., Falkenmark, M., Hirsch, R.M., & W. Zbigniew. (2008). Climate change – stationarity is dead: whither water management? *Science* 319: 573-574.

Moriasi, D. N., Gitau, M. W., Pai, N., & Daggupati, P. (2015). Hydrologic and water quality models: Performance measures and evaluation criteria. Transactions of the ASABE, 58(6), 1763-1785. DOI 10.13031/trans.58.10715

Mukheibir, P. (2007). Possible climate change impacts on large hydroelectricity schemes in Southern Africa. *Journal of Energy in Southern Africa*, 18(1), 4–9.

National Aeronautics and Space Administration NASA, E. S. C. T. (2016). Climate Change: Vital Signs of the Planet: Effects. Retrieved October 8, 2016, from http://climate.nasa.gov/effects/

Nash, J., & Sutcliffe, J. V. (1970). River flow forecasting through conceptual models part I – a discussion of principles. Journal of hydrology, 10 (3), 282-290.

Neitsch, S. L., Arnold, J. G., Kiniry, J. R., Williams, J. R., & King, K. W. (2005). Soil and water assessment tool theoretical documentation. Grassland. Soil and Water Research Laboratory, Temple, TX.

Neitsch, S. L., Arnold, J. G., Kiniry, J. R., Srinivasan, R., & Williams, J. R. (2010). Soil and Water Assessment Tool Input/Output File Documentation Version 2009. Texas Water Resource Institute Technical Report No. 365, Texas A & M University System

Neitsch, S. L., Arnold, J. G., Kiniry, J. R., & Williams, J. R. (2011). Soil and water assessment tool theoretical documentation version 2009. Texas Water Resources Institute Technical Report No. 406, Texas A & M University System College Station, Texas 77843-2118.

Niger State Bureau of Statistics (NSBS) (2011). 2011 Niger State Statistical year book.

Obada, E. M., & Oladejo, I. O. (2013). Groundwater Quality Appraisal in Southern Parts of Kaduna State, Nigeria. *American Journal of Environmental Engineering*, 3(1), 77–83. http://doi.org/10.5923/j.ajee.20130301.11

Okpara, J. N., Tarhule, A. A., & Perumal, M. (2013). Study of Climate Change in Niger River Basin, West Africa: Reality Not a Myth. In Climate Change-Realities, Impacts Over Ice Cap, Sea Level and Risks. InTech.

Olugboye, M.O. (2008). Hydrogeological Practices with Application to Nigeria ground water terrain, PIOS publications, Ilorin.

Omanayin, Y. A. & Ogunbajo, M. I. (2016). Geology and Environmental Impact of Artisanal Gold Mining around Kataeregi Area, North-Central Nigeria. 2, 135–146.

Omotosho, J. B. & Abiodun, B. J. (2007). A numerical study of moisture build-up and rainfall over West Africa. *Meteorol Appl*, 14: 209-225. DOI: 10.1002/met.11

Önöz, B., & Bayazit, M. (2003). The power of statistical tests for trend detection. *Turkish Journal of Engineering and Environmental Sciences*, 27(4), 247-251.

Oyedepo, S. O. (2013). Energy and Sustainable Development in Nigeria: the way forward. *Energy, Sustainability and Society*, 2: 15. https://doi.org/10.1186/2192-0567-2-15

Oyerinde, G. T., Wisser, D., Hountondji, F. C. C., Odofin, A. J., Lawin, A. E., Afouda, A., & Diekkrüger, B. (2016). Quantifying Uncertainties in Modelling Climate Change Impacts on Hydropower Production. *Climate, MDPI*, 4(34), 1–15. http://doi.org/10.3390/cli4030034

Panwar, N. L., Kaushik, S. C., & Kothari, S. (2011). Role of renewable energy sources in environmental protection: A review. *Renewable and Sustainable Energy Reviews*, 15(3), 1513–1524. http://doi.org/10.1016/j.rser.2010.11.037

Pervez, M. S. & Henebry G. M. (2014). Projections of the Ganges-Brahmputra precipitation-downscaled from GCM predictors. *J. Hydrol.*, 517, 120-134

Pervez, M. S. & Henebry, G. M. (2015). Assessing the impacts of climate and land use cover change on freshwater availability in the Brahmaputra River Basin. *J. Hydrol.*, 3,285-311. https//:doi.org/10.1016/j.ejrh.2014.09.003

Prudhomme, C., & Davis, H. (2006). Comparison of different sources of uncertainty in climate change impact studies in Great Britain. Hydrological Processes: Special Issue of International Workshop "Climatic and Anthropogenic Impacts on Water Resources Variability". Technical Document in Hydrology No. 80/, UNESCO, Paris/ UMR 5569, HydroSciences Montpellier. 2007. 183-190. http://unesdoc.unesco.org/images/001502/150251M.pdf.

R Core Team (2017). R: A language and environment for statistical computing. R Foundation for Statistical Computing, Vienna, Austria.URL https://www.R-project.org/.

Ravazzani, G., Dalla V., F., Mendlik, T., Galeati, G., Gobiet, A., & Mancini, M. (2015). Assessing climate impacts on hydropower production of Toce Alpine basin. In Engineering Geology for Society and Territory-Volume 1 (pp. 9-12). Springer International Publishing. http://doi.org/10.1007/978-3-319-09300-0

Rydgren, B., Graham, P., Basson, M, & D. Wisaeus. 2007. Addressing Climate Change-Driven Increased Hydrological Variability in Environmental Assessments for Hydropower Projects – a Scoping Study for the World Bank. Vattenfall Power Consultants, Sweden.

Saha, S., Moorthi, S., Pan, H.-L., Wu, X., Wang, J., Nadiga, S., Tripp, P., Kistler, R., Woollen, J., Behringer, D., Liu,X., Stokes, D., *et al.* (2010). The NCEP climate forecast system reanalysis. Bull. *Am. Meteorol. Soc.*, 91, 1015–1057.

Santander Meteorology Group (2012). FUME package – A set of functions for fire danger and climate analysis – version 1.0. R software packages, retrieved from https://CRAN.R-project.org/src/contrib/Achive/fume/.

Schaefli, B., Hingray, B., & Musy, A. (2007). Climate change and hydropower production in the Swiss Alps: quantification of potential impacts and related modelling uncertainties. *Hydrology and Earth System Sciences,* 11(3), 1191–1205. http://doi.org/10.5194/hess-11 1191-2007

Schuol J., Abbaspour K. C., Yang H., Srinivasan R. & Zehnder A. J. B. (2008). Modelling blue and green water availability in Africa. *Water Resour.* Res., 44, W07406, doi: 10.1029/2007WR006609.

Sen, P.K. (1968). Estimates of the regression coefficients based on Kendall's tau. *Journal of the American Statistical Association*, 63 (324), 1379–1389. doi: 10.1080/01621459.1968.10480934

Seyam, M., & Othman, F. (2015). Long-term variation analysis of a tropical river's annual streamflow regime over a 50-year period. *Theoretical and Applied Climatology*, 121(1-2), 71-85.

Srinivasan, R. (2013). Soil and Water Assessment tool – introductory manual – version 2012. Texas Water Resources Institute, College Station, TX. Retrieved from http://swat.tamu.edu/documentation/ (accessed on 20 December, 2016)

Strzepek, K., & McCluskey, A. (2006). District level hydro-climatic time series and scenario analysis to assess the impacts of climate change on regional water resources and agriculture in Africa. Pretoria: Centre for Environmental Economics and Policy in Africa (CEEPA).

Suleiman, Y. M., Ifabiyi, I. P. (2015). The role of rainfall variability in reservoir storage management at Shiroro Hydropower dam, Nigeria. *An International Journal of Science and Technology*, 3(2), 18-30. http://dx.doi.org/10.4314/stech.v3i2.2.

Sylla, M. B., Giorgi, F., Pal, J. S., Gibba, P., Kebe, I., & Nikiema, M. (2015). Projected changes in the annual cycle of high intensity precipitation events over West Africa for the late 21st century. *J. Clim.*, 28, 6475–6488.

[CrossRef]

Tadross, M., Jack, C., & Hewitson, B. (2005). On RCM-based projections of change in Southern Africa summer climate. *Geophysical Research Letters*, 32.

Teutschbein, C., & Seibert, J. (2012). Bias correction of regional climate model simulations for hydrological climate-change impact studies: Review and evaluation of different methods. Journal of Hydrology, 456, 12-29.

Traore, S. S., Landmann, T., Forkuo, E. K., & Traore, P. C. S. (2014). Assessing Long-Term trends in Vegetation Productivity change over the Bani River Basin in Mali (West Africa). *Journal of Geography and Earth Sciences,* 2 (2), 21–34. http://dx.doi.org/10.15640/jges.v2n2a2

United State Geological Survey (2016), Hydroelectric power water use. Retrieved from https://water.usgs.gov/edu/wuhy.html

Wang, X. L., (2008a). Accounting for autocorrelation in detecting mean-shifts in climate data series using the penalized maximal t or F test. *J. Appl. Meteor. Climatol*., 47, 2423-2444.

Wang, X. L., (2008b) Penalized maximal F-test for detecting undocumented mean-shifts without trend-change. *J. Atmos. Oceanic Tech*., 25 (No.3), 368-384. DOI:10.1175/2007/JTECHA982.1

Wang, X. L. (2010). Quick Guide for the RClimDex and RHtests Users. Climate Research Division, Atmospheric Science and Technology Directorate, Science and Technology Branch, Environment Canada.

Wang, X. L. and Y. Feng (2013). RHtestsV4 User Manual. Climate Research Division, Atmospheric Science and Technology Directorate, Science and Technology Branch, Environment Canada. 28 pp. [Available online at http://etccdi.pacificclimate.org/software.shtml]

Willems, P. & Lloyd-Hughes, B. (2016). Projected Change – River Flow and Urban Drainage. In: Quante, M., Colijn, F. (eds) North Sea Region Climate Assessment. Regional Climate Studies. *Springer*, Cham. https//:doi.org/10.1007/978-3-319-39745-0_7

World Commission on Dams (WCD) (2000). Dams and development: a new framework for decision-making. The report of the World Commission on Dams. London: Earthscan Publications Ltd.

World Energy Council (2015). World Energy Resources: Charting the Upsurge in Hydropower Development, 55.

World Meteorological Organization (WMO). What is Climate? Retrieved October 4, 2016, from http://www.wmo.int/pages/prog/wcp/ccl/faqs.php

World Resource Institute (2017). These Interactive Chart explains World's Top 10 Emitters, and How They've Changed. Retrieved from www.wri.org/blog/2017/04/interactive-chart-explains-worlds-top-10-emitters-and-how-theyve-changed.

Yue, S., Pilon, P., & Cavadias, G. (2002). Power of the Mann – Kendall and Spearman's rho tests for detecting monotonic trends in hydrological series. *Journal of Hydrology,* 259, 254–271.

Yue, S., & Wang, C. (2004). The Mann-Kendall Test Modified by Effective Sample Size to detect trend in serially correlated hydrological series. *Water Resources Management,* 18, 201–218.

APPENDICES

Appendix A: Annual output from Energy Model in the Near Future (2021 – 2045).

Year	Streamflow (m^3/s)		Energy (KWh/year)		Revenue (Million Naira)	
	RCP 4.5	RCP 8.5	RCP 4.5	RCP 8.5	RCP 4.5	RCP 8.5
2021	262.86224	372.42532	1206.5978	1605.9144	9044.0994	18354.393
2022	361.91391	270.8844	1268.3788	985.01801	10314.506	3725.9458
2023	381.24735	372.95898	1381.3227	1250.2501	11037.402	10091.757
2024	367.93397	392.88245	1348.2199	1477.5742	12026.065	14398.771
2025	441.60822	379.16276	1797.7508	1210.9294	19610.616	9148.0623
2026	294.72509	455.08544	864.44031	1810.1174	831.84549	21298.25
2027	474.06593	303.71966	2014.457	1067.8307	24658.307	5713.5682
2028	343.17439	488.53371	1117.2104	1603.0264	6898.5686	15677.018
2029	593.57853	353.64755	2269.4046	1424.3533	29672.394	14270.354
2030	211.02909	611.69366	1000.9886	2075.3398	4109.3636	25371.914
2031	395.4397	217.46939	1253.4236	951.85017	10167.804	2929.8035
2032	451.86262	407.50792	1687.1833	1322.5517	18558.473	11826.878
2033	597.51707	465.65279	2342.3932	1623.3359	30138.406	18012.593
2034	507.97235	615.75239	1661.0794	2333.389	18329.014	30631.169
2035	235.26928	523.4749	1206.4364	1873.0481	8614.0996	22721.916
2036	342.8672	242.44935	1234.4749	1068.5202	9712.7946	5730.0051
2037	284.13628	353.33099	843.41654	1092.0219	327.1564	6294.0453
2038	712.69842	292.8077	2312.294	900.0946	30358.663	1687.7881
2039	604.0228	734.44891	2393.5269	2308.2766	30551.911	30249.129
2040	524.55633	622.45667	1771.4971	2370.3301	19502.13	31287.202
2041	492.75732	540.565	1842.9998	1857.0844	22066.176	21566.41
2042	215.77007	507.79553	1188.8085	1833.4415	8616.9203	22243.393
2043	641.04868	222.35505	1882.3333	1072.9824	20222.214	5837.0953
2044	275.28518	660.61253	1136.8697	1912.5969	7370.5096	20932.082
2045	303.96907	283.68647	1227.9035	1157.2132	9555.4381	7858.6352

Source: Authors compilation, 2017.

Appendix B: Annual output from SWAT model and Energy Model in the Mid Future (2046 – 2070).

Year	Streamflow (m^3/s)		Energy (KWh/year)		Revenue (Million Naira)	
	RCP 4.5	RCP 8.5	RCP 4.5	RCP 8.5	RCP 4.5	RCP 8.6
2046	545.47003	364.93279	2189.4881	1103.0503	27820.374	6558.8472
2047	286.78199	670.01299	1382.145	1965.7049	13257.118	23681.232
2048	435.52441	352.26071	1339.9613	1182.4511	11703.516	8464.3429
2049	507.61277	534.96433	1909.3009	1464.1137	22804.374	14574.939
2050	178.95695	623.51207	1003.9506	2041.8485	4180.333	26031.536
2051	219.90196	219.81681	1107.8576	861.7358	-1117.8134	766.93564
2052	326.01147	270.11047	1220.8563	787.4313	9385.8304	-1016.4892
2053	362.73686	400.44715	1084.3478	1141.8467	6109.8592	7467.6723
2054	712.26044	445.55777	2187.7112	1157.2972	26921.806	7159.029
2055	665.18034	874.88536	2544.8844	2292.2598	33767.581	29456.898
2056	484.44149	817.05583	1884.3814	2583.8735	23006.039	34703.894
2057	375.61394	595.05028	1374.0443	1716.1068	13062.699	18561.677
2058	509.36229	461.37497	1905.0547	1674.0158	22736.394	20146.291
2059	462.9452	625.66105	1895.9024	1703.3639	23355.553	18386.299
2060	561.15752	568.6459	2149.0639	1895.6662	27634.494	23692.499
2061	226.18571	689.28228	1132.0361	2131.2668	7254.5053	27393.922
2062	261.38344	277.82895	702.52366	1104.1915	-3054.3922	6586.235
2063	454.58454	321.06311	1524.7112	844.24936	15781.12	347.25831
2064	262.44892	558.37632	1144.2815	1490.4238	7548.5111	13889.5
2065	352.73747	322.37186	1356.7774	1312.4003	12648.53	11583.485
2066	551.87786	433.2753	2109.5085	1055.2402	26146.631	5084.9407
2067	734.37199	677.88387	2077.2591	2167.4377	26463.435	28027.76
2068	210.37104	902.04548	1237.2037	2009.07	6880.2785	24831.578
2069	225.31576	258.40344	946.93554	1090.5497	-507.37931	6258.8313
2070	540.09201	276.76036	1701.1748	810.60965	16825.067	-460.09064

Source: Authors compilation, 2017.

Appendix C: Annual output from SWAT model and Energy Model in the Far Future (2071 – 2095).

Year	flow		Energy		Revenue	
	RCP 4.5	RCP 8.5	RCP 4.5	RCP 8.5	RCP 4.5	RCP 8.5
2071	509.79341	404.16414	2208.4716	1776.6127	28697.503	18468.482
2072	176.9369	388.02724	1033.3138	2003.505	4885.0495	24926.005
2073	486.11138	134.67483	1483.1803	878.66872	13767.544	1173.4491
2074	214.59806	370.00176	1025.5679	1645.4272	4699.1478	17882.105
2075	842.60076	163.34046	2461.381	1037.9711	31932.924	4996.8232
2076	403.88526	641.34224	1597.6971	2383.8339	17051.626	29847.92
2077	481.58873	307.41567	2054.1491	1560.4838	26228.305	17152.869
2078	374.57281	366.55936	1307.5985	1930.5394	9359.5133	23047.05
2079	306.35229	285.10462	1358.2425	1568.8426	12098.951	15451.483
2080	277.13988	233.17884	971.72832	1193.5491	3406.6361	6796.0699
2081	776.96506	210.94393	2276.6678	917.19797	28286.014	2098.0304
2082	230.20272	591.38389	1048.6282	2363.6082	4607.8904	31006.833
2083	228.49518	175.21789	910.05385	1164.6416	1926.5705	8036.9171
2084	241.26177	173.9182	865.28154	845.69531	851.67683	381.96694
2085	441.06539	183.63544	1360.4379	897.33304	12736.265	1004.7507
2086	554.44393	335.71518	2159.0563	1489.857	27287.745	15307.106
2087	778.49363	422.01281	2754.6067	2104.4306	37435.585	26398.643
2088	346.90444	592.54736	1435.2976	2742.9944	14113.879	37194.533
2089	362.5048	264.04494	1584.121	1524.5814	18104.661	16246.802
2090	485.61884	275.9191	1605.2034	1382.9004	18235.469	13275.605
2091	595.85202	369.62686	2300.6253	1854.1521	30171.924	22505.557
2092	754.36031	453.53041	2593.3017	2182.5178	34854.747	27370.319
2093	580.06713	574.17837	2222.4326	2587.268	28280.495	34696.486
2094	271.76785	441.51581	1331.2603	2212.5645	10969.837	28762.991
2095	378.68964	206.85503	1426.3799	1410.3298	14177.533	13245.067

Source: Authors compilation, 2017.

Appendix D: R Scripts for Mann-Kendall Analysis

```
#timeseries Analysis (Mann-Kendall)

getwd()

setwd("~/Homogenisation_QC/Trend/")

getwd()

require(zoo); library(trend); require(ggplot2);require(Kendall)

require(fume); require(hyfo) ;library(zoo); library(tis); library(plyr); library(trend); library(MASS); library(zyp); library(gimme)

#read in data 1.Kaduna

Kaduna <- read.table("Kad_Ann.csv",header=T,sep=",",dec=".")

Kaduna2 <- read.table("Kaduna_h.csv",header=T,sep=",",dec=".")

head(Kaduna)

Kadmax <- as.vector(Kaduna[,3])

k1=ts(Kadmax,start=c(1981),frequency= 1)

k1m=ts(Kaduna2[,2],start=c(1981),frequency= 12)

Kadmin <- as.vector(Kaduna[,4])

k2=ts(Kadmin,start=c(1981),frequency= 1)

Kadpcp <- as.vector(Kaduna[,2])

k3=ts(Kadpcp,start=c(1981),frequency= 1)

#Autocorrelation

Kadautocorrtmax <- acf(k1, type = "correlation")

plot(Kadautocorrtmax, main="Autocorrelation ACF",xlim=c(1,16), panel.first = grid())

Kadpautocorrtmax <- pacf(k1)

plot(Kadpautocorrtmax)

Kadautocorrtmin <- acf(k2, type = "correlation")

plot(Kadautocorrtmin, main="Autocorrelation Function",xlim=c(1,16), panel.first = grid())

Kadpautocorrtmin <- pacf(k2)

Kadautocorrtpcp <- acf(k3)

plot(Kadautocorrtpcp, main="Autocorrelation Function",xlim=c(1,16), panel.first = grid())

Kadpautocorrtpcp<- pacf(k3)
```

```
#save data
write.csv(Kadautocorrtmax$acf, file = "acf_Kadmin.csv", row.names = T)
write.csv(Kadautocorrtmin$acf, file = "acf_Kadmin.csv", row.names = T)
write.csv(Kadpautocorrtmax$acf, file = "pacf_Kadmax.csv", row.names = T)
write.csv(Kadpautocorrtmin$acf, file = "pacf_Kadmax.csv", row.names = T)
write.csv(Kadautocorrtpcp$acf, file = "pacf_Kadpcp.csv", row.names = T)
write.csv(Kadpautocorrtpcp$acf, file = "pacf_Kadpcp.csv", row.names = T)
# Tmax (Maximum Temperature).
Kaduna_maxtrend <- mkTrend(as.vector(k1), ci=0.95)
Kad_sstmax <- sens.slope(k1)
# Tmin
Kaduna_mintrend <- mkTrend(as.vector(k2), ci=0.95)
Kaduna_mintrend
summary(MannKendall(k2))
Kad_sstmin <- sens.slope(k2)
#pcp
Kaduna_pcptrend <- mkTrend(as.vector(k3), ci=0.95)
Kaduna_pcptrend
summary(MannKendall(k3))
Kad_sstpcp <- sens.slope(k3)
# Sen.slope significance test (Slope magnitude) with library(trend)
# Tmax
write.csv(Kaduna_mintrend, file = "trend_Kadmin.csv", row.names = T)
write.csv(Kad_sstmin, file = "sst_Kadmin.csv", row.names = T)
write.csv(Kaduna_maxtrend, file = "trend_Kadmax.csv", row.names = T)
write.csv(Kad_sstmax, file = "sst_Kadmax.csv", row.names = T)
write.csv(Kaduna_pcptrend, file = "trend_Kadpcp.csv", row.names = T)
write.csv(Kad_sstpcp, file = "sst_Kadpcp.csv", row.names = F)
#Kad_sstpcp
```

```
#-------------------------------------------------------------------------------
#3. Jos
Jos <- read.table("J_Ann.csv",header=T,sep=",",dec=".")
head(Jos)
Jmax <- as.vector(Jos[,2])
J1=ts(Jmax,start=c(1981),frequency= 1)
Jmin <- as.vector(Jos[,3])
J2=ts(Jmin,start=c(1981),frequency= 1)
Jpcp <- as.vector(Jos[,4])
J3=ts(Jpcp,start=c(1981),frequency= 1)
#Autocorrelation
Jautocorrtmax <- acf(J1, type = "correlation")
plot(Jautocorrtmax)
Jpautocorrtmax <- pacf(J1)
plot(Jpautocorrtmax)
Jautocorrtmin <- acf(J2, type = "correlation")
Jpautocorrtmin <- pacf(J2)
Jautocorrtpcp <- acf(J3)
Jpautocorrtpcp<- pacf(J3)
#save data
write.csv(Jautocorrtmax$acf, file = "acf_Jmin.csv", row.names = T)
write.csv(Jautocorrtmin$acf, file = "acf_Jmin.csv", row.names = T)
write.csv(Jpautocorrtmax$acf, file = "pacf_Jmax.csv", row.names = T)
write.csv(Jpautocorrtmin$acf, file = "pacf_Jmax.csv", row.names = T)
write.csv(Jautocorrtpcp$acf, file = "ACF_Jpcp.csv", row.names = T)
write.csv(Jpautocorrtpcp$acf, file = "pacf_Jpcp.csv", row.names = T)

# Tmax
J_maxtrend <- mkTrend(as.vector(J1), ci=0.95)
J_sstmax <- sens.slope(J1)
```

```
# Tmin
J_mintrend <- mkTrend(as.vector(J2), ci=0.95)
J_mintrend
summary(MannKendall(J2))
J_sstmin <- sens.slope(J2)

#pcp
J_pcptrend <- mkTrend(as.vector(J3), ci=0.95)
J_pcptrend
summary(MannKendall(J3))
J_sstpcp <- sens.slope(J3)

#-------------------------------------------------------------------------------------------
#4. Minna
#Minna
Minna <- read.table("Min_Ann.csv",header=T,sep=",",dec=".")
head(Minna)
Mmax <- as.vector(Minna[,2])
M1=ts(Mmax,start=c(1981),frequency= 1)
Mmin <- as.vector(Minna[,3])
M2=ts(Mmin,start=c(1981),frequency= 1)
Mpcp <- as.vector(Minna[,4])
M3=ts(Mpcp,start=c(1981),frequency= 1)
M3
#Autocorrelation
Mautocorrtmax <- acf(M1, type = "correlation")
plot(Mautocorrtmax)
Mpautocorrtmax <- pacf(M1)
plot(Mpautocorrtmax)
Mautocorrtmin <- acf(M2, type = "correlation")
```

```
Mpautocorrtmin <- pacf(M2)
Mautocorrtpcp <- acf(M3)
Mpautocorrtpcp<- pacf(M3)
#save data
write.csv(Mautocorrtmax$acf, file = "acf_MINNAmax.csv", row.names = T)
write.csv(Mautocorrtmin$acf, file = "acf_MINNAmin.csv", row.names = T)
write.csv(Mpautocorrtmax$acf, file = "pacf_MINNAmax.csv", row.names = T)
write.csv(Mpautocorrtmin$acf, file = "pacf_MINNAmin.csv", row.names = T)
write.csv(Mautocorrtpcp$acf, file = "ACF_MINNApcp.csv", row.names = T)
write.csv(Mpautocorrtpcp$acf, file = "pacf_MINNApcp.csv", row.names = T)
# Tmax
M_maxtrend <- mkTrend(as.vector(M1), ci=0.95)
M_sstmax <- sens.slope(M1)
# Tmin
M_mintrend <- mkTrend(as.vector(M2), ci=0.95)
M_mintrend
summary(MannKendall(M2))
M_KENDAL_Min = mk.test(M2)
M_sstmin <- sens.slope(M2)

#pcp
M_pcptrend <- mkTrend(as.vector(M3), ci=0.95)
M_pcptrend
summary(MannKendall(M3))
M_sstpcp <- sens.slope(M3)

#-------------------------------------------------------------------------------------
#5. Zaria
#ZARIA
Zaria1 <- read.table("Za_Ann1.txt",header=T)
```

```
head(Zaria1)
Zmax <- as.vector(Zaria1[,2])
Zmax
Z1=ts(Zmax,start=c(1981),end=c(2015), frequency= 1)
Z1
Zmin <- as.vector(Zaria1[,3])
Zmin
Z2=ts(Zmin,start=c(1981),end=c(2015), frequency= 1)
Z2
Zpcp <- as.vector(Zaria1[,4])
Z3=ts(Zpcp,start=c(1981),frequency= 1)
#Autocorrelation
Zautocorrtmax <- acf(Z1, type = "correlation")
plot(Zautocorrtmax)
Zpautocorrtmax <- pacf(Z1)
plot(Zpautocorrtmax)
Zautocorrtmin <- acf(Z2, type = "correlation")
Zpautocorrtmin <- pacf(Z2)
Zautocorrtpcp <- acf(Z3)
Zpautocorrtpcp<- pacf(Z3)
#save data
write.csv(Zautocorrtmax$acf, file = "acf_ZARIAmax.csv", row.names = T)
write.csv(Zautocorrtmin$acf, file = "acf_ZARIAmin.csv", row.names = T)
write.csv(Zpautocorrtmax$acf, file = "pacf_ZARIAmax.csv", row.names = T)
write.csv(Zpautocorrtmin$acf, file = "pacf_ZARIAmin.csv", row.names = T)
write.csv(Zautocorrtpcp$acf, file = "pacf_ZARIAPCP.csv", row.names = T)
write.csv(Zpautocorrtpcp$acf, file = "pacf_ZARIAPCP.csv", row.names = T)
# Tmax
Z_maxtrend <- mkTrend(as.vector(Z1), ci=0.95)
Z_sstmax <- sens.slope(Z1)
```

```
# Tmin
Z_mintrend <- mkTrend(as.vector(Z2), ci=0.95)
Z_mintrend
summary(MannKendall(Z2))
Z_sstmin <- sens.slope(Z2)

#pcp
Z_pcptrend <- mkTrend(as.vector(Z3), ci=0.95)
Z_pcptrend
summary(MannKendall(Z3))
Z_sstpcp <- sens.slope(Z3)

#-------------------------------------------------------------------------------------------------
----
flow=read.table("flow_annual1.csv",header=T,sep=",", dec=".")
head(flow)
fl=as.vector(flow[,2])
f1=ts(fl,start=c(1990),frequency= 1)
fautocorr <- acf(f1, type = "correlation")
plot(fautocorr)
fautocorr <- acf(f1, type = "correlation")
plot(fautocorr)

setwd("C:/Users/Peter Rock Ebo Odoom/Documents/Homogenisation_QC/Trend/")
Evap=read.table("evapo.csv",header=T,dec=".",sep=",")
class(Evap)
Ev=as.vector(Evap[,1])
E1=ts(Ev,start=c(1990), frequency = 1)
```

Appendix E: Climate forecast System Stations used in the study showing the number of raindays.

STATION	WLATITUDE	WLONGITUDE	WELEV	RAIN_YRS
9869	9.835	6.875	377	33
9872	9.835	7.188	501	33
9875	9.835	7.5	605	33
9884	9.835	8.438	795	33
9888	9.835	8.75	1170	33
10169	10.147	6.875	367	33
10172	10.147	7.188	513	33
10175	10.147	7.5	523	33
10178	10.147	7.813	649	33
10181	10.147	8.125	600	33
10184	10.147	8.438	733	33
10188	10.147	8.75	912	33
10572	10.46	7.188	659	33
10575	10.46	7.5	608	33
10578	10.46	7.813	641	33
10581	10.46	8.125	606	33
10584	10.46	8.438	606	33
10588	10.46	8.75	844	33
10872	10.772	7.188	628	33
10875	10.772	7.5	646	33
10878	10.772	7.813	615	33
10881	10.772	8.125	603	33
10884	10.772	8.438	691	33
11172	11.084	7.188	637	33
11175	11.084	7.5	645	33
11178	11.084	7.813	624	33
11181	11.084	8.125	666	33
11472	11.396	7.188	629	33

Source: Authors compilation, 2017.

Appendix F: Paper presented at Conference

Hydrological modelling of Shiroro Dam Catchment using Climate Forecast Reanalysis data in Soil and Water Assessment Tool model for sustainable water use in Nigeria

Peter Rock Ebo Odoom[1] and Onemayin David Jimoh[2]

[1]West Africa Science Service Centre for Climate Change and Adapted Land Use: Federal University of Technology, Minna

[2]Department of Civil Engineering: Federal University of Technology, Minna

Email: podoom21@yahoocom, odjimoh@futminna.edu.ng

+2347054174214, +2348035862472

ABSTRACTS

The study evaluate the application of National Center for Environmental Prediction's Climate Forecast System Reanalysis data for forcing Soil and Water Assessment Tool in Shiroro catchment to assess its suitability for predicting streamflow. Freely available remote sensing datasets such as FAO soil map, Digital Elevation Model and Moderate Resolution Imaging Spectroradiometer (MODIS) land cover were utilised in ArcSWAT to set up the watershed. Streamflow data obtained were divided into two with the first part used for calibration and the other part for validation of the watershed model. The calibration results were unsatisfactory for R^2 = 0.51 and NSE=0.43 whiles PBIAS = -2 was very good. The uncertainty criteria of the model p-factor was 0.79 and r-factor 1.27 which were within the recommended range. The R^2= 0.79 and NSE= 0.77 and PBIAS = 15 values were good during the validation period with p-factor = 0.77 and r-factor = 0.77. With improvement being made in CFSR with introduction of CFSv2, its performance for rainfall-runoff modelling the catchment is likely to increase.

Key Words: SWAT; CFSR; Hydrological Modelling; MODIS; Shiroro

INTRODUCTION

Water is huge resource which directly or indirectly influences the quality of life of people living in any community or country. It comes as no surprise that access to clean water supply and sanitation is part of the major goals of sustainable development. Globally, the risk of water scarcity are as a result of increasing population growth, climate change, globalization (Srinivasan *et al.*, 2012) and poor water management practices. Increasing population contributes to the gradual loss in wetland over the past decade and in increase contamination of water resources in developing nation. It is an established fact that Climate change will disrupt the hydrological cycle as a result of variability in precipitation and temperature. Assessment of hydrology and their resilience to changes in the environment becomes unavoidable.

Hydrological models have been developed to assess blue and green water quantity and quality to aid in management decisions and disaster planning. Hydrological models are used in the simulation of the hydrology of a location as they attempt to mimic the underlining physiochemical processes in the watershed for the prediction of streamflow, flood modelling, irrigation, groundwater and source of pollution (Benke *et al*, 2007). Most hydrological models are simulate the close interaction between precipitation events and runoff components in a hydrological system. Quality of precipitation data are important in understanding the hydrological cycle. In developing countries, accessibility of climatic data still remains a challenge as they are marred with in insufficient in-situ weather stations with low spatial resolution (Gruber *et al.*, 2017; The World Bank, 2017) and in some cases missing data (Fuka *et al*, 2013;). In Nigeria, the situation is not different (Leary *et al.*, 2008) with the Nigerian Meteorological Agency (NiMeT) making frantic efforts to improve the density of observation in the country through the use of Automatic Weather System (Aderinto, 2006; www.nimet.gov.ng/press/nimet-establish-1000-automatic-weather-stations). Precipitation products from reanalysis and satellites which are freely available to users provide good alternatives to in-situ observed data in hydrological modelling. Agunbiade and Jimoh (2013), Oyerinde *et al* (2016), Oyerinde *et al.* (2017) and Schuol *et* al (2008) have utilised reanalysis or satellite based precipitation products for understanding the interrelationship between rainfall and runoff in Nigeria. There are a number of reanalysis datasets at high resolution with provides a wide range hydrometeorological variables such as European Centre for Medium-Range Weather Forecasts (ECMWF) interim Reanalysis (ERA-Interim), National Aeronautics and Space Administration Modern-Era Retrospective Analysis Research Application (MERRA) and National Centers for Environmental Prediction's Climate Forecast System Reanalysis (CFSR) (Saha *et al*., 2010) at both high and temporal resolutions(Dile and Srinivasan, 2014). The Climate Forecast System Reanalysis data have application in climate and hydrological research studies. CFSR have been used in a number of studies such Fuka *et al.* (2013). The CFSR data suitability was evaluated for modelling one watershed in Ethiopia and four other watersheds in United States of America alongside in-situ observed data. Their findings confirmed that CFSR are good as observed in-situ data and even better when in-situ weather stations are more than 10 km apart. Dile and Srinivasan (2014) assessed the application of CFSR in forcing the SWAT model to simulate streamflow in 3 watersheds in Ethiopia. The CFSR was observed to be ideal for locations with scarcity of data whiles the in-situ observed climate data overall performed

better in gauged locations than CFSR. Precipitation is highly variable in West Africa due to the complex geography and coastline (Gbobaniyi *et al*, 2013). This makes it difficult to simulation of the features of West African Monsoon. Thus it is necessary to investigate the suitability of reanalysis datasets for modelling different locations in West Africa. This study aims to assess the suitability of SWAT model with forcing CFSR data in predicting streamflow in Shiroro catchment.

Methodology

Study Area

Shiroro Hydroelectric Dam is situated in the Kaduna River Basin at Shiroro village in the Niger State of Nigeria. It is a dam constructed on the course of River Kaduna and located at latitude 9^0 58' N and longitude 6^0 50' E. The Shiroro reservoir covers a total land area of about 320 km^2 and has total storage capacity of 7 billion cubic metres (Suleiman and Ifabiyi, 2015). The entire catchment is in the Guinea Savannah zone of Nigeria and the rainfall of the catchment is influenced by the movement of the Inter Tropical Convergence Zone, the African Easterly Jet and the Tropical Easterly Jet (Omotosho and Abiodun, 2007). The rainfall pattern is unimodal where the onset is in April and cessation in October. Figure 1 illustrate the Shiroro catchment with land use classification for SWAT model.

Input Data

Land use and Land Cover (LULC) is one of the most important factors that affect surface erosion, runoff, sedimentation load, and evapotranspiration in a watershed. Land Use Land Cover data was accessed from Moderate Resolution Imaging Spectroradiometer (MODIS) annually compiled Land cover data (MCD12Q1). MODIS Reprojection Tool software (MRT) provided by NASA EODIS LP DAAC was used reproject sinusoidal projection of the MODIS dataset to GCS WGS 84 coordinate system. The MODIS land cover datasets for the year 2013 was acquired and processed for the model input. The MODIS land cover datasets are provided by NASA EODIS Land Process Distributed Active Archive Center (LP DAAC) and available at Earth Explorer data portal (https://earthexplorer.usgs.gov/).

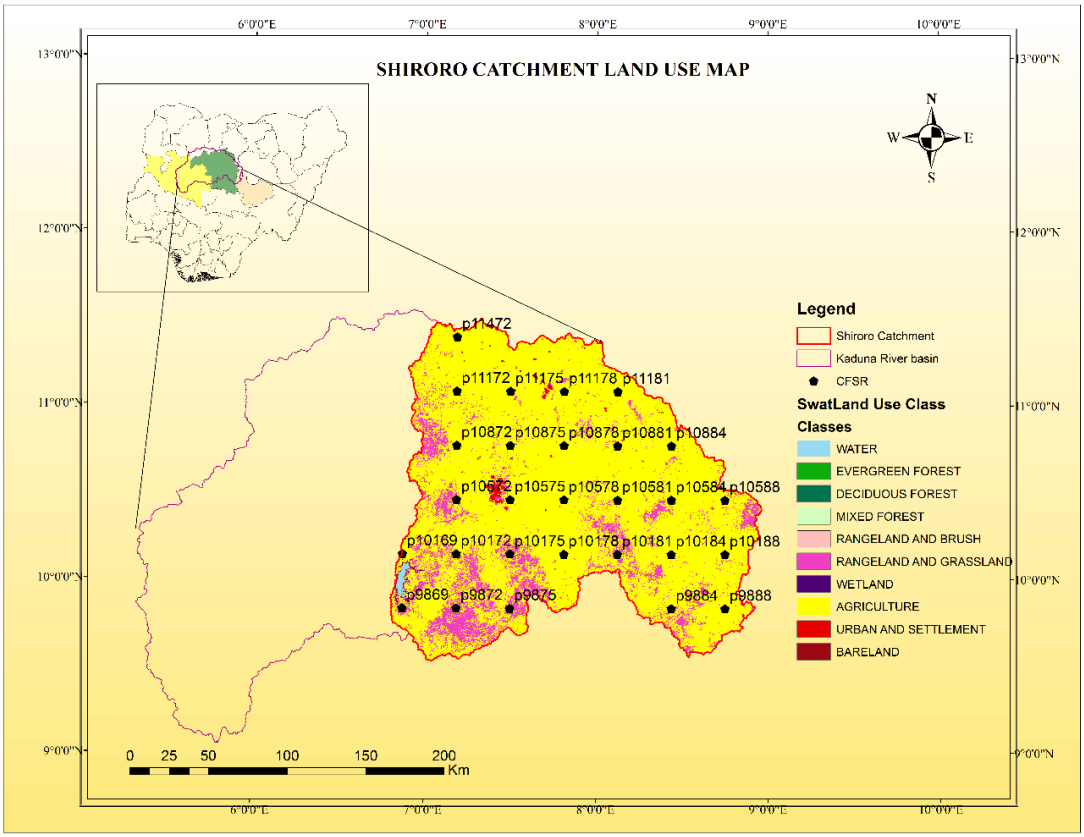

Figure 1: Land use map of Shiroro Catchment showing CFSR point weather stations

The International Geosphere–Biosphere Programme (IGBP) land cover classification was selected. The MODIS land cover was re-classified into land use types similar to existing SWAT model land use by creating a lookup table (Table 1). Topography of the watershed was defined by a DEM that describes the elevation of any point in a given area at a specific spatial resolution. A 90 m by 90 m resolution DEM was obtained from The Consortium for Spatial Information of the Consultative Group for International Agricultural Research (CGIARS-CSI) SRTM (Shuttle Radar Topography Mission) website srtm.csi.cgiar.org/ which are post processed and freely distributed (Jarvis et al., 2008). Soil information such as soil type, organic carbon content, hydraulic conductivity and texture influences the prediction of available water content, infiltration rate, and surface runoff of the catchment area. The Food and Agriculture Organisation (FAO) Digital Soil Map of the World (FAO, 2003) was retrieved from waterbase website (http://www.waterbase.org/download_data.html). River discharge data to the Shiroro dam over the span of 25 years was obtained from Shiroro Hydroelectric Power Station. The Climate Forecast System Reanalysis (CFSR) data used to force the model during the calibration and validation process was taken from www.globalweather.tamu.edu. The

CFSR data were download from the year 1981 to 2013 from the SWAT global weather website for the study area. CFSR points weather stations located in the catchment is illustrated in Figure 1.

Soil and Water Assessment Tool

Soil and Water Assessment Tool (SWAT) is a semi-distributed physical based model capable of modelling complex watersheds with varying soils and land use as a result of land use practices on water resources (Arnold *et al.*, 1998). Soil and Water Assessment Tool (SWAT) model have been widely used worldwide to assess water quantity and quality issues. SWAT model possess ability to simulate single watershed or a network of multiple watersheds which are hydrological linked in a location. The SWAT model divides the watershed into sub-basins, then sub-basins to hydrological response units (HRU) based on the land use, soil (Table 2) and slope distribution in the watershed. The hydrology of the SWAT model is based on the water balance equation.

Table 1: Reclassification of land cover types into SWAT database land Use classes.

SWAT LAND USE type	**IGBP land cover type**
Water	Water
Evergreen Forest	Evergreen Needleleaf and Broadleaf forest
Deciduous Forest	Deciduous Needleleaf and Broadleaf Forest
Mixed Forest	Mixed forest
Rangeland and Brush	Closed shrublands, Open shrublands, Woody savannahs,
Rangeland and grassland	Savannahs, Grasslands
Urban	Urban and built-up
Agriculture	Croplands, Cropland/Natural vegetation mosaic
Bareland	Barren or sparsely vegetated, Snow and ice
Wetland	Permanent wetlands,

The slope as a topographical parameter of the watersheds were generated from the DEM using the Slope function. Five slope classes were identified in degrees. The slope classes

used in the Hydrological Response Unit definition were 0^o – 2.868^o, 2.868^o – 5.497^o, 5.497^o – 8.844^o, 8.844^o – 12.668^o and greater than 12.668^o. The highest elevation in the study area was 1582 m high, the mean elevation was 676.47 m and the lowest was 283 m above sea level. The delineation of the watershed was based on subjective judgement on the threshold value that best define the rivers and stream from the DEM. The area used was 80,000 ha which fell within the ranges 32,403 to 6,480,537 ha indicated during automatic watershed delineation for the stream definition. The dam location was used as the outlet for the delineation of Shiroro catchment area. A total of 109 HRUs were derived from 21 sub-basins based on the soil, land use and slope classification specified with a watershed area of 34,684.1025 km.

Table 2: Soil types present in the catchment and their percentage in the catchment.

Dominant Soil Name	**Soil classification**	**Hydrologic Group**	**TEXTURE**	**Watershed Area %**
Lithosols	I-60	C	LOAM	0.76
Lithosols	I-c-99	C	LOAM	0.46
Ferric Acrisols	Af12-2b-1020	D	SANDY_CLAY_LOAM	1.54
Orthic Acrisols	Ao43-1b-1056	C	LOAMY_SAND	1.56
Lithosols	I-Lf-1255	C	SANDY_CLAY_LOAM	1.46
Lithosols	I-bc-1324	C	LOAM	0.42
Ferric Luvisols	Lf1-1420	C	SANDY_CLAY_LOAM	0.02
Ferric Luvisols	Lf41-1-2a-1468	C	SANDY_LOAM	0.98
Ferric Luvisols	Lf42-1a-1470	C	SANDY_LOAM	11.77
Ferric Luvisols	Lf49-1a-1476	C	SANDY_LOAM	39.1

Sensitivity analysis, Calibration, Validation and Performance Evaluation

Parameters in SWAT are calibrated either manually or automatically. The sensitivity analysis is carried out to identify the most influential parameters in the SWAT model for streamflow simulation before calibration takes place (Griensven *et al.*, 2006). Parameters selection were also based on parameters sensitive to streamflow in Abbaspour *et al.* (2004), other parameters likely to influence streamflow, Schuol *et al.* (2008) and Akpoti *et al.* (2016), with the latter two working in similar climatic zone as the study area. The Global Sensitivity Analysis was used to analyse the sensitivity of the parameters after each calibration run. Fourteen (14) parameters were used in the calibration process. The parameters selected for the calibration of the model were r__SOL_K(…).sol, v__ALPHA_BF.gw, r__CN2.mgt, v__CH_N2.rte, v__ESCO.hru, v__CH_K2.rte, r__SOL_BD(…).sol, v__GW_REVAP.gw, v__OV_N.hru, v__CANMX.hru, v__RCHRG_DP.gw, v__GWQMN.gw, v__GWHT.gw and r__SOL_AWC(…).sol. The Global Sensitivity employs multiple regression systems that regresses Latin hypercube generated parameters against the objective function (Abbaspour, 2015). The relative significance of each parameter is determined by using the statistical test *t*-test. The sensitivities values obtain give average changes in objective function derived from changes in parameter while all other parameters are simultaneously changing. The *t*-stats refers to the coefficients of the parameter divided by the standard error and is the extent of the precision to which the coefficient of regression is measured, hence the larger the values in absolute and the smaller the p-value (less than 0.05), the more sensitive the parameter (Abbaspour, 2015).

The SWAT model performance is evaluated after the calibration and validation on the initial model simulation run. The model is evaluated by performance on its ability to simulate and project flow by using primarily three objective functions namely the coefficient of determination (R^2), Nash-Sutcliffe Efficiency (NSE) and Percent Bias (PBIAS) (Abbaspour *et al.*, 2015). These goodness of fit statistics were used to evaluate the performance of the model. The equations below define these statistical objective functions.

$$NSE = 1 - \frac{\sum_{i=1}^{n}(Q_{sim,i} - Q_{obs,i})^2}{\sum_{i=1}^{n}(Q_{obs,i} - Q_{obs})^2} \qquad PBIAS = 100 \times \frac{\sum_{i=1}^{n}(Q_{obs} - Q_{sim})_i}{\sum_{i=1}^{n} Q_{obs,i}}$$

$$R^2 = \frac{\left[\sum_{i=1}^{n}(Q_{obs,i} - \bar{Q}_{obs})(Q_{sim,i} - \bar{Q}_{sim})\right]^2}{\sum_{i=1}^{n}(Q_{obs,i} - \bar{Q}_{obs})^2 \sum_{i=1}^{n}(Q_{sim,i} - \bar{Q}_{sim})^2}$$

where $Q_{obs,i}$ is the observed flow at time i (m^3/s), $Q_{sim,i}$ is the simulated flow at time i (m^3/s), Q_{obs} is the measured variable (m^3/s), Q_{sim} is the simulated variable (m^3/s), i is the i^{th} measured or simulated data.

About 65 % of the observed streamflow records from the gauging station at dam were used for calibration and the rest used for validation of the model. The Soil and Water Assessment Tool – Calibration and Uncertainty Programs (SWAT-CUP) which is a standalone program was used for the calibration and validation of the SWAT model. The model is initially run for the calibration between the periods 1990 – 2005 and for validation period from 2006-2013 in the SWAT-CUP program. The SUFI-2 algorithm was used for the calibration. The calibration are based on improvement of the goodness fit after each iteration. The calibration ends when the goodness of fit statistics stops improving with iterations. Under the SUFI-2 approach, 200 runs were done for each iterations and each parameters updated automatically, the new values fall within the Absolute Swat values range of parameters in the SWAT-CUP program. More iterations are performed to improve the statistics of the goodness of fit of the model. In this study, five iterations were performed and the best solution amongst them selected.

Results and Discussion

Sensitivity Analysis, Calibration and Validation of the Model

Soil Water Assessment integrates several parameters which are used for the calibration of models. Some of these parameters are location specific (Temperate regions and Tropical Regions) and also differs in sensitivity in different watersheds and even sub-watersheds during the calibration process of the model. The Global Sensitivity analysis was used to identify most sensitive parameters for the model calibration. The most sensitive parameters during the calibration stage are illustrated in Table 4. Four parameters were sensitive out of the fourteen parameters used for the calibration of the model.

Table 0: Parameters Most Sensitive to flow in the Shiroro catchment.

Parameter Name	t-stat	p-value
R_CN2.mgt	-4.94	0.000002
V_GW_REVAP.gw	4.86	0.000003
V_GWQMN.gw	4.12	0.000057
V_ESCO.hru	-3.10	0.002255

SUFI-2 algorithm fitted these parameters as sensitive with values having absolute t-stats values and lower p-value less than 0.05 significant level. The most sensitive parameter was the CN2 and least sensitive among the parameters was the ESCO. Monthly time steps of streamflow data were used in calibrating the model in the SWAT-CUP. Nash-Sutcliffe Efficiency was the objective function employed during the calibration of the model. A Nash-Sutcliffe objective function ranges between negative infinity (-∞) to one (1) (Abbaspour, 2015). Table 5 indicates the results of calibration from the five iterations with 200 simulations using SUFI-2 algorithm.

Table 5: Calibration results for 200 simulations for each iterations

Iteration	**Summary Statistics**					
	NSE	***R^2***	***PBIAS***	**P-factor**	**r-factor**	**Mean Sim (mean Obs value)**
1st	0.38	0.49	2.9	0.92	2.80	277.77 (286.01)
2nd	0.43	0.51	-0.2	0.79	1.27	286.64 (286.01)
3rd	0.46	0.55	17.8	0.67	0.80	235.08 (286.01)
4th	0.47	0.55	13.9	0.56	0.50	246.32 (286.01)
5th	0.22	0.47	-14.4	0.82	1.52	327.14 (286.01)

Sim refers to the simulation values obtained and Obs is the observed values measured.

Based on Moriasi *et al.* (2016), the results of NSE and R^2 from the five iteration were unsatisfactory for monthly scale calibrations whilst the PBIAS for the 1st and 2nd iteration could be said to be very good. PBIAS of the 3rd iteration was unsatisfactory whilst those of the 4th and the 5th iteration suggest a satisfactory results for the calibration. Although an NSE value of one represents the models simulated streamflow values having perfect agreement with the observed streamflow values, values of NSE higher than zero of a model is considered acceptable performance level and a less than or equal to zero value shows that the average of the observed data is a better at prediction than the model (Dile and Srinivasan, 2014). The 2nd iteration simulated streamflow average (286.64 m^3/s) value was the closest the observed average streamflow value of 286.01 m^3/s for the calibration period also indicating an overestimation. The 1st iteration simulated average streamflow of 277.77 m^3/s (underestimation), this was the next in good estimate closer to average observed streamflow. Other iterations such as 4th iteration, 246.32 m^3/s (underestimation), 5th iteration 327.14 m^3/s (overestimation) and 3rd iteration 235.08 m^3/s (underestimation) follow in the order of difference of simulated streamflow values from the observed streamflow values. In accounting for uncertainty criteria in the calibration of the model, all the p-factor representing the amount of observed streamflow

values enclosed by the 95PPU band were all greater than 0.5 for all iterations revealing that higher amount of observed streamflow were bracketed. The r-factor being the depth of the enclosed 95PPU band bracketing the observed data were also good except for the value obtained in the 1st iteration which was rather large.

In selecting the goodness of fit iteration for as the best solution out of these results, the recommendations of Abbaspour *et al*. (2015) based on uncertainty analysis was adopted. They recommended a p-factor greater than 0.7 and r-factor less than 1.5. Therefore, the 2nd iteration was selected as a good fit using this criteria. The 2nd iterations had the best average simulated streamflow to average observed streamflow in prediction. The value of PBIAS of -0.2 was significantly good even though the negative sign suggested an overestimation of the simulated streamflow to the observed streamflow. The NSE value obtained during calibration range was in agreement with the range stipulated in the results of Schuol *et al.* (2008) in the basin. Figure 2 shows the plot of the simulated and observed streamflow during the calibration, while Figure 5 shows the result of the validation exercise.

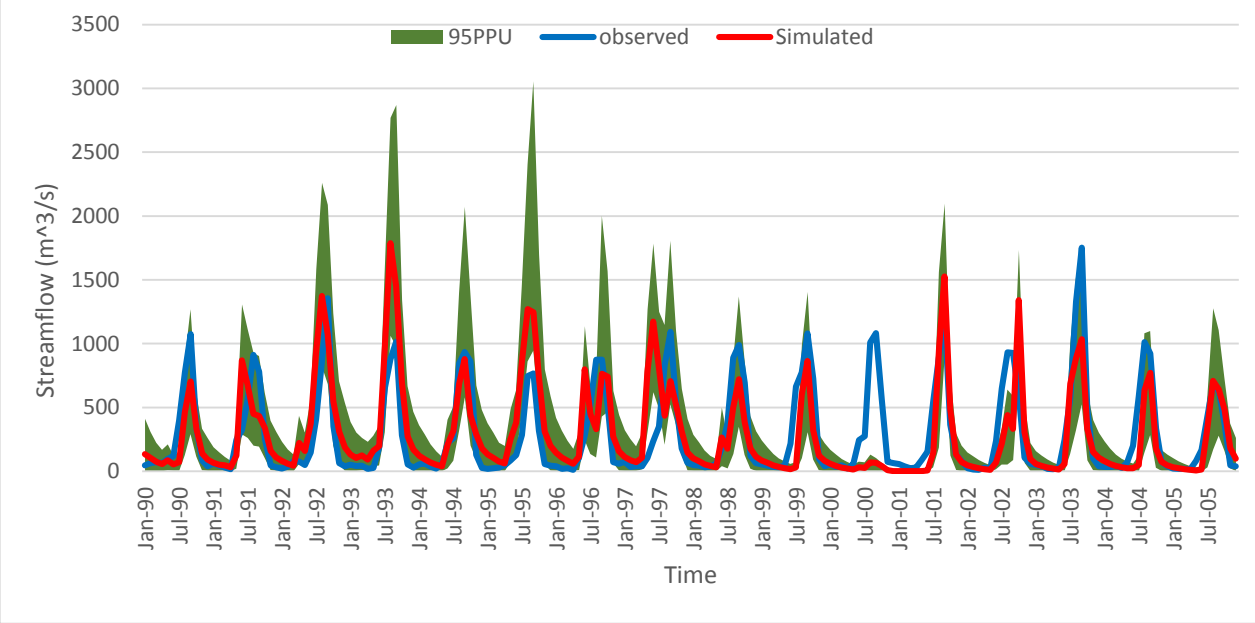

Figure 2: Calibration from 1990 to 2005

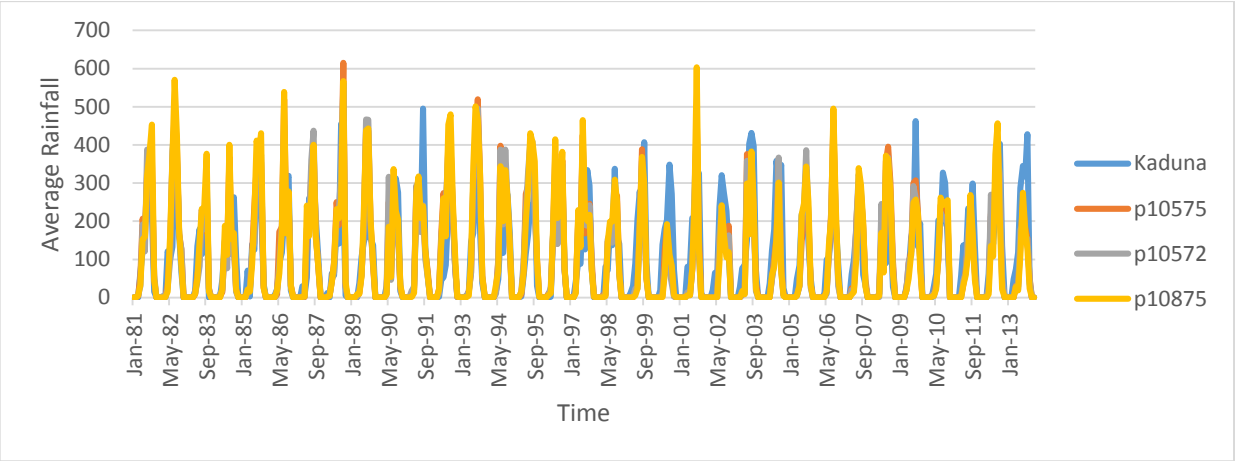

Figure 3: Average rainfall for Kaduna weather station and CFSR from 1981 to 2013

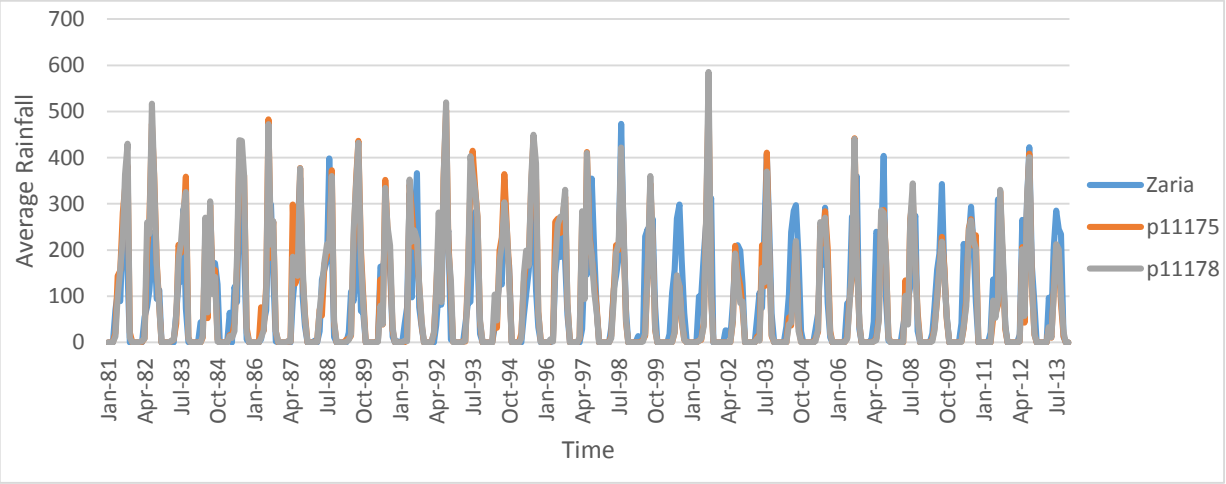

Figure 4: Average rainfall for Zaria weather station and CFSR from 1981 to 2013

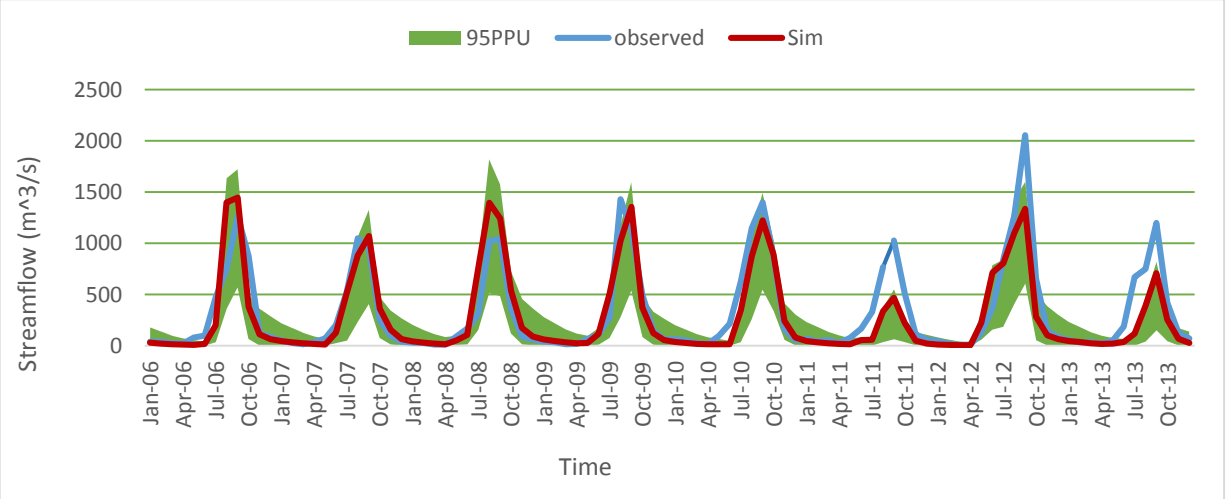

Figure 5: Validation from 2006 to 2013

The calibrated model was able to simulate flow peaks at similar periods as the observed peak flow but the simulated discharge reveals patterns of underestimation and overestimation of flow in a number of the years. Between the periods June 1990 to Dec 1990, July 1998 to January 1999, July 1999 to January 2000, July 2003 to January 2004 and July 2004 to January 2005 indicates the period where underestimation of simulated peak flow by the calibrated model. The model overestimate of peak flow between July 1993 to January 1994, July 1995 to January 1996 and July 2002 to January 2003. A drought year was recorded by the simulated flow between the periods of June 2000 to January 2001 where reasonable hit of peak flow was recorded in the simulated flow as against the observed flow for that period. This is as a result of the precipitation data used in modelling (Srinivasan, 2013). During that period NCEP CFSR precipitation data from all the stations recorded very low rainfall. Applying an assumption that closer weather stations of CFSR to an in-situ weather station should have similar climatic features, in-situ observed weather stations Kaduna and Zaria (both located in the Shiroro catchment) monthly precipitation series (Figures 3 and 4) were compared with CFSR point weather stations close-by to investigate the low peak recorded between the periods of June 2000 to January 2001. The CFSR peak precipitation records fell below the observed in-situ average precipitation peak amount by about 44.44 and 54.84 % of observed peak for Kaduna and Zaria stations respectively.

The statistical results from the validation of the model revealed improved values of NSE and R^2 compared to the calibration period. The NSE value for the validation period was 0.77, R^2 was 0.79 and PBIAS was 15 which good. The p-factor of 0.77 and the r-factor of 0.77 values were within the recommended range of p-factor > 0.7 and r-factor < 1.5. The average simulated streamflow values was 300.49 m^3/s whiles the observed streamflow values was 327.65 m^3/s indicating underestimation by the model during the validation period.

Conclusion

The CFSR data used to force the SWAT model in the catchment produced unsatisfactory results during calibration of the model. Nevertheless, the value obtained for NSE and R^2 were not far from the acceptable target of satisfactory in modelling watersheds with SWAT. The validation of the model and uncertainty were good. This findings opens up

the assessment of other reanalysis datasets suitability for modelling the hydrology of the Shiroro catchment. There also exist the opportunity of using CFSR dataset with in-situ weather data to improve their performance in modelling.

Acknowledgement

This research is supported by West African Science Centre on Climate Change and Adapted Land Use (WASCAL) for providing grants towards the completion of this project.

References

Abbaspour, K. C., Rouholahnejad, E., Vaghefi, S., Srinivasan, R., Yang, H., & Kløve, B. (2015). A continental-scale hydrology and water quality model for Europe: Calibration and uncertainty of a high-resolution large-scale SWAT model. *Journal of Hydrology*, *524*. http://doi.org/10.1016/j.jhydrol.2015.03.027

Abbaspour, K. (2015a). SWAT-Calibration and uncertainty programs (CUP)-User Manual. Swiss Federal Institute of Aquatic Science and Technology, Eawag, Duebendorf, 1-100.

Aderinto, S. A. (2006). Implication of Automatic Weather Observing Stations in Nigerian Meteorological Agency. Unpublished IMO report. http://www.wmo.int/pages/prog/www/IMOP/publications/IOM–94–TECO2006 P, 3

Agunbiade, O. A. & Jimoh, O. D. (2013). Flood modelling of upper Gurara watershed using remote sensing data and the geospatial streamflow model. WIT Transactions on Ecology and the Environment, 172, 39-49. Doi: 10.2495/RBM130041

Akpoti K., Antwi E. O. & Kabo-Bah A. T. (2016). Impact of Rainfalll Variability, Land Use and Land Cover Change on Streamflow of Black Volta Basin, West Africa. *Hydrology*, 3, 26. doi: 10.3390/hydrology3030026

Arnold, J. G., Srinivasan, R., Muttiah, R. S., Williams, J. R. . (1998). Large Area hydrologic modeling and assessment part I: Model development. JAWRA Journal of American Water Resources Association , 73-89.

Benke, K. K., Lowell, K. E., & Hamilton A. J. (2007). Parameter uncertainty, sensitivity analysis and prediction error in water-balance hydrological model. Mathematical and Computer Modelling, 47 (11-12), 1134-1149. https://doi.org/10.1016/j.mcm.2007.05.017.

Food and Agriculture Organization of the United Nations (FAO) (2003). Digital Soil Map of the World (DSMW): based on the FAO/UNESCO Soil Map of the World, Original Scale 1:5 000 000. FAO-AGL (Land and Water Development Division), Rome.

Fuka, D. R., Walter, M. T., MacAlister, C., Degaetano, A. T., Steenhuis, T. S., & Easton, Z. M. (2013). Using the Climate Forecast System Reanalysis as weather input data for watershed models. Hydrol. Process., DOI: 10.1002/hyp.10073

Gbobaniyi, E., Sarr, A., Sylla, M. B., Diallo, I., Lennard, C., Dosio, A., Dhiédiou, A.,

Kamga, A, Klutse, N. A. B., Hewitson, B., Nikulin, G. & Lamptey, B. (2014). Climatology, annual cycle and interannual variability of precipitation and temperature in CORDEX simulations over West Africa. International Journal of Climatology, 34(7), 2241-2257. DOI: 10.1002/joc.3834

Gubler, S., Hunziker, S., Begert, M., Croci-Maspoli, M., Konzelmann, T, Brönnimann, S., Schwierz, C., Oria, C., & Rosas, G. (2017). The influence of station density on climate data homogenization. International Journal of Climatology, 37 (13), 4670-4683. DOI: 10.1002/joc.5114

Jarvis, A., Reuter, H.I., Nelson, A. & Guevara, E. (2008). Hole-filled SRTM for the globe Version 4, available from the CGIAR-CSI SRTM 90m Database (http://srtm.csi.cgiar.org).

Jimoh, O. D., & Ayodeji, O. S. (2003). Impact of the Gurara River (Nigeria) interbasin water transfer scheme on the Kaduna River at Shiroro Dam. Proceedings of Symposium IUGG2003- Hydrological Risk Management and Development, IAHS Publication, Saporo 281:277-286.

Leary, N., Adejuwon, J., Barros, V., Burton, I., Kulkarni, J., & Lasco, R. (Eds.) (2008). Climate change and adaptation. London, UK: Earthscan.

NASA LP DAAC (2013). MODIS Land Cover Type Yearly L3 Global 500 m SIN Grid – Version 051. NASA EODIS LP DAAC, USGS Earth Resources Observation and Science Center, Sioux Falls, South Dakota (https://lpdaac.usgs.gov). Accessed March 12, 2017.

Neitsch, S. L., Arnold, J. G., Kiniry, J. R., & Williams, J. R. (2011). Soil and water assessment tool theoretical documentation version 2009. Texas Water Resources Institute Technical Report No. 406, Texas A & M University System College Station, Texas 77843-2118.

Omotosho, J. B. & Abiodun, B. J. (2007). A numerical study of moisture build-up and rainfall over West Africa. Meteorol Appl, 14: 209-225. DOI: 10.1002/met.11

Oyerinde, G. T., Wisser, D., Hountondji, F. C. C., Odofin, A. J., Lawin, A. E., Afouda, A., & Diekkrüger, B. (2016). Quantifying Uncertainties in Modeling Climate Change Impacts on Hydropower Production. Climate, MDPI, 4(34), 1–15. http://doi.org/10.3390/cli4030034

Oyerinde, G. T., Fademi, I. O., & Denton, O. A. (2017). Modeling runoff with satellite-based rainfall estimates in the Niger basin. Cogent Food & Agriculture, 3(1), 1363340. http://doi.org/10.1080/23311932.2017.1363340

Saha, S., Moorthi, S., Pan, H.-L., Wu, X., Wang, J., Nadiga, S., Tripp, P., Kistler, R., Woollen, J., Behringer, D., Liu,X., Stokes, D., et al. (2010). The NCEP climate forecast system reanalysis. Bull. Am. Meteorol. Soc., 91, 1015–1057.

Schuol J., Abbaspour K. C., Yang H., Srinivasan R. & Zehnder A. J. B. (2008). Modeling blue and green water availability in Africa. Water Resour. Res., 44, W07406, doi: 10.1029/2007WR006609.

Srinivasan, R. (2013). Soil and Water Assessment tool – introductory manual – version 2012. Texas Water Resources Institute, College Station, TX. Retrieved from http://swat.tamu.edu/documentation/ (accessed on 20 December, 2016)

Suleiman, Y. M., Ifabiyi, I. P. (2015). The role of rainfall variability in reservoir storage management at Shiroro Hydropower dam, Nigeria. An International Journal of Science and Technology, 3(2), 18-30. http://dx.doi.org/10.4314/stech.v3i2.2.

Srinivasan, V., Lambin, E. F., Gorelick, S. M., Thompson, B. H. & Rozelle, S. (2012). The nature and causes of the global water crisis: Syndromes from a meta Analysis of coupled human-water studies. Water Resour. Res, 48, W10516. DOI: 10.1029/2011WR011087.

The World Bank (2017). Hydromet in Africa. Retrieved from http://www.worldbank.org/en/region/afr/brief/hydromet-in-africa.